Theses, Dissertations and Capstones

1-1-2002

PKCα Translocation and Actin Remodeling in Contracting A7r5 Smooth Muscle Cells

Chenwei Li

Recommended Citation

PKCα Translocation and Actin Remodeling in Contracting

A7r5 Smooth Muscle Cells

by

Chenwei Li

Dissertation submitted to the Graduate College of

Marshall University

in Partial Fulfillment of the Requirements for

the Degree of

Doctor of Philosophy

Approved by

Gary L. Wright, Ph.D., Committee Chairperson
Patrick I. Brown, Ph.D.
Todd L. Green, Ph.D.
William D. McCumbee, Ph.D.
Michael L. Norton, Ph. D.

Department of Physiology

Acknowledgments

To my Advisor, Dr. Gary L. Wright, who taught me to think independently and to seek the truth in science, because of him, I believe I will be a better scientist and person...

To my doctoral committee members, Dr. Brown, Dr. Green, Dr. McCumbee and Dr. Norton, who gave me wisdom and assistance with my education and research...

To my wife Manxue, and my son Michael, who always remained understanding and loving throughout this time...

To my friends and colleagues, who encouraged and supported me...

Abstract

Recent research indicates that protein kinase C (PKC) plays an important role in smooth muscle contraction. Because PKC activation and specificity of substrate phosphorylation is believed to be associated with the relocalization of the enzyme to specific cell sites, we first investigated the subcellular translocation of PKCα in A7r5 smooth muscle cells by confocal microscopy through use of standard immunohistologic staining and PKCα - enhanced green fluorescent protein (PKCα -EGFP) fusion protein expression. PKCα was diffusely distributed throughout the cytosol in the unstimulated A7r5 cell. Upon stimulation with phorbol 12, 13 dibutyrate (PDBu), PKCα was translocated primarily to either the perinuclear region of the cell or to subplasmalemmal sites depending on the concentration of the stimulating agent. Specifically, PKCα was translocated to the perinuclear area in response to high PDBu concentrations (10^{-5} M to 10^{-6} M) and relocated to the plasma membrane at lower PDBu concentrations (10^{-7} M to 10^{-8} M). Translocation of PKCα to the perinucleus but not the plasmalemma was blocked by the use of colchicine to disrupt cell microtubules. By comparison, cytochalasin B disruption of actin microfilaments had no significant effect on PKCα translocation to either the plasmalemma or the perinucleus. The results indicate that the target site of PKCα translocation may vary with activating stimulus strength in A7r5 cells and that the translocation of the isoform to the perinuclear region of the cell is dependent on an intact microtubular cytoskeleton. This suggests that multiple pathways are available for the redistribution of PKCα that may employ different mechanisms to regulate the movement and/or docking of the isoform at specific target sites.

We next compared the spatial and temporal pattern of PKCα translocation in response to different stimulating agents in live A7r5 smooth muscle cell preparations utilizing cells transfected with PKCα-EGFP. PDBu (10^{-8} M) induced a slow but robust and irreversible relocation of the PKCα -EGFP fusion protein from the cytosol to the plasmalemma. By comparison, thapsigargin (10^{-5} M) and A23187 (2 X 10^{-5} M) induced a rapidly transient translocation to the cell membrane, which was completed within 4 minutes. In contrast to these agents, angiotensin II (Ang II, 10^{-6} M) caused only partial relocalization of cytosolic PKCα-EGFP to brightly fluorescing patches at the cell periphery. Moreover, the translocation of the kinase to peripheral patches was completed within seconds and the fusion protein returned to the cytosol within 2 minutes. The PKC inhibitor staurosporine blocked cellular contraction to PDBu but not to A23187 and had no effect on PKCα-EGFP translocation. By comparison, the calcium chelators EDTA and BAPTA-AM blocked the contraction to A23187, attenuated the contraction to PDBu, and abolished the translocation of PKCα-EGFP by both agents. The results show that A7r5 cells retain the ability to respond to several types of contractile agents and the spatial and temporal characteristics of individual PKC isoform translocation may differ markedly, depending on the stimulating agent.

The mechanism of vascular smooth muscle contraction is not well understood. Early research from our laboratory has suggested that stimulation of contraction in A7r5 smooth muscle cells with phorbol ester (PDBu) results in remodeling of the actin component of the cytoskeleton. Because the elevation of intracellular calcium ($[Ca^{2+}]i$) is

thought to be the initiating event of smooth muscle cell contraction to the majority of physiological agonists, we examined the effect of increasing $[Ca^{2+}]i$ by A23187 and thapsigargin on α- and β-actin remodeling. Contraction of A7r5 cells induced by A23187 and thapsigargin was earlier in onset and more quickly completed than PDBu-induced contractions. During the interval of contraction induced by A23187 and thapsigargin, β-actin cables shortened without evidence of disassembly. In marked contrast, elevation of intracellular calcium resulted in the partial or complete dissolution of α-actin cables and blocked further α-actin remodeling in response to PDBu. The α-actin associated cross-linking protein α-actinin showed a similar pattern of dissolution in response to high calcium, while the distribution of anchor protein talin was unchanged. Finally, incubation of the cells in the calcium-free medium prevented α-actin dissolution by A23187/thapsigargin and blocked PDBu-mediated α-actin remodeling. The results suggest that extracellular calcium is necessary for α-actin remodeling and that the elevation of $[Ca^{2+}]i$ beyond a threshold level initiates disassembly of α-actin cable structure in a highly selective fashion. We have further observed that of six kinase inhibitors investigated only ML-7, a myosin light chain kinase (MLCK) inhibitor, blocked the dissolution of α-actin cables induced by increased $[Ca^{2+}]i$. This finding may be suggesting a novel role of MLCK in destabilizing α-actin structure in the $[Ca^{2+}]i$ activated smooth muscle cell.

Table of Contents

List of Figures

List of Tables

I Literature Review

Smooth Muscle Contraction: Smooth muscle is found to be mainly present in the cylindrical or hollow organs of six different systems: gastrointestinal, ocular, reproductive, respiratory, urinary and vascular. Therefore, the functions of the organs containing smooth muscle are storage and transport, and smooth muscle is often considered a tissue of conductance and capacitance. This does not indicate that smooth muscle is an inert tissue, serving only as a conduit for various fluids. In the cardiovascular system, the active nature of smooth muscle is best observed. After contraction of the heart and propulsion of blood through the vasculature, it is the resting tone of the vessels that is the major determinant of the fluid dynamics of the system. The functions carried out by the smooth muscle in all systems are based on its excitable nature and ability to contract.

Major unanswered questions concerning smooth muscle contractile properties include concerned with the mechanism by which it develops force and the complete signal pathway. Most of the information available on how cells develop force was derived from the study of striated muscle that is characterized by an ordered arrangement of regularly spaced sarcomeres that move closer together upon contractile stimulation. Early research revealed the sarcomeres in striated muscle to be mainly comprised of actin and myosin. The basic principles of sliding filament theory, which evolved from structural and biochemical studies of the sarcomere, indicate that the initial increases in intracellular calcium after muscle stimulation results in calcium binding to troponin. This binding causes a shift of tropomyosin from its resting position in the grooves within the actin helices, thereby removing inhibition of interaction between actin and myosin. The interaction of actin and myosin activates the ATPase in the myosin head, and stable crossbridges between the sarcomeric actin and myosin filaments are formed. Following

this, the hydrolysis of ATP and the conformational change of myosin induced by hydrolysis of ATP provide the force necessary to pull the actin and myosin past each other. These biochemical events combined with the opposing interdigitation of the actin and myosin filaments produce a shortening of each individual contractile unit sarcomere and force development.
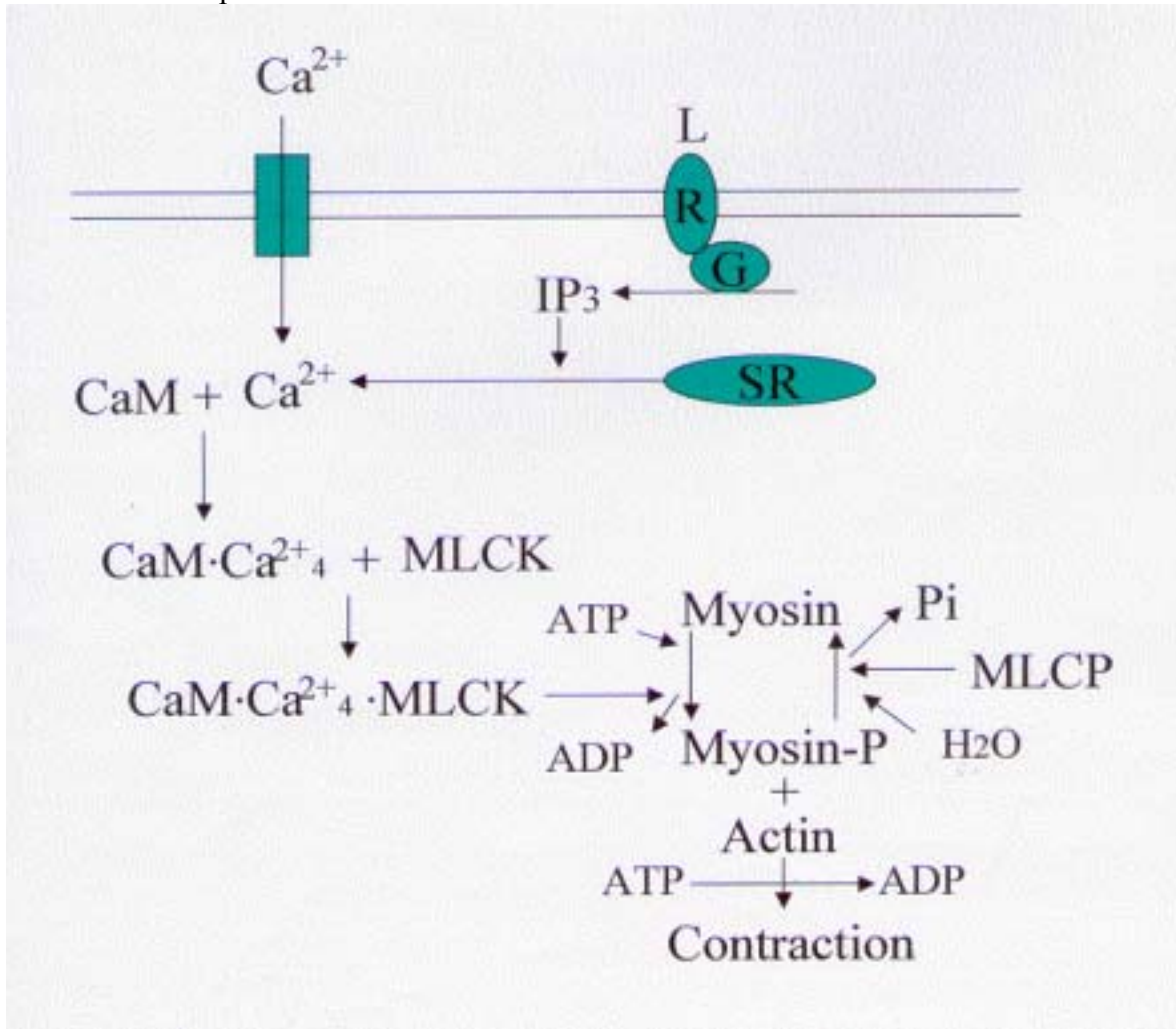
Figure 1.
Activation scheme of smooth muscle contraction. G, heterotrimeric GTP-binding protein; R, receptor; L, ligand; IP3, inositol 1,4,5-trisphosphate; SR, sarcoplasmic reticulum; CaM, calmodulin; MLCK, myosin light-chain kinase; MLCP, myosin light-chain phosphatase.

Smooth muscle has no morphologically recognizable sarcomere. Despite the gross morphological differences between striated and smooth muscle, most of the initial work concerning the biochemistry and biophysics of smooth muscle contraction was analyzed and presented within the existing parameters that had been determined for striated muscle contraction. The most widely accepted mechanism is that the contraction of smooth muscle is induced by the elevation of $[Ca^{2+}]i$ which, in turn, activates myosin light chain kinase to initiate the actin/myosin interaction and contraction (Fig. 1). A number of extracellular signals, including neural, humoral, ionic, and mechanical forces, result in an increase in intracellular calcium from 120-270 nM to 500-700 nM and the high intracellular calcium induces binding of free calcium to calmodulin (CaM) to form Ca^{2+}_4-CaM complex. Formation of this complex induces a conformational change in CaM with exposure of a site of interaction with the target protein myosin light chain kinase (MLCK), resulting in formation of the complex Ca^{2+}_4-CaM-MLCK, which is the active from of kinase. The active MLCK phosphorylates the serine 19 in each of the two 20-kD myosin light chains (LC20), triggering the cross-bridge cycling of actin-myosin and development of force with the hydrolysis of ATP. After an excitation, relaxation and calcium homeostasis are achieved by calcium reuptake into intracellular stores and the extrusion into extracellular space.

Intracellular Calcium   The main site of calcium storage inside smooth muscle cell is the sarcoplasmic reticulum (SR), and this organelle plays a major role in maintaining low intracellular $[Ca^{2+}]$. Although the volume of SR appears to vary between smooth muscles, the SR forms an extensive intracellular network, which is capable of calcium uptake,

storage, and specialized release. SR volume is estimated to be 1.5-7.5% of smooth muscle cell volume. SR is typically more abundant in tonic (for example, aorta) than phasic (such as portal vein) smooth muscle. Most of the surface of SR in smooth muscles is closely associated with the plasma membrane (Devine et al., 1972), so release of calcium can greatly affect the concentration of calcium near the inner surface of the plasma membrane as well as the calcium concentration in the cytosol. The SR is surrounded by a membrane that is not freely permeable to calcium. Active calcium-ATPases, which are known as SERCA pumps, exist in the SR membrane and generate and maintain about a 10,000-fold calcium gradient between the SR lumen and the cytoplasm. Three genes encode SERCA pumps, and two subgroups of SERCA2 (SERCA2a and SERCA2b) have been identified. SERCA pumps utilize the energy from ATP hydrolysis to move calcium from the cytoplasm to the lumen of the SR. After calcium is pumped into the SR, it is buffered by calcium binding proteins, such as calreticulin and calsequestrin. Studies of the function of SERCA pumps have been strongly aided by specific SERCA pump inhibitors, such as thapsigargin. When SERCA pumps are inhibited by thapsigargin, a major source of calcium regulation is lost and calcium leaks into the cytoplasm. Because cells are unable to maintain typically low cytoplasmic concentrations, intracellular calcium concentrations increase. This effect will induce further increase of intracellular calcium concentration or extend periods of contraction. Evidence from a variety of cell types suggests that mitochondria also play an important role in calcium homeostasis

Stimulation of smooth muscle by agonists that bind to certain types of G-protein-coupled membrane receptors results in the activation of phospholipase C and production of IP3 by

hydrolysis of phosphatidylinositol. IP3 induces calcium release from the SR by activating one type of calcium release channel, which is called the IP3 receptor. Three genes encode IP3 receptors and each channel is made up of four subunits of about 300 kDa that form a homotetrameric or heterotetrameric structures. An increase of calcium concentration from basal level to 300nM will further increase the potency of IP3 in activating calcium channels, and cause more calcium release. However, higher calcium concentrations reduce the effectiveness of IP3 and result in negative feedback for release of calcium. Another major source of calcium channel-associated SR release of calcium involves the ryanodine receptor. Cytoplasmic calcium can activate ryanodine receptors, and, as a result, this release pathway is referred as the calcium –induced calcium release channel. It is possible that the release of calcium from IP3 receptors stimulates the release of calcium from ryanodine receptors.

The Cytoskeleton The smooth muscle cytoskeleton is composed of three principal types of protein filaments (actin filaments, intermediate filaments and microtubules), which form protein filament networks extending throughout the cytoplasm. The cytoskeleton is a dynamic structure that is continually reorganized as cells move, change shape, or contract.

Actin The major smooth muscle cytoskeleton protein, actin, is involved in vesicle trafficking, cell division, cell motility and muscle contraction (Barkalow and Hartwig, 1995). Actin exists as monomeric, G-actin, or as filamentous, F-actin. The G-actin polymerizes to form F-actin filaments which are thin, flexible fibers approximately 7 nm is diameter and up to several mm in length. The formation of F-actin from G-actin is a two-step process. *In vitro*, the first step, the rate-limiting step for filament assembly, is nucleation: formation of actin dimers and trimers (Cooper et al., 1983; Frieden, 1983; Tobacman et al., 1983). The nucleation of actin filaments *in vivo* is poorly understood,

but research indicates that the Arp2/3 complex plays a possible key role in nucleation. After nucleation, rapid elongation of actin filaments occurs (Korn, 1982). Since all actin monomers are oriented in the same direction, actin filaments have a distinct polarity with the two ends (plus and minus ends) being distinguishable from one another. These two ends of an actin filament grow at different rates. The G-actin is added to the plus end five to ten times faster than to the minus end. Therefore the plus end is kinetically favored for assembly. This polarity of actin filaments is important in establishing a unique direction of myosin movement relative to actin.

There is a very high degree of conservation of actin sequence within cell types with a 95 percent amino acid sequence homology (Pollard and Cooper, 1986). In vertebrate animals, six distinct actin isoforms have been identified: α-skeletal, α-cardiac, α-vascular, γ-enteric, γ-cytoplasmic and β-cytoplasmic. Each is encoded by a distinct gene (Vandekerckhove and Weber, 1978; Reddy et al., 1990). The isoforms found in smooth muscle are α-actin, β-actin, and γ-actin (Herman, 1993), they only differ in their N-termini (Vandekerckhove and Weber, 1981). These isoforms are categorized into muscle actin (α-actin and γ-actin) and cytoplasmic actin (β and γ-actin). Of the cytoplasmic actins, β-actin is the most predominant, comprising up to thirty percent of the total cellular actin complement (North et al., 1994a). There appears to be a cellular compartmentalization of these isoforms. Antibodies directed against the α and γ-actin but not β-actin colocalized with the myosin containing contractile region (North et al., 1994b). It was suggested that this compartmentalization was a reflection of function by Small (1986) who hypothesized that contraction was generated through the actin:myosin containing portion of the cell.

The idea that there is a relationship between contraction and cytoskeleton remodeling was first proposed in the early 1990s. Based on studies of single smooth muscle cells, it was

shown that the length-tension relationship changed depending on the initial length at which the cells were activated. It was first suggested by Harris and Warshaw (1991) that there was a disassociation of cell length and contractile element length. Subsequent studies showed that velocity of shortening decreased as the tissue was activated at increasing lengths, leading Gunst and coworkers (1993) to conclude that their results were consistent with an the hypothesis of Harris and Warshaw (1990), who proposed that the decrease in velocity of shortening in single cell contractions is due to an internal load that increases as the cell shortens. Gunst suggested that the internal load could represent resistance to shortening resulting from the compression of the cytoskeleton. It was further speculated by Gunst et al. (1993) that the inverse relationship between tissue length at activation and velocity of shortening could reflect the reorganization of the cytoskeleton in response to activation at different muscle lengths. They suggested that reorganization would serve to maximize contractile function at each tissue length and could involve the activation-induced attachment of the contractile component of the cytoskeleton to stabilizing cell structures. This research group proposed later that the depression of force seen during the oscillation in length of canine tracheal smooth muscle was due to the resetting of contractile element length as a result of muscle stretch (Shen et al., 1997).

Our laboratory first demonstrated that inhibition of actin polymerization by cytochalasin caused a selective blockade of the slow tension increase in rat aortic smooth muscle (Wright and Hurn, 1994). Rather than a fixed resetting of the cytoskeleton to optimize length-tension at activation, Wright and Hurn (1994) suggested that slow tension development by smooth muscle required a capability for dynamic remodeling of a portion of the actin cytoskeleton during the interval of contraction. Their conclusion has been supported by recent studies of Mehta and Gunst (1999), who showed that inhibition of actin polymerization by latrunculin-A depressed force development without affecting

7

myosin light chain phosphorylation, further suggesting that actin polymerization contributes directly to force development. Wright and Battistella-Patterson (1998) have shown that inhibition of actin polymerization blocks calcium-dependent stress relaxation in vascular smooth muscle, suggesting that remodeling of the actin cytoskeleton may also serve to decrease cellular tension following abrupt stretch. Taken together, it is clear that effects of inhibition of actin polymerization on the contractile and stress relaxant properties of smooth muscle cannot be attributed to a simple loss in cytoskeletal structure. However, Wright's conclusions are consistent with an inhibition of dynamic actin cytoskeletal remodeling which could serve to continuously modulate the optimal positioning of actin and myosin filaments during the interval of force development and cell constriction (Battistella-Patterson et al., 1997; Fultz et al., 2000). Nevertheless, the cytochalasin-based studies have been the subject of controversy.

Cytochalasins are a class of fungal metabolites first derived from cultures of Helminthosporium dematioideum and Metarrhizium anisopliae in the late 1960's (Carter, 1967). Cytochalasins were shown to cause microfilaments to lose their filamentous nature (Schroeder, 1970; Wessells, 1971). These microfilaments were later shown to be the actin filaments (Spudich, 1972; Spudich and Lin, 1972). Cytochalasin B inhibits actin polymerization by binding to the plus end of actin filaments, thereby inhibiting the addition of actin monomers to existing filaments (Cooper, 1987). It was unknown whether the inhibitory effect of cytochalasins on smooth muscle contraction was through the effect of cytochalasin on the polymerizing actin cytoskeleton or due to an unknown or nonspecific effect of the drug (Wessells, 1971). For example, there is some evidence indicating the effect of cytochalasin on smooth muscle contraction could be through the blockade of calcium influx (Dresel and Ogbaghebriel, 1988), the blockade of glucose uptake (Dresel and Knickle, 1987), the inhibition of myosin light chain phosphorylation or the inhibition of myosin ATPase activity. However, Obara and Yabu (1994) have

shown that treatment of smooth muscle tissues with cytochalasin at a concentration that induced a maximal inhibition of the contraction, had no effect on cell calcium current, myosin light chain phosphorylation or myosin ATPase activity in response to high potassium contraction. It was reported by Tseng et al (1997) that there was an absence of an effect of cytochalasin on glucose transport at the concentration necessary to produce maximal inhibition. Because the stable actin structure of striated muscle is not affected by cytochalasin, it may suggest that the fast phase of smooth muscle contraction, which is also unaffected by cytochalasin (Wright and Hurn, 1994), is produced by a mechanism comparable to sliding filament-based systems. At this time, however, the role of dynamic actin cytoskeleton remodeling as a potential factor in the development of slow phase smooth muscle contraction has yet to be clearly elucidated.

Recent studies of the contractile response of A7r5 smooth cells to phorbol ester, which activates slow tension development, indicate significant actin remodeling, with the remodeling of α and β-actin being distinctly different (Fultz et al., 2000). Both isoforms were incorporated into stress cables in the unstimulated cell. During the interval of contraction, β-actin cables were stable and observed to shorten without evidence of disassembly. In contrast, α-actin cables were clearly observed to disassemble and reform into a system of peripheral column-like structures with associated clusters of randomly oriented fibers. Although subject to controversy, there is evidence that the phorbol ester-induced contraction of smooth muscle may occur in the absence of an elevation in $[Ca^{2+}]i$ (Nakajima et al., 1993) or a concomitant increase in myosin light chain phosphorylation (Singer and Baker, 1987).

Intermediate Filaments   Intermediate filaments have a diameter of 10 nm. Their main function is to provide mechanical strength to cells. Intermediate filaments have been proposed to play an indirect role in the contractile process through the positioning of

9

dense bodies in the cell. It has been suggested that dense bodies constitute cellular anchorage points in smooth muscle that are analogues to the Z-line in striated muscles (Bond and Somlyo, 1982; Kargacin et al., 1989). Actin filaments anchored at dense bodies have been presumed to transmit tension to the cell surface via connections to subplasmalemmal dense plaques (Pease and Molinari, 1960). These dense bodies have been shown to contain α-actinin (Fay et al., 1983), filamin (Small et al., 1986), talin (Volberg et al, 1986), vinculin (Geiger et al., 1985; Volberg et al., 1986), plectin (Wiche et al., 1983) and actin.

Microtubules There is no evidence to indicate the involvement of microtubules in smooth muscle contraction. Microtubules have been shown to be involved in a variety of cellular functions including: formation of the mitotic spindle, axonal and dendritic extension in neurons, maintenance of intracellular organization and shape, transport of compounds and organelles (Avila, 1991), and cell motility (Bershadsky and Vasiliev, 1993). Microtubules are rigid hollow rods approximately 25 nm in diameter and are formed by the reversible polymerization of tubulin. Like actin filaments, the microtubules have a distinct polarity with a greater addition rate of tubulin at the plus end than at the minus end. There are three types of tubulin that comprise the microtubule, α,β and γ. The α and β-tubulin form dimers and these dimers can attach to the growing microtubule. γ-Tubulin is found at the centrosome, the microtubule organizing center (MTOC), and site for polymerization (Oakley and Oakley, 1989; Zheng et al., 1991). This degree of organization ensures that microtubular polymerization can only occur in a direction away from the MTOC (Brinkley, 1985). The transport function of microtubules is accomplished by microtubule-associated motor proteins: kinesin and dynein. Both of these proteins consist of a heavy chain and of a light chain. The heavy chain binds to the microtubule and generates force through hydrolysis of ATP, while the light chain is responsible for binding a specific "cargo". A major difference between the two motor

proteins is based on the polarity of transport along the microtubules: kinesin is a plus-end oriented motor protein, moving away from the MTOC, and dynein is a minus end-directed motor, moving toward the MTOC. This type of system allows for specific and directed bi-directional transport of compounds and organelles. Colchicine, which causes depolymerization of the microtubules into free tubulin, is known to cause a disruption of the cellular morphology, producing "fractures" within the cytoplasm (Godman, 1955).

Kinases Thought to be Involved in Smooth Muscle Contraction   Although the exact nature of the signaling pathways that regulate smooth muscle contraction are not certain, recent use of pharmacological and molecular approaches indicates that several specific families of kinase are involved in determining the contractile response to different agonists. Those that have been repeatedly demonstrated to be important are discussed below.

Myosin Light Chain Kinase (MLCK) MLCK is a calcium/calmodulin-dependent protein kinase that phosphorylates a serine residue in the N-terminus of the regulatory light chain (RLC) of myosin II (Stull et al., 1986; Gallagher et al., 1997). The RLC of myosin II is its only identified physiological substrate, so the enzyme is recognized as a dedicated kinase. Phosphorylation of the RLC of myosin II by calcium/calmodulin-dependent MLCK plays diverse roles in cellular functions including, potentiated skeletal and cardiac muscle contraction (Sweeney et al., 1993), initiation of smooth muscle contraction (Kamm & Stull, 1985; Hartshorne, 1987; Somlyo & Somlyo, 1994; Gallagher et al., 1997), platelet aggregation and contraction, endothelial cell retraction, fibroblast contraction, secretion, receptor capping and nerve growth cone motility (Hartshorne, 1987; Gallagher et al.,1997).

11

In vertebrates there are two genes for MLCK (Stull et al., 1986; Gallagher et al., 1997). One form is expressed in striated muscles and has distinct catalytic and structural properties that are distinct from the other form. The other form, originally purified from smooth muscle tissues, was described as smooth muscle MLCK. However, emerging biochemical and molecular evidence shows that this form is also found in non-muscle cells (Gallagher et al., 1997). The size of this enzyme ranges from 130 to 150 kDa depending upon the animal species. Because of its ubiquitous distribution, it is now commonly referred to as conventional MLCK. Biochemical and molecular research indicates that MLCK contains a catalytic core that is structurally related to other serine/threonine protein kinases (Stull et al., 1986; Gallagher et al., 1997). The regulatory segment involved in autoinhibition and calmodulin binding extends from the C-terminus of the catalytic core and folds back onto the large lobe of the catalytic core in the absence of calcium/calmodulin, thereby inhibiting intrasterically RLC binding and phosphotransferase activity (Kemp & Pearson, 1991; Knighton et al., 1992). The MLCK contains three immunoglobulin-like and one fibronectin-like motifs and the C-terminal of the catalytic core/regulatory segments (Olsen & Eckstein, 1990; Gallagher et al., 1991; Potier et al., 1995). Immunoglobulin-like and fibronectin-like motifs, consisting of about 100 residues, are also found in giant muscle proteins such as titin. The third immunoglobulin-like motif at the C-terminus has seven strands of an antiparallel β-pleated sheet that form a barrel (Holden et al., 1992).

Calmodulin with calcium has a high affinity for MLCK with an averaged Kd or Kcam value of 1nM (Stull et al., 1986). There are two lobes of calmodulin which can be separated by limited trypsin cleavage. Biochemical studies of the isolated fragments show that each is an effectively independent structure capable of activating target enzymes including MLCK (Newton et al.,1985; Persechini et al.,1994; Persechini et al., 1996). A mixture of the two lobes results in a greater extent of activation than does either

lobe alone. Calcium first binds to the high affinity sites in the C-terminal lobe of calmodulin. As the calcium concentration increases, calcium binds to the two lower affinity sites in the N-terminal lobe of calmodulin. This results in the subsequent binding of the second calcium/calmodulin lobe, displacement of the regulatory segment and exposure of the catalytic cleft for RLC binding. MLCK obviously binds to myosin via a substrate-enzyme interaction. Biochemical studies show it has a higher affinity for non-phosphorylated myosin (substrate) than for the phosphorylated form (Sellers & Pato, 1984).

Biochemical studies have also shown that MLCK binds to F-actin, but the apparent binding affinity, with or without tropomyosin, is low relative to what would be expected from binding to detergent washed myofilaments or skinned fibres (Sellers & Pato, 1984). At relatively high concentrations *in vitro,* MLCK bundles F-actin filaments (Hayakawa et al., 1994) and is able to inhibit the interaction of phosphorylated myosin with F-actin (Sato et al., 1995). Binding studies to detergent-washed gizzard myofilaments showed that the full-length MLCK and ΔC-MLCK (deletion of the C-terminal Ig-like motif alone) bound but the ΔN- (deletion of the N-terminal half-alone) and ΔNC (deletion of both the N-terminal half and C-terminal IG-like motif) forms did not. MLCK bound with an apparent higher affinity to detergent-washed myofilaments and to purified smooth muscle thin filaments than to smooth muscle F-actin or skeletal muscle myofibrils. Because the apparent binding affinity is greater for purified thin filaments than smooth muscle F-actin, there may be another protein that facilitates or anchors MLCK to the actin-containing filaments.

Calcium /Calmodulin -Dependent Protein Kinase II (CaMK II) When calcium binds to calmodulin to form a calcium/calmodulin complex, the complex will activate a number of cellular enzymes. One such enzyme is Calcium /Calmodulin -dependent protein kinase

II (CaMK II). CaMK II is large multimer (~ 600 kDa) protein with 8-10 individual kinase subunits of about 54-60 kDa each. CaMK II is composed of four subunits (α, β, δ and γ). The CaMK II present in cultured rat aortic VSM cells is comprised mainly of the $\delta2$-subunit variant (Schworer et al., 1993). This kinase undergoes autophosphorylation in the presence of Calcium/CaM on a specific conserved threonine residue (Thr 286 in the α-subunit) which results in Calcium/CaM-independent (or "autonomous") kinase activity (Hanson et al., 1992). A total of 70-80% of the Calcium/CaM-dependent kinase activity may become autonomous *in vitro* under optimal autophosphorylation conditions (Hanson et al., 1989). Autophosphorylation on Thr286 has also been reported to result in a 1000-fold increase in the affinity of the kinase subunits for calmodulin (Meyer et al., 1992). Inactive CaMK II has a low affinity for calmodulin. The autophosphorylation of CaMK II is predicted to be a cooperative process requiring at least two activated subunits per holoenzyme. Intact cells have phosphatase activities that are capable of reversing autophosphorylation. The possible effect of CaMKII on smooth muscle contraction is by phosphorylation of myosin light chain kinase. When MLCK is phosphorylated by CaMK II *in vivo*, the affinity of MLCK for calmodulin is decreased and the calcium/calmodulin threshold for activation of MLCK is raised (Stull et al., 1990). In addition, if the CaMKII specific inhibitor, KN-62, is used in these preparations, the phosphorylation of myosin light chain by MLCK is potentiated, indicating that there is an inhibitory effect of CaMKII phosphorylation on MLCK activity (Tansey et al., 1992).

Mitogen-Activated Protein (MAP) Kinase   MAP kinases are unique protein kinases activated in response to many extracellular stimuli. They have been shown to be involved in multiple functions of cells. The MAP kinase family members may be classified by two different standards. First, they may be classified according to the sequence that results in activation when it is phosphorylated. The MAP kinases require dual phosphorylation of threonine and tyrosine and include TEY, TPY and TGY

14

sequences. The second classification scheme is based on the nature of the upstream dual specificity kinases (MAP kinase kinases) that phosphorylate and activate the MAP kinases. Regulation of MAP kinase inactivation by specific MAP kinase phosphatases is stimulus- and cell type-specific.

One TEY member, ERK1/2, is believed to play an important role in mediating phosphorylation of contractile proteins in the maintenance of sustained smooth muscle tone. In porcine carotid arteries stimulated by a mechanical load or by vasoactive agonists, ERK1/2 activity was found to increase by 5- to10-fold (Adam et al., 1995). Immunofluorescence studies in ferret aorta cells showed that phenylephrine-induced translocation of cytosolic PKC to the surface membrane was associated with transient redistribution of ERK1/2 to the surface membrane before cell contraction. Coincident with cell contraction, ERK1/2 undergoes a second redistribution away from the plasmalemma and towards contractile filaments. High molecular weight caldesmon (h-caldesmon) has been proposed to be the ERK1/2 substrate. The thin filament proteins caldesmon and calponin are known to inhibit actomyosin ATPase *in vitro* and prevent actin sliding. Inhibition of actomyosin ATPase is relieved by phosphorylation of caldesmon.

Focal Adhesion Kinase (FAK) Focal adhesion kinase (FAK) is a cytoplasmic tyrosine kinase with a molecular weight of 120-kDa. FAK is activated by autophosphorylation of Tyr397 in response to different ligand engagement with integrins (Schlaepfer et al., 1994; 1997). It has been reported that the time course of the increase in FAK tyrosine phosphorylation in response to contractile stimulation closely follows tension development in tracheal smooth muscle. The role of FAK in the contractile activation of tracheal muscle has been studied by utilizing an antisense oligonucleotide to FAK to selectively deplete FAK protein (Tang et al., 2001). The depletion of FAK protein

resulted in an inhibitory effect on the development of force, intracellular calcium levels, and myosin light-chain phosphorylation in response to contractile stimulation with acetylcholine. After permeabilization with α-toxin and stimulation by increasing intracellular calcium, the FAK-depleted tissues developed active tension that was comparable to control tissues. This indicated that the primary cause for the suppression of contractile activation in the FAK-depleted tissues is possibly the disruption of calcium signaling. These studies are consistent with electrophysiological studies in vascular muscle cells that also suggest a critical role for FAK in the regulation of calcium channels. It has also been suggested that FAK might be part of a complex of proteins that mediate calcium-insensitive signaling pathways which regulate the contractile apparatus and cytoskeletal dynamics in smooth muscle (Tang et al., 1999).

Small Heat Shock Protein (HSP27) There are several families of proteins that are likely to be effectors of actin remodeling, including capping proteins, severing proteins such as gelsolin (Gusev et al., 1994; Butt et al., 2001;), and cross-linking proteins such as filamin and α-actinin. Small heat shock proteins might also be important effectors of actin remodeling or cross-bridge function. HSP27 is a multimer that occurs in various sizes ranging from dimers to 700-kDa oligimers, with the large (>500 kDa) multimers predominating. Multimers form from interaction of unphosphorylated dimers. Phosphorylation of Ser 83 promotes dissociation of multimers (Benndorf et al., 1994), and further phosphorylation of Ser15 may regulate interaction of dimers with actin filaments (Lambert et al., 1999). HSP27 has significant effects on actin cytoskeletal polymerization or depolymerization which are regulated by phosphorylation and dephosphorylation of HSP27. Purified unphosphorylated mouse and chicken HSP27 homologs inhibit actin polymerization *in vitro* (Benndorf et al., 1994; Miron et al., 1991) while phosphorylation reverses the inhibition. This is supported by studies of cultured cells in which the phosphorylation of HSP27 was shown to be necessary for growth

16

factor stimulating F-actin formation (Lavoie et al., 1993a; and 1993b), the stabilization of focal adhesions (Schneider et al., 1998), and the promotion of cell migration (Rousseau et al., 1997). Research of signaling pathways regulating HSP 27 activity in fibroblast and other nonmuscle cells showed that phosphorylation of HSP27 by MAP kinase-activated protein (MAPKAP) kinase 2 (MK2) is necessary for formation of F-actin. Phosphorylation of HSP27 by MK2 increases the rate and extent of actin polymerization *in vitro* (Butt et al., 2001). This suggests that, *in vivo*, the extent of actin polymerization can be increased by phosphorylation of HSP27 by MK2. MK2 is regulated by p38 MAP kinases. The p38 MAP kinases are activated by upstream activators MKK3, MKK4 and MKK6. The pathway between the MKKs and surface receptors is not well defined. RhoA is also reported to be an upstream activator of HSP27 in smooth muscle. HSP27 is constitutively expressed in smooth muscles at relatively high concentrations (2-8μg HSP27/mg total protein) (Miron et al., 1988; Hedges et al., 1999;). HSP27 has been shown to colocalize with contractile proteins in freshly dispersed intestinal smooth muscle cells stimulated with ceramide, and has been coprecipitated with actin, tropomyosin, and caldesmon, suggesting some molecular association with the contractile elements (Ibitayo et al., 1999). "Stress"stimuli also can activate signal transduction pathways that induce HSP27 phosphorylation in smooth muscle

The Protein Kinase C (PKC) Family   Several hypotheses advanced to explain the contractile function of smooth muscle based on the results of *in vitro* research, have proposed mechanisms involving protein phosphorylation by protein kinase C. PKC was discovered in 1977 by Nishizuka and co-workers. This discovery represented a major breakthrough in signal transduction research. PKC has been known as the cellular receptor for diacylglycerol (DAG), and is therefore a key player in phospholipase C-
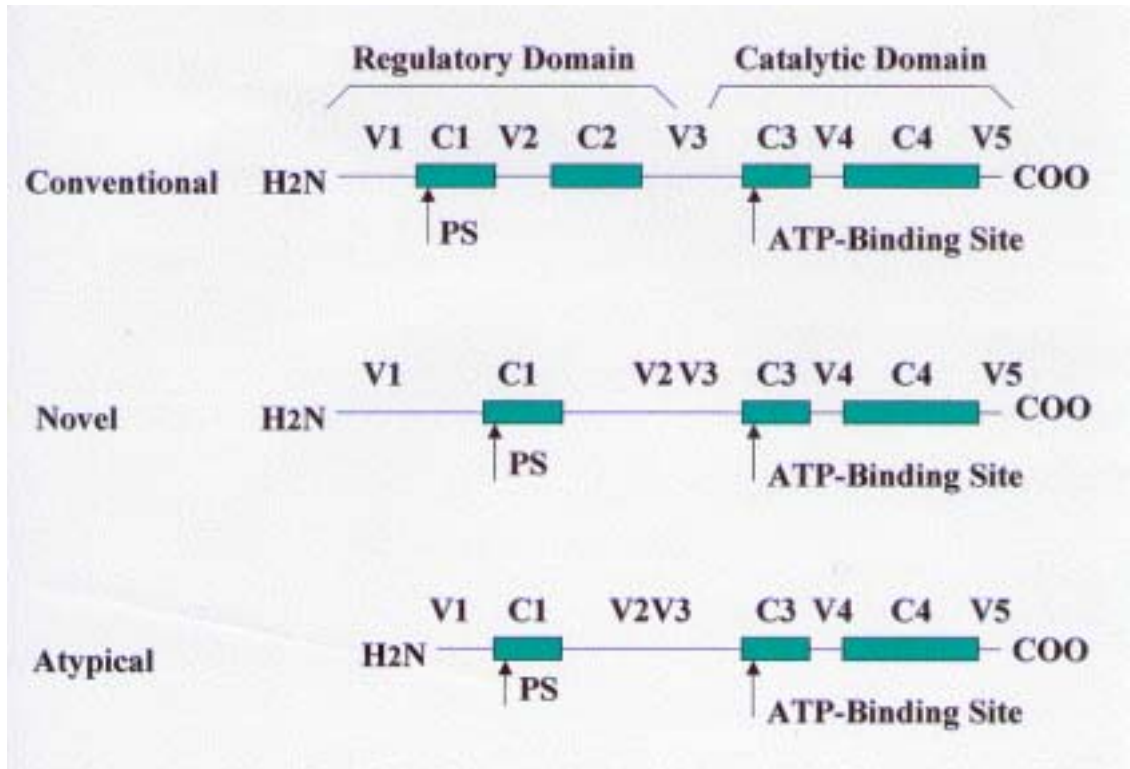
Figure 2.
Schematic representation of structural features of protein kinase C (PKC) isozymes. PKC polypeptides are depicted as linear chains with an amino terminal regulatory domain and a carboxyl terminal catalytic domain. Comparison of deduced amino acid sequences reveals five variable (V1-V5) and four constant (C1-C4) regions. Locations of pseudosubstrate (PS)-and ATP-binding sites are indicated. Cysteine-rich zinc finger sequences are located in C1 domains: two in each of cPKC and nPKC isozymes, and one in the aPKC isozymes. The nPKC and aPKC isozymes lack a C2 domain and exhibit calcium-independent activity.

coupled signal transduction. PKC is also a high-affinity receptor for the phorbol ester, which is a tumor promoter involved in multistage carcinogenesis. The activation-associated translocation, the identification of substrate, and the characterization of its functional role in the cell all form active areas of research.

The PKC family is a group of serine-threonine kinases implicated in various biological functions including signal transduction, cell proliferation and differentiation, and smooth muscle contraction. The PKC family is separated into four subgroups (Fig. 2) based on their structure and activation requirements (Keenan and Kelleher, 1998; Newton et al., 1998). The conventional PKC (cPKCs): α, βI, βII, and γ are activated by calcium, diacylglycerol (DAG) or phorbol ester, and phosphatidylserine (PS). There are additional activators for cPKC, such as cis-unsaturated fatty acids and lysophosphatidylcholine (lysoPC). PKC δ, ε, η, and θ are known as novel PKCs (nPKC). Compared with conventional PKCs, novel PKCs lack a conserved region of homology known as the C2 domain, which allows them to function in a calcium-independent manner. Atypical PKCs (aPKC), PKC ζ and ι/λ, have only one cysteine-rich zinc finger motif located in their C1 domain compared with the other cPKC and nPKC isozymes, which have two. The aPKCs do not require DAG or calcium for activation, but are dependent on PS, the only cofactor required by all three groups. PKCμ (or PKD), a new serine-threonine kinase with homology to PKC, may form a distinct PKC subgroup (Newton et al., 1998).

Each PKC isozyme is the product of a separate gene with the exception of PKC βI and βII, which are alternativly spliced variants of the same gene. All of the PKC isozymes are single chain polypeptides, comprised of an N-terminal regulatory domain (approximately 20-40 kDa) and a C-terminal catalytic domain (approximately 45 kDa). Cloning of the first isozymes revealed four conserved domains: C1-C4 (Coussens, 1986). The function of each of these domains has been established by extensive biochemical and mutational research. The regulatory domain participates in protein-protein interactions that regulate PKC activity and localization. The catalytic region is the kinase domain and includes motifs involved in ATP and substrate binding. The regulatory and catalytic domains are connected by a hinge region that is highly sensitive to proteolytic cleavage by cellular proteases.

The C1 domain contains a pseudosubstrate sequence that resembles the sequence around phosphorylatable serine or threonine residues in the PKC substrate. The pseudosubstrate sequence may bind to the active site in the catalytic domain and inactivate the PKC. Conversely, antibodies to the pseudosubstrate sequence completely activate PKC. In the absence of cofactors, the introduction of a mutation in the pseudosubstrate sequence of PKCα resulted in a substantial increase in effector-independent kinase activity compared with normal controls. The C1 domain also contains two cysteine-rich zinc finger sequences that form the diacylglycerol or phorbol ester binding site. Early experiments using a [3H] PDBu radioligand revealed that PKC isozymes bind phorbol esters with high affinity in the presence of phosphatidylserine and that DAG and phorbol esters bind to the same site. The first implication that cysteine-rich domains act as phorbol ester binding sites originated from experiments performed in Nishizuka's laboratory (Ono et al., 1989), in which either deletion of those motifs in PKCγ or mutation of conserved cysteines resulted in a loss of phorbol ester binding. Each cysteine-rich domain in PKC folds into a globular structure. Phorbol esters bind in a groove formed by pulling apart two β-sheets.

The C2 domain contains the calcium-binging site. PKCs without a C2 domain (novel or atypical PKCs) or PKCs with a mutation in the C2 domain do not require calcium for kinase activity or phorbol binding. A great number of proteins containing C2 domains have been identified to date. Most of them are related to signal transduction mechanisms or membrane trafficking. Structural analysis has revealed that all C2 domains fold similarly into a structure consisting of two four-stranded antiparallel β-sheets connected by variable loops at the end of each strand, with the calcium binding site located at one end of the domain. The calcium domain acts as a membrane-docking module, where the calcium ions and basic residues contribute to electrostatic membrane binding. The

catalytic domain of PKC isozymes includes the C3 and C4 domains. The C3 domain possesses the binding site for ATP, the C4 domain possesses the binding site for substrates. It is thought that PKC is maintained in the inactive state by the pseudosubstrate occupation of this site. Detailed structural information is not available for the PKC kinase domain; however, it is known that the regulatory catalytic domain is separated by a hinge region (V3). [Proteolytically generated kinase domain protein kinase M (PKM)]

Regulation of PKC Activity by Cofactors   Experiments using mixed micelles or lipid bilayers have determined that acidic phospholipids are efficient cofactors for PKC activation, with PKC having a remarkable selectivity for phosphatidylserine. DAG causes a dramatic increase in the affinity of cPKCs and nPKCs for phosphatidylserine. According to the accepted model of PKC activation by lipids, the binding of DAG (or phorbol esters) in the presence of the phospholipid cofactors induces a conformational change in PKC that results in the removal of the pseudosubstrate from its binding site and in the activation of the enzyme. It is believed that the cysteine-rich and C2 domains are not the only regions involved in phospholipid binding. The pseudosubstrate domain, once removed from its binding site, may also contribute to membrane binding through its basic residues. Membrane association is reflected as a shift in the subcellular localization or 'translocation' of cytosolic PKC to membrane compartments in cellular systems, a process that is also tightly controlled by protein-protein interactions. The association to membranes and activation of kinase activity are differentially regulated by the cation, and the concentration of calcium required for membrane binding is substantially lower than that required for activation. The model postulated by Newton (Keranen and Newton, 1997) suggests that low concentrations of the cation promote weak membrane interactions, which are accompanied by conformational changes that are insufficient to promote the activation of the enzyme. Higher calcium concentrations, however, produce

a conformational change in PKC that results in the release of the pseudosubstrate from its binding site in the catalytic domain, leading to enzyme activation.

PKC Binding Proteins Research from the past 10 years has made it clear that in addition to binding to lipids, PKC can also interact with proteins via protein-protein interactions. It was believed that these interactions play an important role in the localization and function of PKC isozymes. PKC in an active conformation will bind to receptors for activated C kinase (RACKs) or substrates that interact with C kinase (STICKs). Inactive PKCs will interact with a kinase anchoring proteins (AKAPs) and 14-3-3. Hence, PKC binding proteins may or may not be PKC substrates. Such proteins serve many functions including localizing inactive (AKAPs) or active (RACKs) PKC isozymes to specific intracellular sites or serving as substrates (STICKs), shuttling proteins (RACK1), PKC activators, or PKC inhibitors.

RACKs were first characterized as Triton-X-100 insoluble proteins that bind PKC isozymes only in the presence of PKC activators. Because a PS bridge should not be sufficient for binding of PKC to these RACKs, it was proposed that the association involved direct protein-protein interaction. Moreover, PKC binding to RACKs should not be inhibited by a substrate peptide, indicating that anchorage does not reflect binding of the catalytic site on PKC to a phosphorylation site on these proteins. The PKC-RACK interaction is mediated, at least in part, by the C2 region in cPKCs and the C2-like region (within the V1 region) in nPKCs (Mochly-Rosen et al., 1992; Johnson et al., 1996; Csukai et al., 1997; Hundle et al., 1997; Yedovitzky et al., 1997; Zhang et al., 1997; Ron et al., 1999). Two RACKs have now been identified by using overlay assays: RACK1, a 36 KDa protein, which specifically interacts with PKCβII (Ron et al., 1994; 1995) and RACK2 (β'-COP), which specifically interacts with PKCε. Neither RACK1 nor RACK2 is a PKC substrate, but both increase PKC phosphorylation of substrates (Ron et al.,

1994; Csukai et al., 1997), suggesting that the PKC-RACK complex may be the active form of the enzyme *in vivo*. It was reported that RACK1 exhibits a translocation response to PKC activation. RACK1 translocates to the same site as activated PKCβII and specifically associates with this isozyme upon activation. These findings suggest a potential role for RACK1 as a PKC shuttling protein. A εPKC-selective RACK, RACK2, has also been identified by expression cloning using a fragment of εPKC that contains the RACK binding site. It selectively binds εPKC colocalized only with activated εPKC (and not other isozymes) to cross-striated structures, the perinucleus, and cell-cell contacts in cardiac myocytes. Prekeris et al. (1996) found that εPKC, and not other PKC isozymes, binds to filamentous actin (F-actin) *in vitro* and in synaptosomes. Because only the activated form of εPKC binds, F-actin appears to have the characteristics of a εRACK. Blobe and collaborators (1996) have found that, *in vivo* and in three different cell lines, F-actin results in stimulation of βIIPKC but not βIPKC. Binding to F-actin results in the stimulation of βIIPKC which displays altered substrate specificity when bound to F-actin. These data suggest that F-actin may also have βIIRACK characteristics. Whether both ε and βIIPKC bind to F-actin in the same cells and whether their binding is competitive remain to be determined.

STICKs require phosphatidylserine for interaction with PKC and they are PKC substrates. Phosphorylation of STICKs regulates their association to PKC. STICKs are involved in a variety of functions. For example, adducin, which is identified as a STICK, is a cytoskeletal protein involved in the interaction between actin and spectrin (Fowler et al., 1998). Clone 72, which is another STICK and a major PKC binding protein in REF52 fibroblasts, is involved in cytoskeleton remodeling and cell growth (Chaplin et al., 1996). Another STICK is the serum deprivation response protein (Sdr) that binds and localizes PKCα within the microdomain of caveolae (Mineo et al., 1998).

23

Scaffolding proteins can enable signaling proteins to cluster. This allows a tight control of cellular pathways and cross talk between different cascades. Scaffolding proteins include caveolin (Mineo et al., 1998; Oka et al., 1997), AKAPs (Klauck et al., 1996), p62/ZIP (Puls et al., 1997), INAD (Xu et al., 1998), and 14-3-3 (Xiao et al., 1995; Meller et al., 1996). Each of these proteins has the ability to cluster PKC to specific intracellular sites. PKC scaffolding proteins bind to PKC in its inactive conformation.

Syndecan-4, another PKC interacting protein, is a transmembrane matrix binding proteoglycan. The cytoplasmic tail of syndecan-4 interacts with the kinase domain of PKCα, resulting in the localization of PKCα to focal contacts and in the activation of the isozymes (Oh et al., 1997A; and 1997B). Syndecan-4 can also be phosphorylated in response to PKC activation (Horowitz et al., 1998). The phosphorylation status of syndecan-4 does not affect its binding to PKCα, although it regulates its activity (Horowitz et al., 1998).

Cytoskeletal proteins interact, in part, with PKC in an isozyme-selective pattern. Examples of this isozyme specificity are PKCζ which associates with tubulin via the pseudosubstrate region (Garcia-Rocha et al., 1997), and PKCε which specifically binds F-actin via an actin-binding site within the C1 region (Prekeris et al., 1998). F-actin activates PKCε in the absence of phospholipids (Prekeris et al., 1998). PKCβII (but not PKCβI) also interacts with the F-actin cytoskeleton upon activation. PKCβII selectively phosphorylates actin, although actin is a poor substrate. The interaction of PKCβII with actin results in a significant increase in autophosphorylation and in an alteration in substrate specificity. It is thought that the interaction between PKCβII and actin protects PKC from degradation and down-regulation (Blobe et al., 1996).

By using an overlay technique and screening of an expression library, Jaken and collaborators (Hyatt et al., 1994) have identified several additional PKC binding proteins. These proteins are all substrates of PKC and bind PS directly. A PS bridge between the binding proteins and PKC has been suggested to mediate this binding. These PKC binding proteins include talin and vinculin, myristoylated alanine-rich C-kinase substrate, a β-adducin homolog, AKAP 79, clone 72, and a related gene product, gravin/AKAP250. The finding that PS alone is sufficient for binding of PKC to these binding proteins suggests that full activation of PKC is not required. Furthermore, they found that αPKC, for example, localizes to focal contact structures, where talin and vinculin are found in nonstimulated fibroblasts and in cultured renal cells. Activation by phorbol esters results in αPKC translocation away from these proteins, as shown by cell fractionation.

There is a proposed model for PKC binding to its anchoring proteins (Daria and Gorgen, 1998). In this model inactive PKC is depicted as a folded rod with the pseudosubstrate autoinhibitory sequence at the amino terminus associated with the substrate site in the catalytic domain (House and Kemp, 1987). Those proteins that anchor inactive C-kinase are referred to as receptors for inactive C-kinase isozymes, or RICKs. In the presence of PKC activators, the rod unfolds and the RACK binding site becomes exposed, resulting in binding of PKC to its RACK. RACK- bound PKC is shown with the substrate binding site exposed and the RICK binding site unavailable for binding. Although there are no direct experiments indicating an ability of RICKs and RACKs to associate with PKC, concomitantly, immunofluoresence data and the inhibition of binding to at least some putative RICKs in the presence of phorbol ester suggest exclusive binding of the enzyme either to RICKs or to RACKs (Yao et al., 1997). This scheme also reflects the findings that although there is a PS bridge between RACK and PKC there is also direct protein-protein interaction (Mochly-Rosen et al., 1991).

PKC Expression and Translocation Different cell types express their own unique complement of PKC isoforms (Dekker and Parker, 1994). Within a cell type, PKC may be involved in the regulation of a variety of different cell functions. PKC isoforms identified in vascular smooth muscle (α, β, ε, δ, ζ) (Andrea et al., 1992) are thought to play key roles in such functions as cell proliferation and differentiation (Montesano and Orci, 1985) and contractile activity (Rasmussen et al., 1987). The expression of multiple isoforms regulating diverse functions within a single cell type suggests that individual isoforms phosphorylate specific substrate(s) and that overlap of PKC isoform activity may be limited under physiological conditions (Mochly-Rosen 1995; Mochly-Rosen et al., 1991). This, in turn, would necessitate strict PKC isoform compartmentalization and/or regulatory control of enzyme activation. The spatial separation of individual isoforms in the stimulated cell is an important mechanism determining substrate specificity. Hence, the regulation of PKC activation and its translocation to isoform-specific sites are presently areas of intense research interest.

Prior to stimulation of the cell, the inactive form of PKC is thought to be diffusely distributed throughout the cytosol or to be localized to specific regions or structures of the cell. Following cell stimulation, PKC isoforms may translocate from inactive pools to their active cell loci. Hence, the intracellular translocation of PKC may represent a major mode of control of isoform function: the targeting of specific isoforms to discrete cell loci would determine access to substrate. It was originally thought that upon cell stimulation, conventional, novel and atypical subgroups of PKC isoforms underwent obligatory translocation to the cell membrane thereby allowing access to lipid co-factors required for enzyme activation. More recent evidence, however, indicates that PKC isoforms may translocate to a variety of subcellular structures including membrane vesicles, perinuclear/nuclear structures, and the cytoskeleton. Colocalization studies have indicated extensive association of different PKC isoforms with components of the actin

microfilament (Murti et al., 1992; Allen and Adarem, 1995), microtubules (Lehtich and Forrest, 1994), and intermediate filaments (Omary et al., 1992; Owen et al., 1996) of the cytoskeleton in different cell types. Recent interest has focused on the role of PKC as a regulator of cytoskeletal function. Activation of PKC results in the phosphorylation of an array of cytoskeletal proteins (Keenan et al., 1998) and is thought to regulate changes in cytoskeletal structure and organization (Hoshi et al., 1987; Inagaki et al., 1988; Chou et al., 1990; Murphy et al., 1993).

Several laboratories have reported that the isoform PKCα is translocated from the cytosol to the plasmalemma in isolated vascular smooth muscle cells (Khalil et al., 1994; Jensen et al., 1996; Haller et al., 1998) and in intact vascular smooth muscle strips (Haller et al., 1990). Haller and coworkers (Haller et al., 1996) have shown that PKCα is translocated from the cytosol to the nucleus in endothelial cells in response to stimulation by a variety of hormones and growth factors. They have further demonstrated (Haller et al., 1998) that passaged vascular smooth muscle grown on fibronectin exhibited PKCα accumulation at both the nucleus and at membrane focal adhesions. Taken together, these results suggest that the translocation signaling movements of a specific isoform are not fixed but may vary significantly with the cell type, cell environment, the stimulus employed, and other factors, possibly including the differentiation state of the cells studied. Plasticity of PKC translocation signaling between cell compartments would be expected to greatly expand the potential range of target substrates and cell functions of individual isoforms.

A7r5 Cell Line   The A7r5 cell line is an embryonic smooth muscle cell line with adult-like characteristics (Kimes and Brandt, 1976). The A7r5 clonal cell line was originally derived from an embryonic rat aorta. A7r5 cells show expression and promoter activity of several highly restricted smooth muscle markers: smooth muscle α-actin, smooth

muscle calponin, smooth muscle myosin heavy chain, tropoelastin, and SM 22 alpha

mRNA which is found exclusively in smooth muscle and is considered one of the earliest

makers of differentiated smooth muscle (Firulli et al., 1998). A7r5 cells are characterized

by an inability to proliferate in serum-free medium, the absence of PDGF-B mRNA and

the ability to contract in culture. Thus, it is concluded that A7r5 cells represent a

transcriptionally differentiated smooth muscle. A7r5 cells also showed high transfection

efficiency compared with other smooth muscle cell lines. All these characteristics of

A7r5 cells make it an excellent *in vitro* model system for smooth muscle research. Their

comparatively slow growth, however, may represent an obstacle for the derivation of

stably transfected cell lines (Firulli et al., 1998).

II Methods

Cell Culture

A7r5 cells, derived from the embryonic rat aorta and exhibiting an adult smooth muscle phenotype, were obtained from American Type Culture Collection (Manasass, VA) and cultured in Dulbeccos modified Eagles medium (DMEM) that was supplemented with 10% fetal bovine serum, 100 units/ml penicillin G, and 100 μg/ml streptomycin. Cultures were maintained in a humidified atmosphere of 5% CO_2 in air at 37°C. The medium was changed every 2 days and cells were passaged at least once a week by addition of trypsin/EDTA solution in HBSS.

PKCα-EGFP Plasmid Constructs

A PKCα-EGFP expression plasmid was constructed by inserting PKCα cDNA into pEGFP-C2 vector (Fig. 3).

PKCα cDNA Digestion: PKCα cDNA in the SRD vector obtained from Dr. Ohno (1987; Department of Molecular Biology, Yokohama City University School of Medicine, Yokahama, Japan) was removed using an EcoRI restriction enzyme. To digest PKCα cDNA, 1.0 μl 10X buffer, 8.5 μl of the PKCα plasmid and 0.5 μl EcoRI were mixed in a reaction centrifuge tube. EGFP vector was also digested with the EcoRI: 1.0 μl 10X buffer, 8.5 μl of the EGFP plasmid, and 0.5 μl EcoRI. The two samples were incubated at 37°C for 1 hour for reaction and inactivated at 65°C for 20 minutes. The sample was run on the gels and appropriate band cut out for purification of the PKCα and for ligation of EGFP cDNA.
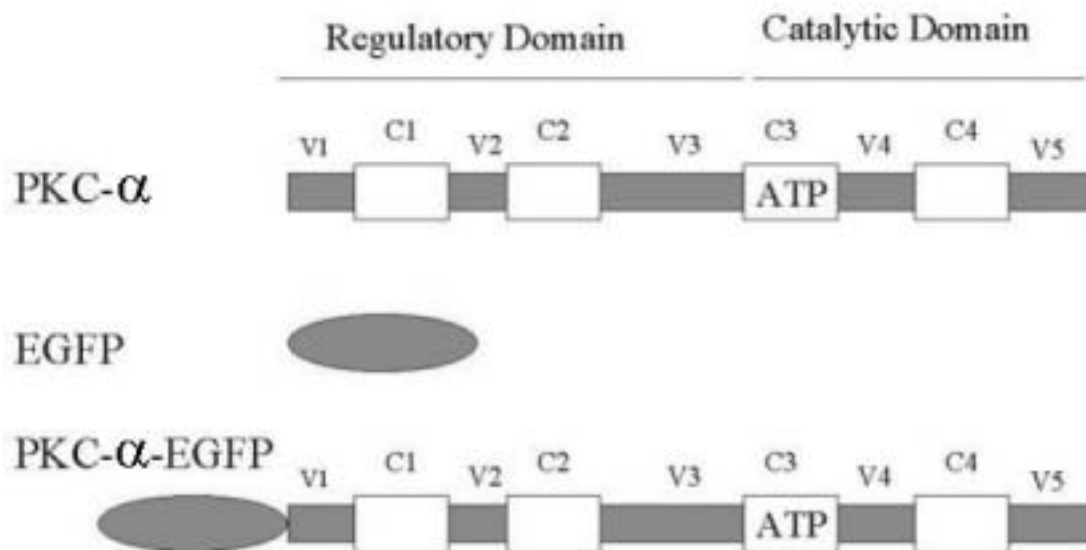
Figure 3.
Construction of the PKCα-EGFP fusion protein. The full length PKCα cDNA
without the stop codon was inserted into the EcoRI site of the pEGFP-C2 vector
downstream of EGFP. The EGFP was ligated to the V1 domain at the N-
terminus of PKCα cDNA.

PKCα and EGFP Ligation: The PKCα cDNA was ligated into the pEGFP-C2 vector (Clontech, Palo Alto, CA) downstream of EGFP at the EcoRI site. Five μl PKCα DNA (~ 150μg) and 3μl EGFP DNA (~ 100μg) were mixed with 1μl 10X buffer and 1μl T4 ligase. This solution was incubated at 16 °C overnight. The sample was then heated at 70 °C for 10 minutes to inactive the ligase reaction. The sample was added to 200μl XL-1 blue competent bacteria (Stratagene: La Jolla, CA) in a microcentrifuge tube, incubated on ice for 30 minutes, mixed with 800μl LB media (10g/L Bacto peptone, 5g/L yeast extract, 85.5mM NaCl, pH 7.4) and incubated at 37 °C for 1 hour. The transformed bacteria (200μl) were spread on agar plates which containing kanamycin (50 μg/ml) antibiotic, and incubated at 37 °C overnight. Purification of the PKCα-EGFP DNA was done by Wizard miniprep columns (Promega, WI) following the manufacturer's instructions.

DNA Sequencing: Correct orientation of PKCα-EGFP fusion protein cDNA was determined by restriction digestion and DNA sequencing. A total of eight samples were initially tested here by BamH1 restriction enzyme cleavage. Based on the BamH1 cleavage site, the correct constructs were expected to yield two fragments of 2.1Kbp and 5.5Kbp. A possible reversed orientation was expected to produce fragments at 0.8Kbp and 6.8Kbp. The correct constructs, identified from restriction enzyme digestion, were further subjected to DNA sequencing to confirm that the inserted DNA was ligated in the exact reading frame. Nucleotide sequences were determined by the dideoxy chain termination method (Sanger et al., 1977) using a Sequenase 2.0 sequencing kit (Amersham; Arlington Hts, IL), following the manufacturer's instructions. The resulting plasmid, PKCα-EGFP, contained PKCα fused in frame downstream of EGFP.

31

Cell Transfection

Cells were seeded at a density of 4 x 10^6 cells/100 mm culture dish and transfected with 12 to 18 μg of plasmid using lipofectamine (Life Technologies; Gaithersburg. MD), according to the manufacturer's standard protocol. During the course of the project, two different plasmids were used to transfect A7r5 cells: PKCα-EGFP and a β-actin-EGFP expression plasmid (Clontech, Palo Alto, CA). First, 12 to 18 μg of plasmid were diluted in 600 μl serum-free and antibiotic-free DMEM medium (solution A) while 30 μl lipofectin were diluted in 600 μl serum-free and antibiotic-free DMEM medium (solution B). Both solutions were incubated at room temperature for 30 minutes, and then combined and incubated at room temperature for an additional 30 to 45 minutes after which 4800 μl serum-and antibiotic-free medium were added to the mixed solution. Cells were rinsed with 6 ml serum-and antibiotic-free medium and then overlaid with the DNA-lipofectin solution. They were then incubated in a humidified atmosphere of 5% CO_2 in air at 37°C for 10 hours, after which they were returned to complete medium containing 10% serum. Fluorescence indicating expression of fusion protein, was typically detected within 2 days. Experiments were performed within 3 or 4 days after transfection.

Immunostaining of A7r5 Cells

A7r5 cells were fixed and permeabilized by the addition of ice-cold acetone for 1.0 minute. They were then washed with phosphate-buffered saline (PBS) containing 0.5% TWEEN-20 (PBS-T; pH 7.5) and incubated for 10 minutes in blocking solution (5% nonfat dry milk in PBS-T). For PKCα staining, the fixed cells were incubated with a

1:1000 dilution of monoclonal anti-PKCα antibody (UBI, Lake Placid, NY) for 30

minutes at room temperature, washed in PBS-T, and then incubated with Alexa 488-

labeled anti-mouse secondary antibody (Molecular Probes, Eugene, OR) for 30 minutes.

For PKCα/microtubule or PKCα EGFP/microtubule colocalization experiments, PKCα

was visualized with an Alexa 594-labeled secondary antibody (Molecular Probes,

Eugene, OR). A FITC-labeled anti-β-tubulin primary antibody (Sigma, St. Louis, MO)

was utilized for visualization of microtubules. For α-actin staining, cells were incubated

in a 1:1000 dilution of monoclonal anti-α-smooth muscle actin clone 1A4 FITC-labeled

antibody (Sigma Chemical Co., St. Louis, MO) for 30 minutes at room temperature. For

F-actin staining, the fixed cells were incubated with 2.5μM TRITC-labeled phalloidin

(Sigma Chemical Co., St. Louis, MO) for 30 minutes at room temperature. For alpha-

actinin and talin staining, the fixed cells were incubated with a 1:1000 dilution of

monoclonal anti-α-actinin (Sigma Chemical Co., St. Louis, MO) and anti-talin antibody

(UBI, Lake Placid, NY) for 30 minutes at room temperature, washed in PBS and then

incubated with Alexa 488-labeled anti-mouse secondary antibody (Molecular Probes,

Eugene, OR) for 30 minutes. Nonspecific binding was determined by incubating cells

with secondary antibody in the absence of primary antibody or by mixing the primary

antibody with an excess of purified PKCα protein prior to incubation with cells.

Confocal Microspcopy

For fixed cells, the coverslips were mounted on a Nikon Diaphot microscope and

confocal microscopy was performed with a BioRad Model 1024 scanning system at 488

nm krypton/argon excitation using a 515 nm long pass barrier filter. This included

experiments with PKCα-EGFP transfected cells, PKCα, α-actin, talin, and α-actinin antibody stained cells and phalloidin stained cells. For colocalization studies, confocal microscopy was performed at 633 nm krypton/argon excitation using a 665 nm red glass filter with cells immunostained for PKCα or at 488 nm krypton/argon excitation using a 515 nm long pass barrier filter in studies with PKCα-EGFP transfected cells or cells stained for β-tubulin. Final micrograph images were built by projecting serial Z-plane image acquisitions and were analyzed using Lasersharp and Confocal Assistant Software (BioRad, Hercules, CA).

Prior to observation, live A7r5 cells were plated onto 25 mm circle glass coverslips one day before the experiments. Dynamic change of PKCα-EGFP transfected cells or β-actin-EGFP transfected cells was observed by utilizing the BioRad Model 1024 scanning system at 488 nm krypton/argon excitation using a 515 nm long pass barrier filter. Each experiment was performed a minimum of three times with at least 30 cells from fixed preparations and 4 to 6 cells from live preparations evaluated per experiment. Results were confirmed by at least two observers and phenomenon were judged significant if observed in 70% or more cells.

Cell Treatments:

A. Concentration-Dependent Phorbol-Induced PKCα Translocation:

Translocation of PKCα was induced by the addition of phorbol 12, 13 dibutyrate (PDBu) to the incubation medium at final concentrations ranging from 10^{-5}M to 10^{-9}M. Unless stated otherwise, images were obtained at 10 minutes after cell activation with PDBu. The microtubular cytoskeleton was disrupted by the addition of colchicine (40 μg/ml)

and The actin cytoskeleton was disrupted by addition of cytochalasin B (1 µg/ml) to the medium 20 minutes prior to PDB (10^{-6}M to 10^{-8}M) stimulation.

B. Multi-Agonists-Induced PKCα Translocation:

In studies of live cell preparations, cells were stimulated by phorbol 12, 13 dibutyrate (PDBu, 10^{-8} M), thapsigargin (10^{-5}M), A23187 (10^{-5}M), angiotensin II (10^{-6}M) or potassium (10^{-2}M) addition to the incubation media. The PKC inhibitor staurosporine (10^{-8} M) or a calcium chelator cocktail (EGTA, 10^{-3}M; BAPTA-AM, 10^{-5}M) was added to the medium 15 minutes prior to additions of contractile agents. Colchicine (40 µg/ml) and cytochalasin B (1 µg/ml) were added to the medium 20 minutes prior to PDBu stimulation. In experiments using calcium-free medium, cells were washed (2X) with calcium-free medium and then incubated in calcium-free medium for an hour before addition of PDBu and A23187.

C. Actin Remodeling Experiments:

Actin cytoskeletal reorganization was studied in A7r5 cells contracted by additions of 2 x 10^{-5}M A23187 and 2 x 10^{-6}M thapsigargin (Sigma Chemical Co., St. Louis, MO). In experiments examining the effect of these agents on phorbol ester-induced cytoskeletal remodeling, cells were activated by additions of 10^{-8}M phorbol 12, 13 dibutyrate (PDBu) at either 30 minutes before or 20 minutes following the additions of A23187 and thapsigargin to the medium. In order to determine the effect of calcium-free conditions on remodeling, cells were washed twice with and then incubated in Ca^{2+}-free DMEM (Gibco BRL Products, Life Technologies, Rockville, MD) for 1 hour before the addition of agonists. In a final series of experiments, we examined the effects of 6 different protein kinase inhibitors (Table 1) on A23187/thapsigargin-induced α-actin

depolymerization. Each kinase inhibitor was added at 10X its published IC_{50}

concentration 30 minutes prior to the addition of the agonists. Each experiment was

conducted a minimum of three times with the results verified by two observers. Unless

stated otherwise, conclusions were based on the observation that at least 80% of the cells

exhibited the phenomenon.

Table 1. Six different kinase inhibitors were studied in actin remodeling experiments.

Inhibitor	Target Kinase
Staurosporine	General kinase
Bisindolymaleimide I	PKC
H-89	PKA
ML-7	MLCK
KN-93	CaMK II
Genistein	Tyrosine Kinase

Verification of Effective PKCα-EGFP Transfection

After being washed twice with phosphate-buffered saline solution (PBS), A7r5 cells were collected at 3 days post-transfection by scraping with a rubber spatula followed by centrifugation. The harvested cells were suspended in 150 µl of lysis buffer (10 mM Tris, pH 7.4; 1 mM EDTA, 1 µg/ml leupeptin, 1 µg/ml pepstatin, 50 µg/ml aprotinin, 0.5 mM phenylmethylsulfonyl fluoride (PMSF), and 1% glycerol). Protein concentration was determined by the BCA (Pierce) protein assay. Equal amounts of protein samples were electrophoretically separated on 10% SDS-PAGE. The resolved bands were electrophoretically transferred to a nitrocellulose membrane (Amersham, Piscataway, NJ). The membrane was incubated with blocking solution (5% nonfat dry milk in PBS) for 2 hours, repeatedly rinsed with PBS, and then further incubated in a 1:1000 dilution of either monoclonal anti-PKCα (UBI, Lake Placid, NY) or anti-EGFP (Clontech, Palo Alto, CA). The blot was washed 3 times in PBS/0.5% Tween and then incubated one hour incubation with rabbit anti-mouse horseradish peroxidase-conjugated secondary (Sigma Chemical Co., St. Louis, MO). Reactive bands were visualized by the ELC-enhanced chemoluminescence method (Amersham).

Immunoprecipitation of PKCα and EGFP

As an initial step in the kinase activity determinations the PKCα-EGFP and PKCα proteins were immunoprecipitated for assay. Control A7r5 cells and A7r5 cells transfected with PKCα-EGFP were harvested from 100 mm culture dishes into 2 ml of ice-cold lysis buffer [250 mM NaCl, 25 mM Tris-HC1 (pH 7.5), 5 mM EDTA, 1% Triton 100, 2 µg/ml aprotinin, 1 mM phenylmethysulfonyl fluoride (PMSF)] and homogenized

by repeated pipetting. After centrifugation at 14000 g for 10 minutes, the supernatant was divided into two aliquots for the addition of anti-PKCα monoclonal antibody or anti-EGFP monoclonal antibody. The samples were incubated at 4°C for an additional hour in a rotary mixer after which protein A was added. The samples were incubated for an additional hour at 4 °C. The samples were then centrifuged and the pellets were washed 3 times by resuspension in 2 ml of rinse buffer (lysis buffer without Triton 100). The washed pellet was suspended in 50 µl PBS for the kinase activity assay.

PKCα Activity Assays

PKCα activity was measured using the Pep Tag Assay for non-radioactive detection of protein kinase C (Promega, Madison, WI) according to the manufacturer's instructions (Fig. 4). This assay utilizes a brightly fluorescent peptide substrate that is very specific for PKC. The amino acid sequence of the PKC-specific substrate, Pep Tag C1 peptide, is P-L-S-R-T-L-S-V-A-A-K. Phosphorylation of C1 Peptide by PKC changes the peptide's net charge from +1 to −1, and this change in the net charge of the substrate allows the phosphorylated and nonphosphorylated substrate to be separated on an agarose gel at neutral pH. Phosphorylated substrate moves toward the positive electrode while the nonphosphorylated substrate migrates toward the negative electrode. Briefly, 10 µl of sample were mixed with reaction buffer (100 mM HEPES, 6.5 mM $CaCl_2$, 5 mM DTT, 50 mM Mg Cl_2, 5 mM ATP, pH 7.4), activator solution (1 mg/ml phosphatidyl serine) and Pep Tag Cl peptide. The solution was incubated at 30°C for 30 minutes. The reaction was stopped by placing the sample in a 95°C heating block for 10 minutes. The samples were electrophoresed on a 0.8% agarose gel at 100V for 20 minutes. The gel
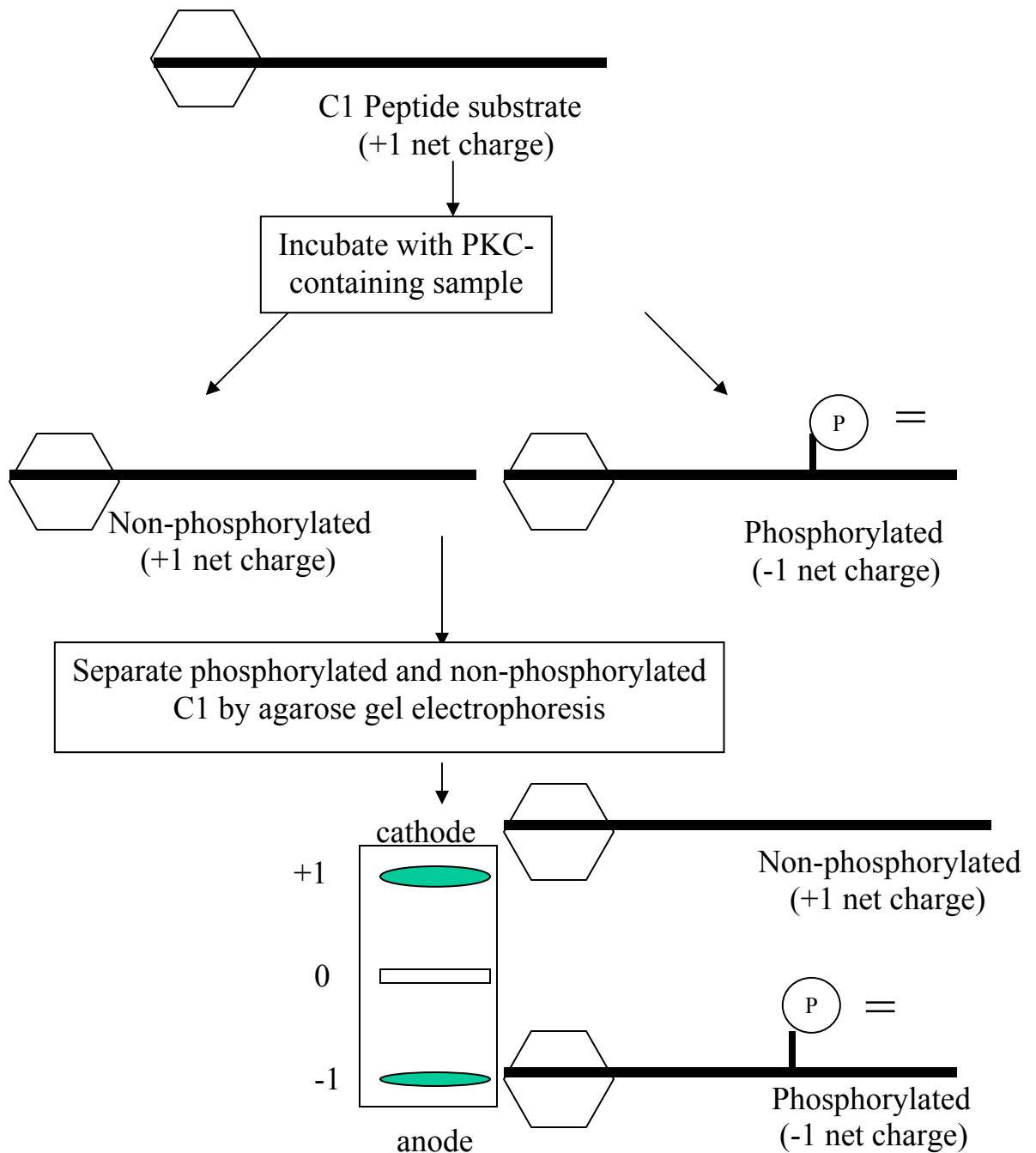
Figure 4.
Mechanism and procedure of the Pep Tag non-radioactive protein kinase assay. Two μg of Pep Tag C1 peptide were incubated as described in the standard PKC assay with PKC sample in a final volume of 25 μl for 30 minutes at room temperature. The reactions were stopped by incubation at 95°C for 10 minutes, and the samples were electrophoresed on a 0.8% agarose gel at 100V for 20 minutes. Phosphorylated peptide migrated toward the anode (+), while nonphosphorylated peptide migrated toward the cathode (-).

was photographed under UV light and the signal intensity was quantitated with a Molecular Dynamic densitometer. The activity of PKCα was normalized for the protein content of each immunoprecipitation sample and expressed as units/μg protein.

Intracellular Calcium Determination

Loading of Cells with Fura-2:

A7r5 cells were placed in a six well culture plate containing 25 mm diameter glass coverslips and allowed to grow for 1 to 2 days until they reached 70 to 80% confluency. The coverslips containing A7r5 cells were removed asceptically from the six well culture plates, rinsed with HBSS (GIBCO-BRL, NY) and then placed in a Narishige Microincubation Chamber (Narishige International USA, Inc., NY). The cells were then incubated in 1 ml HBSS containing 5 μM Fura-2AM (Molecular Probes, Inc., Eugene OR) and 0.05% w/v Pluronic F-127, a non-ionic detergent that helps to disperse Fura-2AM and thus facilitate dye loading into the cells (Molecular Probes, Inc., Eugene, OR) at 37^0C for 30 minutes. The cells were then washed three times with HBSS and incubated in HBSS for 10 min at 37^0C so as to completely hydrolyse the Fura-2AM. Prior to imaging the solution was replaced with a 1 ml fresh HBSS.

Digital Video Fluorescence Imaging:

The Narishige microincubation chamber containing Fura-2 loaded A7R5 cells on the coverslip in HBSS was placed on the stage of a Nikon Diaphot TMD inverted fluorescence microscope (Nikon Corporation, Tokyo, Japan) maintained at 37°C and equipped for ratio fluorescence microscopy. The cells were successively excited at 340 nm and 380 nm, and the fluorescence emitted at 510 nm was intensified by a

DAGE-MTI GenIISys image intensifier (DAGE-MTI, Inc., Michigan City, Indiana) and finally captured by a DAGE-MTI CCD72 video camera (DAGE-MTI, Inc., Michigan City, Indiana). The video signals from the CCD72 camera were digitized at 8 bits per pixel. The fluorescence images were acquired every 15 sec with each set representing an average of 16 video frames. The ratio images were calculated in real time by pixel to pixel division of fluorescence images obtained by 340 nm excitation to that by 380 nm excitation. Metfluor Imaging System, version 4.1.7, software (Universal Imaging Corporation, Westchester, PA) was used for image acquisition and analysis. The $[Ca^{2+}]_i$ was calculated according to equation of Grynkiewicz et al. (1985) as follows:

$$[Ca^{2+}]_i = K_D \, \beta \, (R - R_{min}) / (R - R_{max})$$

where R is ratio of Fura-2 fluorescence emission due to excitation at 340 nm divided by 380 nm excitation, R_{max} is the ratio when Fura-2 is saturated with Ca^{2+} ions (achieved by using 5 μM ionomycin), R_{min} is the ratio when Fura-2 is in the acid form (achieved by chelating intracellular calcium ions with 20 mM EGTA), β is the ratio of fluorescence of free Fura-2 in acid form divided by fluorescence of Fura-2 saturated with Ca^{2+} ions with 380 nm excitation and K_D is the dissociation constant for the binding of Fura-2 to Ca^{2+} ions (a value of 224 nM was used). The in situ calibration of $[Ca^{2+}]_i$ was performed at the end of the experiment by using 5 μM ionomycin followed by 20 mM EGTA. Finally, 50 mM $MnCl_2$ was used to completely quench the fluorescence and thus to obtain background image emission. All images were corrected for the background emission.

III   Results

Study of Concentration-Dependent Phorbol Induced PKCα Translocation

Characterization of PKCα-EGFP Fusion Protein

In order to determine if the PKCα-EGFP fusion protein was effectively expressed and

retained PKCα enzymatic properties, Western Blot and kinase activity assays were

performed on PKCα-EGFP expressing A7r5 cells. Western Blot analysis indicated PKCα

and PKCα-EGFP exhibited bands at approximately 80 kDa and 110 kDa, respectively

(Fig. 5). Visualization of cells with anti-EGFP antibody yielded a single band at

approximately 30 kD in cells transfected with EGFP vector and a single band at about

110 kD in cells transfected with PKCα-EGFP indicating little or no detectable breakdown

of PKCα-EGFP. Furthermore, significant levels of kinase activity were observed in

samples obtained both by immunoprecipitation of PKCα or EGFP (Fig. 6), indicating that

PKCα-EGFP retained enzymatic activity. Finally, colocalization studies of PKCα and

EGFP indicated identical cellular distribution of endogenous PKCα and PKCα-EGFP

both in control and stimulated cells (Fig. 7).

Translocation of PKCα in Response to Different Concentrations of PDBu

Results from experiments utilizing either standard immunostaining methods (Fig. 8) or

A7r5 cells expressing the PKCα-EGFP fusion protein (Fig. 9) were consistent in

indicating concentration-dependent effects of PDBu on PKCα translocation.

Immunostaining indicated that PKCα was diffusely distributed throughout the cell prior

to stimulation (Fig. 8A). Addition of PDBu to the medium at final concentrations of 10^{-5} M and 10^{-6}M resulted in intense immunostaining in the perinuclear/nuclear region with minor or no fluorescence seen at the cell membrane (Fig. 8 B, C). By comparison, PDBu at final concentrations of 10^{-7}M and 10^{-8}M caused significant accumulations of PKCα at the cell membrane with only slight staining noted at the perinucleus (Fig. 8 D, E). PDBu at 10^{-9}M did not result in PKCα translocation in A7r5 cells (Fig. 8 F). Similar to the results from immunostaining experiments, A7r5 cells expressing PKCα-EGFP also showed a diffuse distribution of fluorescence in unstimulated cells although discrete areas of intense fluorescence at the membrane were often noted in these control cells (Fig. 9). Addition of 10^{-6}M PDBu resulted in an obvious translocation of the fusion protein to the perinucleus, whereas 10^{-8}M PDBu caused translocation to the cell membrane (Fig. 9).

Control experiments (data not shown) in which cells were incubated with secondary antibody in the absence of primary antibody demonstrated that PKCα translocation was not influenced by nonspecific staining or autofluorescence. In addition, the addition of a 2X molar excess of purified PKCα enzyme with the primary antibody used in the present experiments resulted in the almost total blockade of immunostaining, further indicating the specificity of PKCα staining in the A7r5 cell preparation. Finally, it was shown that the addition of the inactive phorbol ester, 4α-phorbol 12, 13-didecanoate (4α-PDD) had no detectable effect on PKCα intracellular distribution (Fig.9), indicating that the translocation phenomenon observed was associated with PKC activation.

Role of the Cytoskeleton in PKCα Translocation in A7r5 Cells

Figure 10 shows the effect of colchicine treatment on the structure of the microtubule cytoskeleton of A7r5 cells. The typical A7r5 cell exhibited a pattern of dense central microtubular structure connected by distinct filaments to an extensive subplasmalemmal microtubular structure (Fig. 10A). The central microtubular structure and connecting filaments were disrupted within 10 minutes (Fig. 10 B, C) and the entire microtubular cytoskeleton was abrogated within 20 minutes after the addition of colchicine to the medium (Fig.10 D).

Disruption of the microtubules with colchicine had no significant effect on the distribution of PKCα in unstimulated cells (Figs. 11 A', 12A'). However, disruption of the microtubules by a 20 minutes treatment of colchicine consistently resulted in the blockade of PKCα translocation to the perinuclear region of cells stimulated by the addition of 10^{-6}M PDB (Figs. 11 B', 12 B'). By comparison, treatment with colchicine did not affect the peripheral translocation of PKCα induced by 10^{-8} M PDB in A7r5 cells (Figs. 11 C', 12 C').

Dual immunostaining for β-tubulin and PKCα indicated little or no direct association of PKCα with the microtubular system in unstimulated cells (Fig. 13B). Similarly, there was no evidence of colocalization of PKCα and microtubular structure in A7r5 cells stimulated by additions of 10^{-6} M PDB (Fig. 13 D) or 10^{-8}M PDB (Fig. 13 F) to initiate perinuclear and peripheral translocation, respectively.

A7r5 cells stained with TRITC-labeled phalloidin showed a system of densely packed actin stress fibers arranged in parallel and extending across the whole cell body. Treatment with cytochalasin B caused disruption of actin fibers, primarily at the central region of the cells (data not shown). Cytochalasin B had no effect on the distribution of PKCα in unstimulated cells (Fig. 14 A') and, unlike colchicine, cytochalasin B had no effect on the translocation response to either 10^{-6}M PDBu (Fig. 14 B') or 10^{-8}M PDBu (Fig. 14 C').

Colocalization of PKCα with p62 and BiP/GRP 78 in Response to 10^{-6}M PDBu

In order to determine whether PKCα was associated with the nuclear envelope or endoplasmic reticulum in response to 10^{-6}M PDBu stimulation, colocalization studies of PKCα with nucleoporin p62 and the ER marker BiP/GRP78 were performed. Data indicated some degree of colocalization of PKCα with p62 and BiP/GRP78 in unstimulated cells which appears to be increased in 10^{-6}M PDBu stimulated cells (Fig. 15).
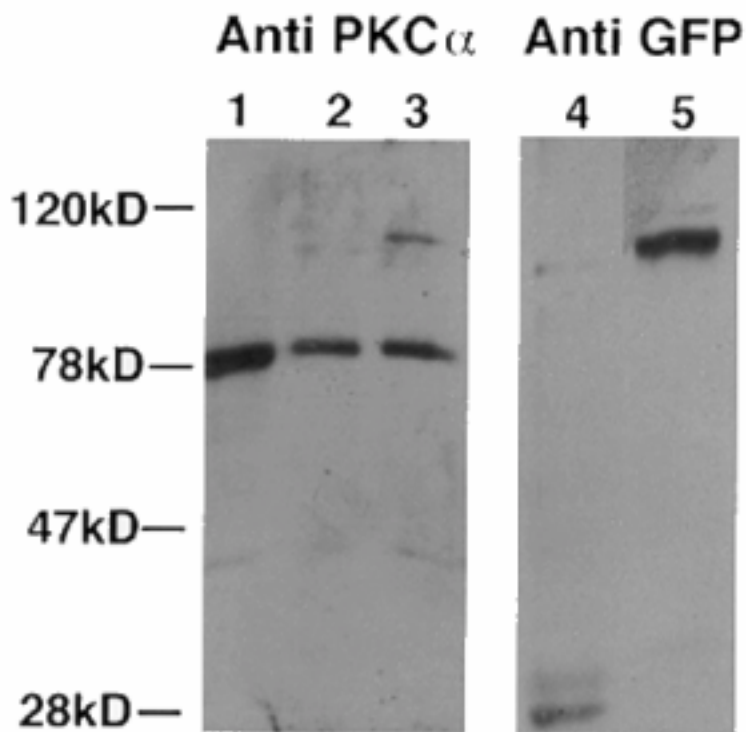
Figure 5.

Immunoblot analysis of the PKCα-EGFP fusion protein from A7r5 cells. Lane 1, rabbit brain positive control for PKCα; lane 2, control A7r5 cells; lane 3, A7r5 cells transfected with PKCα-EGFP; lane 4, A7r5 cells transfected with EGFP; lane 5, A7r5 cells transfected with PKCα-EGFP. Bands detected with anti-PKCα monoclonal antibody (lanes 1-3) indicated immunoreactivity only at 80 kDa in control A7r5 cells and at both 80 kDa and 110 kDa in cells transfected with PKCα-EGFP. Detection by anti-EGFP monoclonal antibody (lanes 4, 5) indicted immunoreactivity at approximately 29 kDa in cells transfected with EGFP (lane 4) and only at 110 kDa in cells transfected with PKCα-EGFP (lane 5) indicating insignificant degradation of the PKCα-EGFP. The figure shown is a typical of results from three individual experiments.
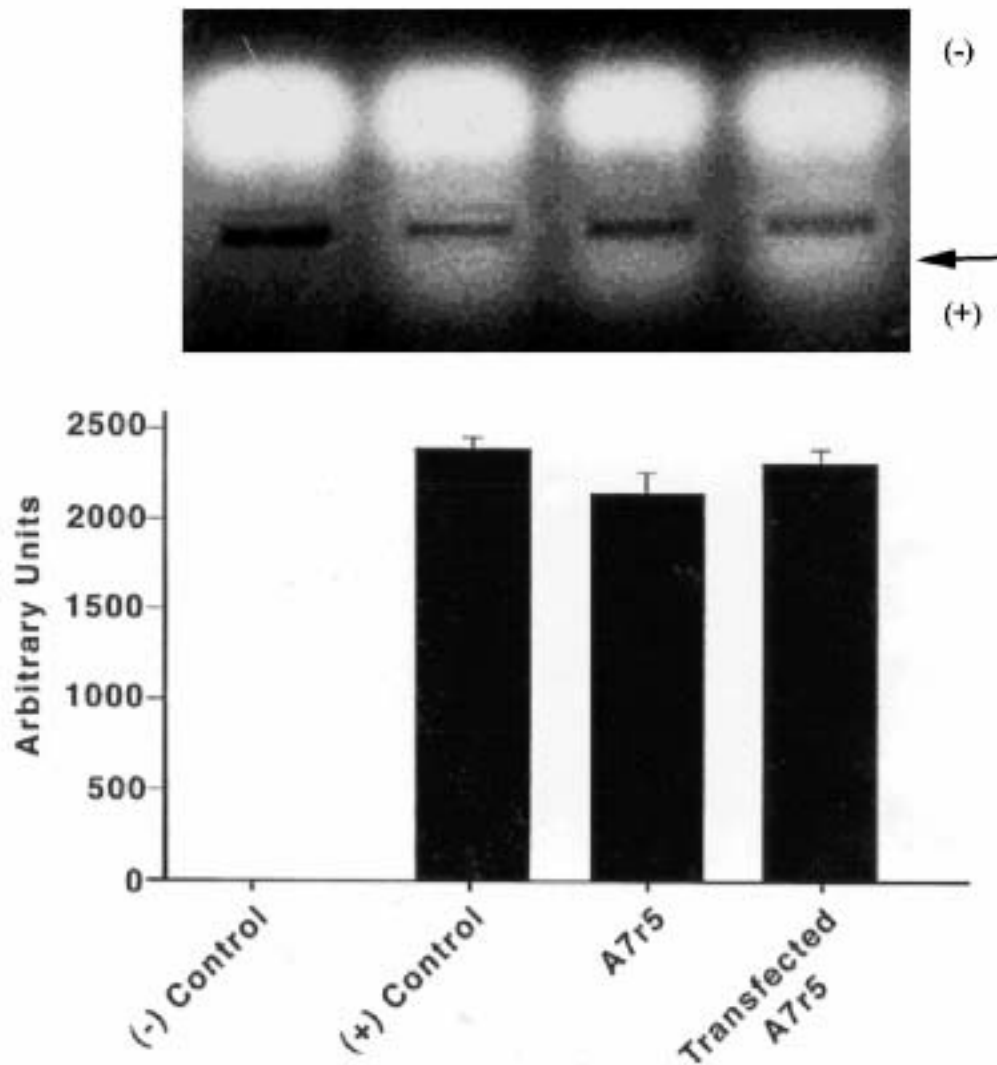
Figure 6.

PKCα kinase activity of the PKCα-EGFP fusion protein obtained from A7r5 cells. Anti-PKCα and anti-PKCα-EGFP monoclonal antibodies were utilized to immunoprecipitate PKCα and the PKCα-EGFP, respectively from A7r5 cell samples. PKCα kinase activity was then measured using the Pep Tag assay method. Precipitated samples were mixed with PKC activity reaction solution, electrophoresed on a 0.8% agarose gel, and photographed on a transilluminator under UV light. Phosphorylated peptide can be seen to migrate toward the (+) (an arrow indicates the phosphorylated peptide), while nonphosphorylated peptide migrates to the cathode (-). Positive control was purified PKCα protein while negative control contained distilled water. Results reflect the average of three individual experiments.
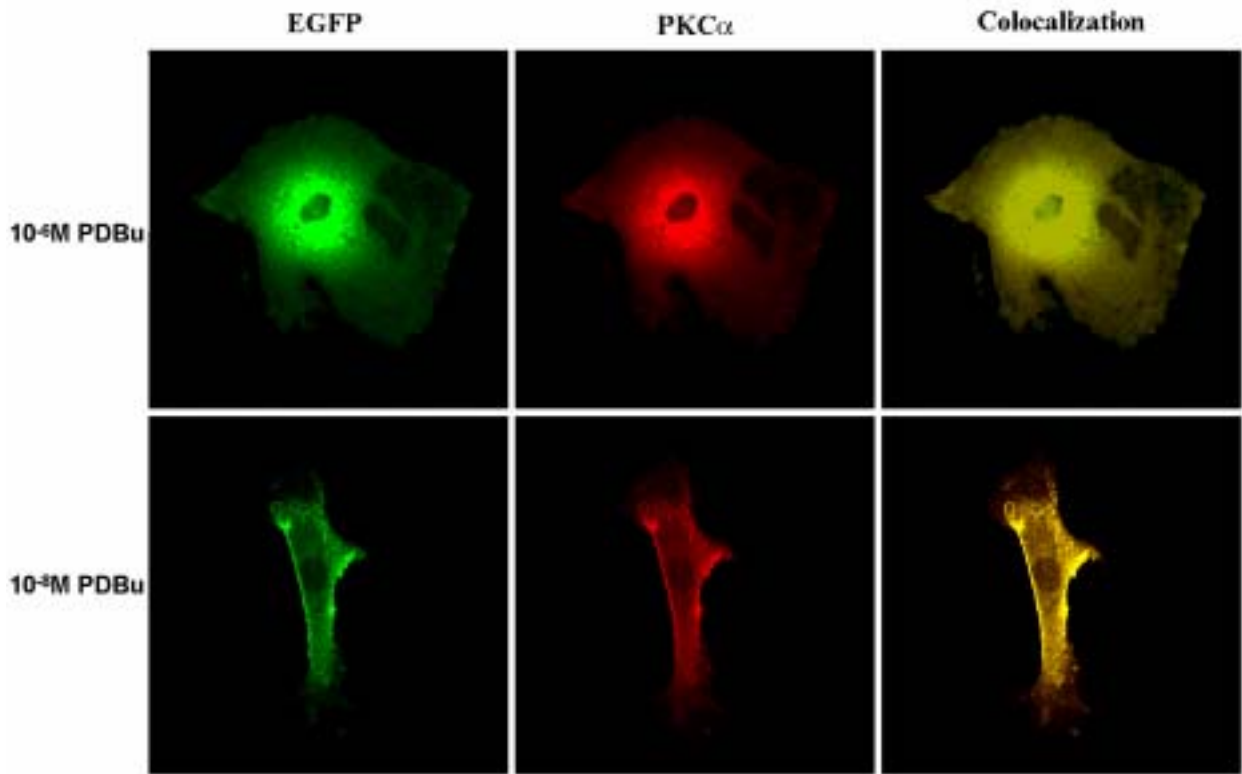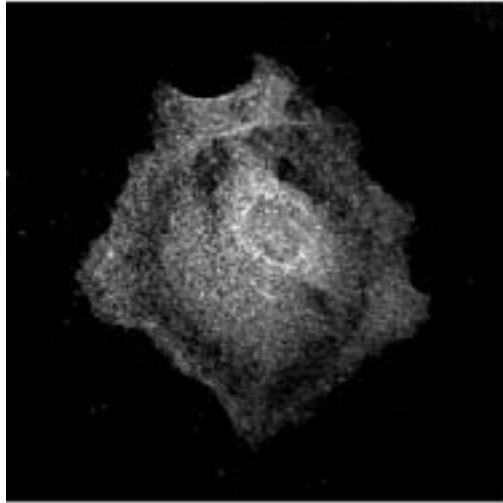
Figure 7.

Confocal micrographs showing dual imaging for PKCα and EGFP in A7r5 cells stimulated at 10^{-8} M and 10^{-6} M concentrations of phorbol 12, 13 dibutyrate (PDB). PKCα was visualized using an Alexa 594-labeled secondary antibody. Images were collected in separate channels to prevent overlap of fluorophores. Yellow color in panels at the right of the figure indicates areas of colocalization of EGFP and PKCα. Because there was no evidence of significant degradation of PKCα-EGFP, the results indicate that the fusion protein is translocated in response to cell stimulation in a fashion identical to native PKCα. Magnification was 600X. The micrographs reflect the results from 3 experiments in which a total of 88 cells were evaluated.
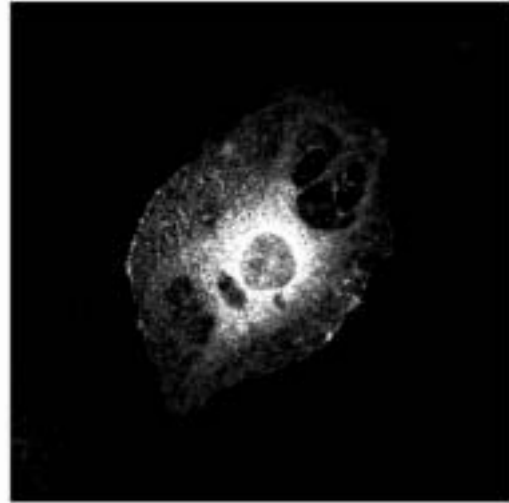
Figure 8.

Confocal micrographs showing the concentration-dependent perinuclear and plasmalemma translocation of PKCα in A7r5 at 10 minutes after exposure to vehicle (A) or PDBu concentrations of 10^{-5}M (B), 10^{-6}M (C), 10^{-7}M (D), 10^{-8}M (E), and 10^{-9}M (F). PKCα was visualized by standard immunostaining methods using unlabeled anti-PKCα primary antibody followed by Alexa 488-labeled anti-mouse IgG secondary antibody. Magnification was 600X. The micrographs reflect the results from 5 experiments in which a total of 456 cells were evaluated. It was estimated that at least 90% of cells exhibited the indicated phenomenon.
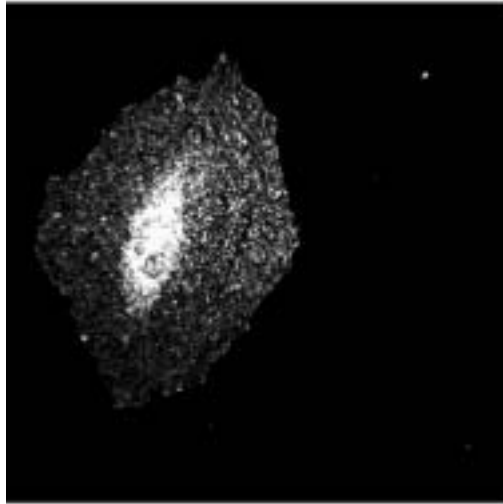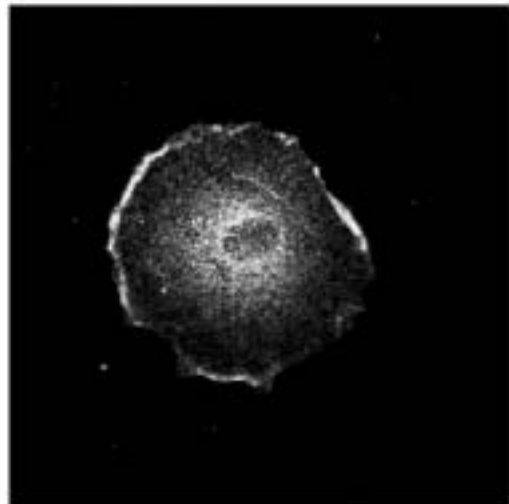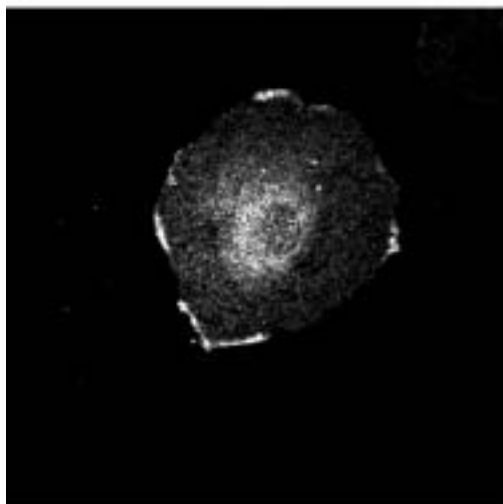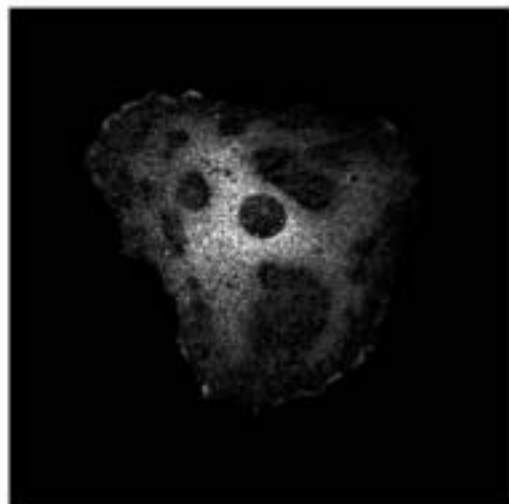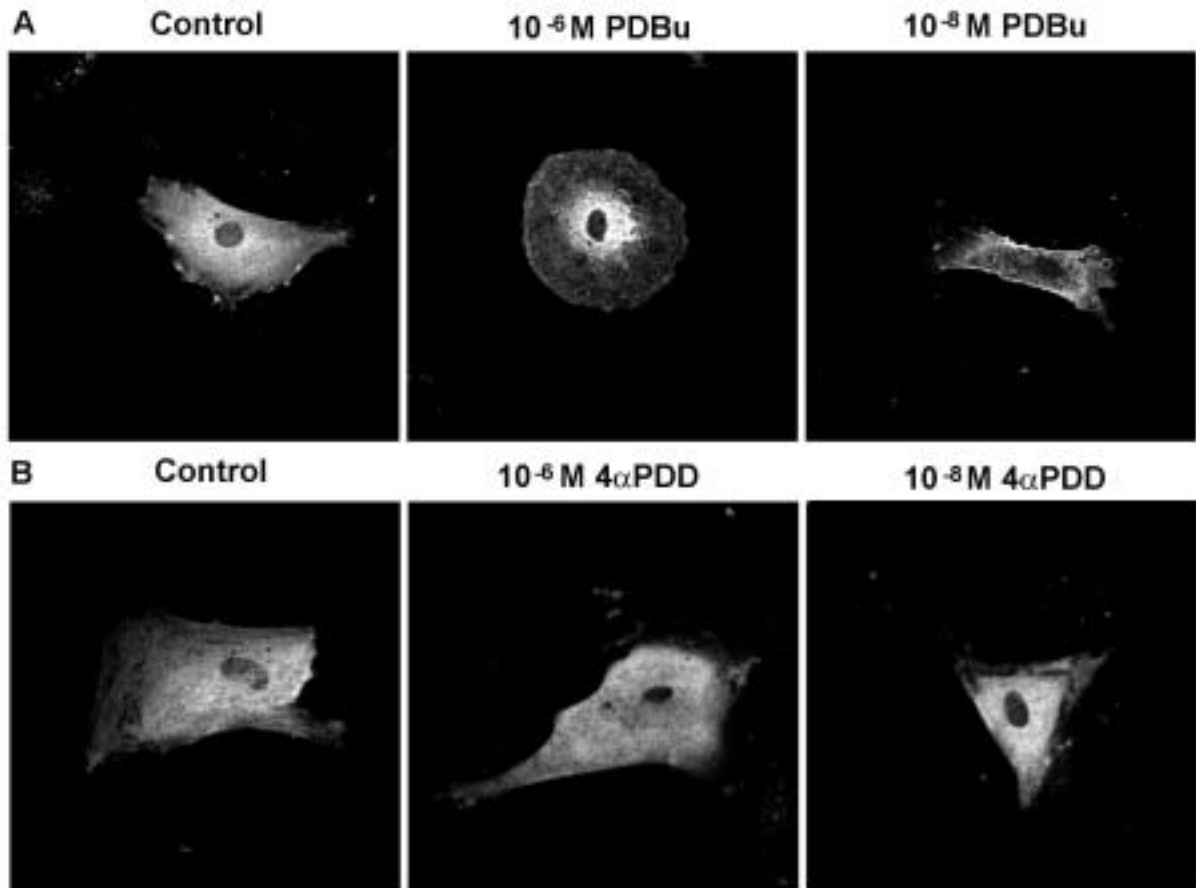
Figure 9.

Confocal micrographs showing the distribution of PKCα-EGFP fusion protein in unstimulated control A7r5 cells and in cells stimulated by the addition of 10^{-6}M or 10^{-8}M PDBu. Results are identical to those obtained with standard immunostaining in indicating that cells stimulated with 10^{-6}M and 10^{-8}M PDBu translocate PKCα primarily to the perinucleus and plasmalemma, respectively. Inactive phorbol 4αPDD had no effect on distribution of PKCα. Magnification was 600X. The micrographs reflect the results from 3 experiments in which a total of 212 cells were evaluated. It was estimated that at least 90% of cells exhibited the indicated phenomenon.

51

Figure 10. 1010.10.10.
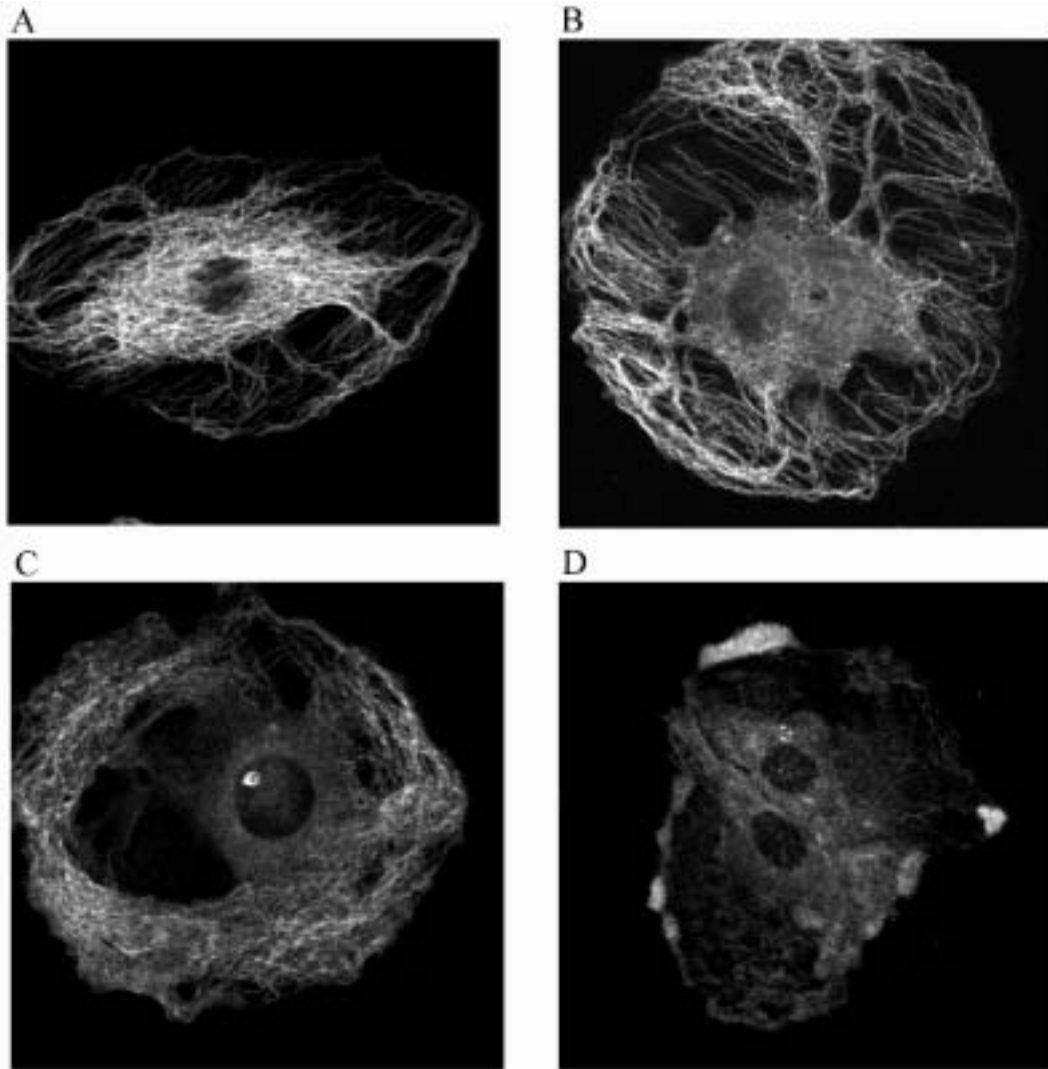
Normal A7r5 cell microtubular structure (A) and the effects of the microtubule disrupting drug colchicine on these structures at 5 minutes (B), 10 minutes (C), and 20 minutes (D) exposures. Microtubules were visualized using a FITC-labeled-β-tubulin antibody. Magnification was 600X. The micrographs reflect the results from 3 experiments in which a total of 410 cells were evaluated.

Figure 11.

The effect of treatment with colchicine to disrupt microtubules on the distribution of PKCα in unstimulated and PDBu-stimulated A7r5 cells. Control cells received vehicle (A) or additions of PDBu at 10^{-6}M (B) or 10^{-8}M (C). Treated cells were exposed to colchicine (40 µg/ml, 20 min) prior to receiving vehicle (A'), 10^{-6}M PDBu (B') or 10^{-8}M PDBu (C'). PKCα was stained with unlabeled anti-PKCα primary antibody (UBI) followed by Alexa 488-labeled anti-mouse IgG secondary antibody (Molecular Probes). Magnification was 600X. The micrographs reflect the results from 4 experiments in which a total of 428 cells were evaluated. It was estimated that an average of $87 \pm 6\%$ of cells exhibited colchicine blockade of perinuclear translocation at 10^{-6}M PDBu.
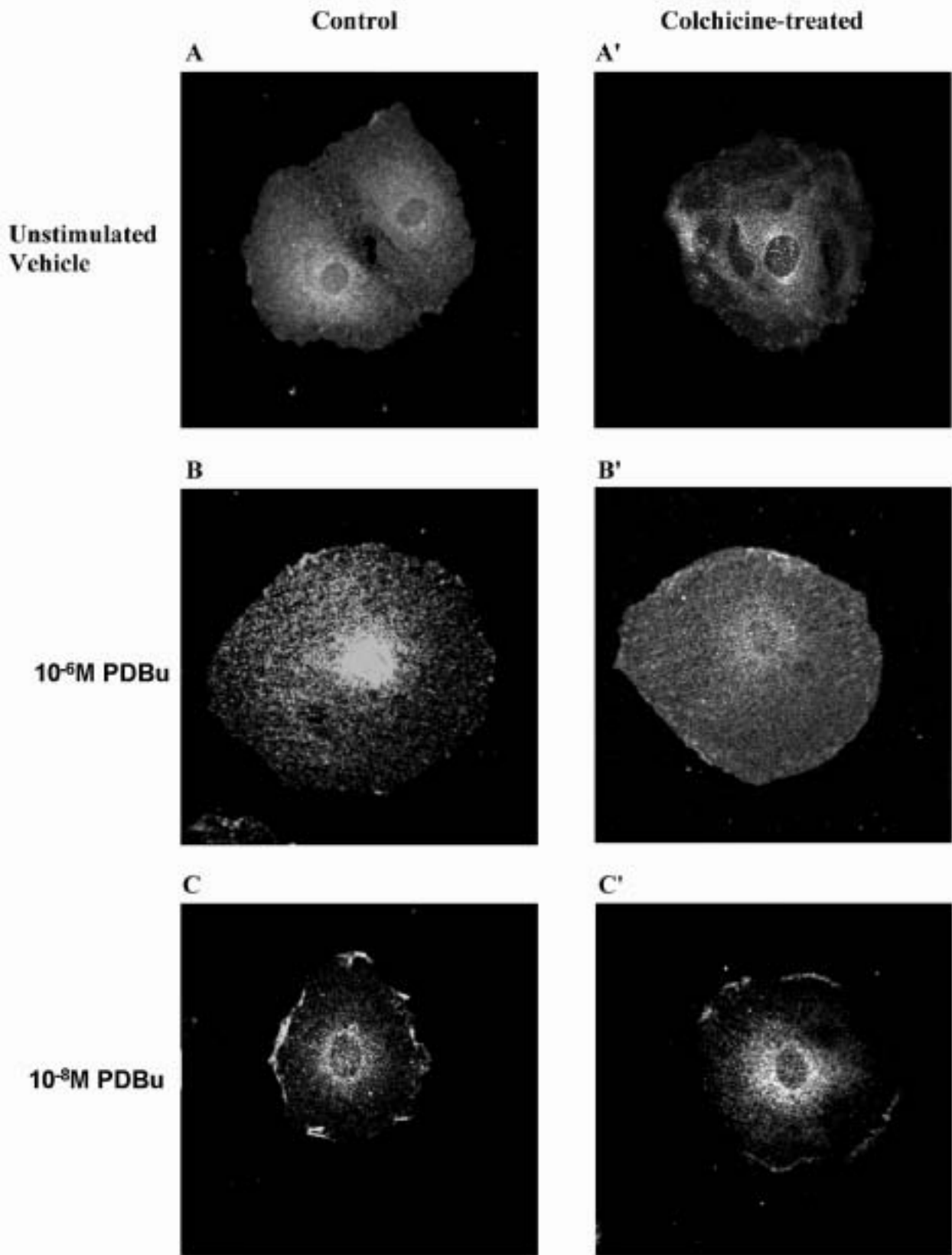
Control Colchicine-treated

A A'

Unstimulated
Vehicle

B B'

10^{-6}M PDBu

C C'

10^{-8}M PDBu

Figure 12.

The effect of treatment with colchicine to disrupt microtubules on the distribution of PKCα -EGFP fusion protein in unstimulated and PDBu-stimulated A7r5 cells. Untreated cells received vehicle (A) or additions of PDBu at 10^{-6}M (B) or 10^{-8}M (C). Treated cells were exposed to colchicine (40 µg/ml, 20 min) prior to receiving vehicle (A'), 10^{-6}M PDBu (B' or 10^{-8}M PDBu (C'). The results were consistent with those from experiments using standard immunostaining methods in indicating that disruption of microtubules blocked the perinuclear accumulation of PKCα-EGFP induced by 10^{-6}M PDBu but had no significant effect on 10^{-8}M PDBu-stimulation of PKCα-EGFP translocation to the plasmalemma. Magnification was 600X. The micrographs reflect the results from 4 experiments in which a total of 350 cells were evaluated. It was estimated that $86 \pm 3\%$ of cells examined exhibited the loss in perinuclear translocation.
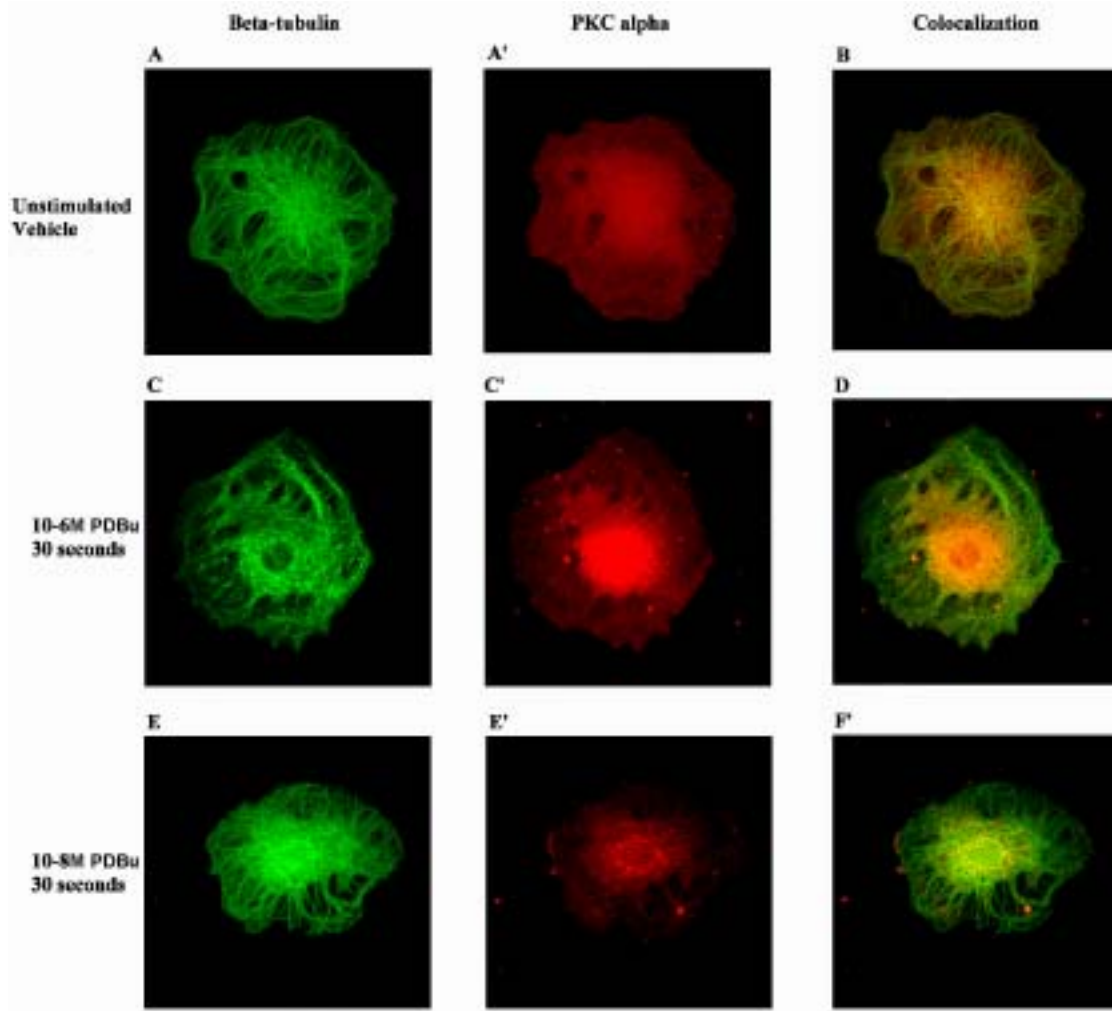
Control | Colchicine-treated

A | A'

Unstimulated

B | B'

10^{-6}M PDBu

C | C'
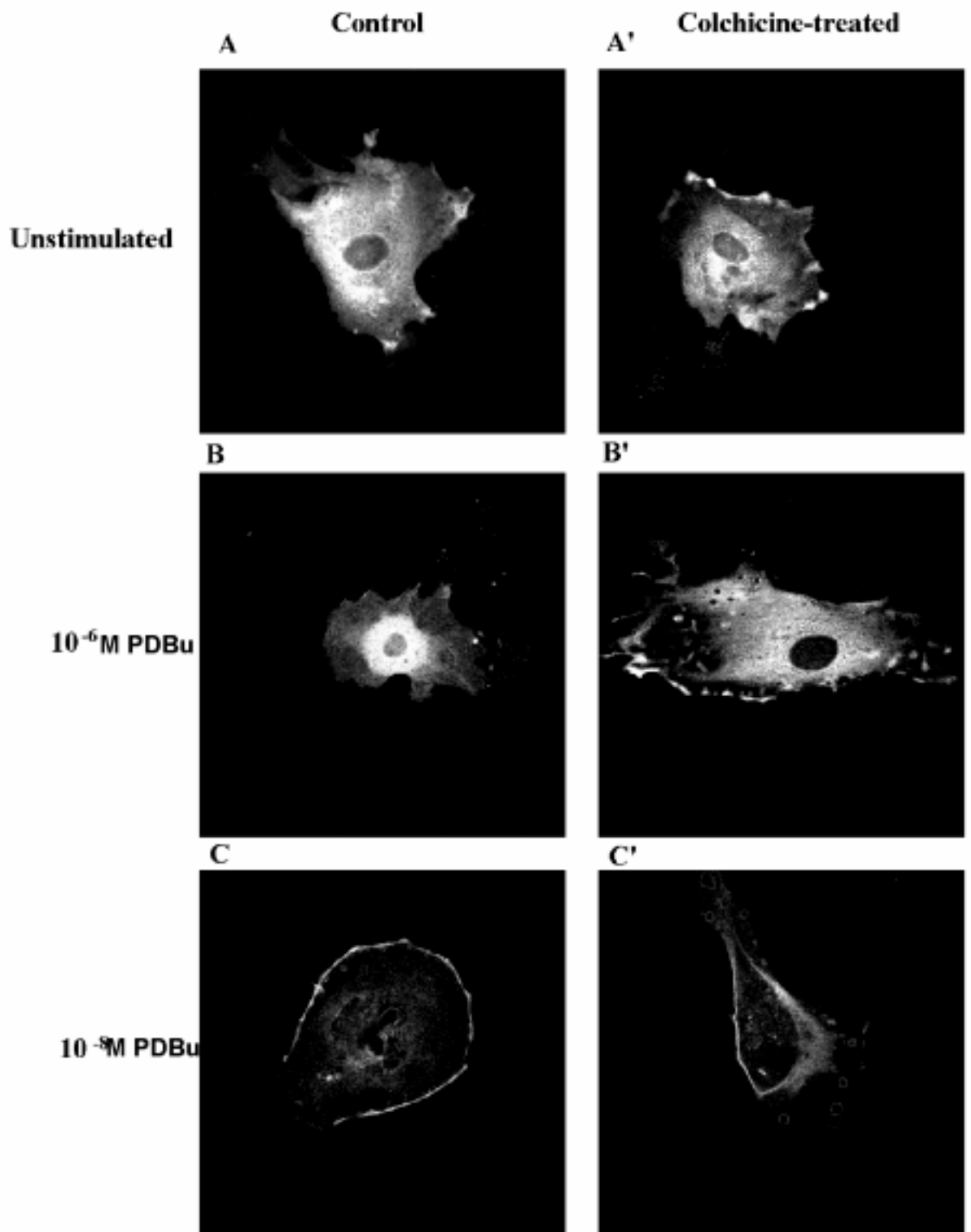
10^{-8}M PDBu

Figure 13.

Dual immunostaining for β-tubulin and PKC α in unstimulated (A, A') A7r5 cells and 30s after the addition of 10^{-6}M PDBu (C, C') or 10^{-8}M PDBu (E, E'). Microtubules were stained with FITC-labeled anti-β-tubulin antibody while PKCα was visualized with Alexa 594-labeled secondary antibody. Images were collected in separate channels at laser power settings below 10% to eliminate bleedover of fluorphores. Rightside panels indicate areas of overlap in fluorescence (yellow). The micrographs are representative of images collected in six individual experiments in which a total of 102 cells were evaluated. Magnification was 600X.

Figure 14.

The effect of treatment with cytochalasin B to disrupt actin stress fibers on the distribution of PKCα in unstimulated and PDBu-stimulated A7r5 cells. Control cells received vehicle (A) or additions of PDBu at 10^{-6}M (B) or 10^{-8}M (C). Treated cells were exposed to cytochalasin B (1μg/ml, 15 min.) prior to receiving vehicle (A'), 10^{-6} PDBu (B') or 10^{-8}M PDBu (C'). PKCα was stained with unlabeled anti-PKCα primary antibody followed by Alexa 488-labeled anti-mouse IgG secondary antibody. The original magnification was 600X. Micrographs reflect the results from 3 experiments in which a total of 298 cells were evaluated.
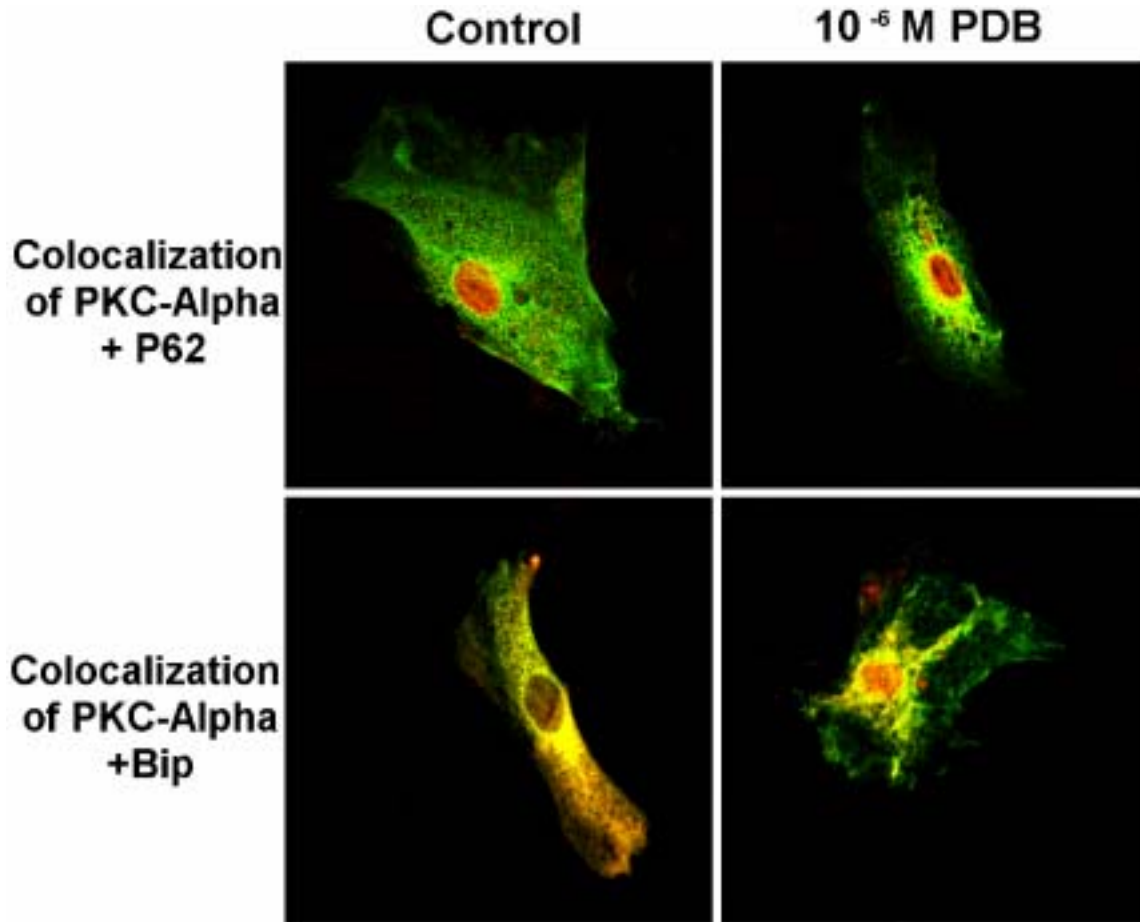
Control   Cytochalasin B-treated

A   A'

Unstimulated

B   B'

10^{-6} M PDBu

C   C'

10^{-8} M PDBu
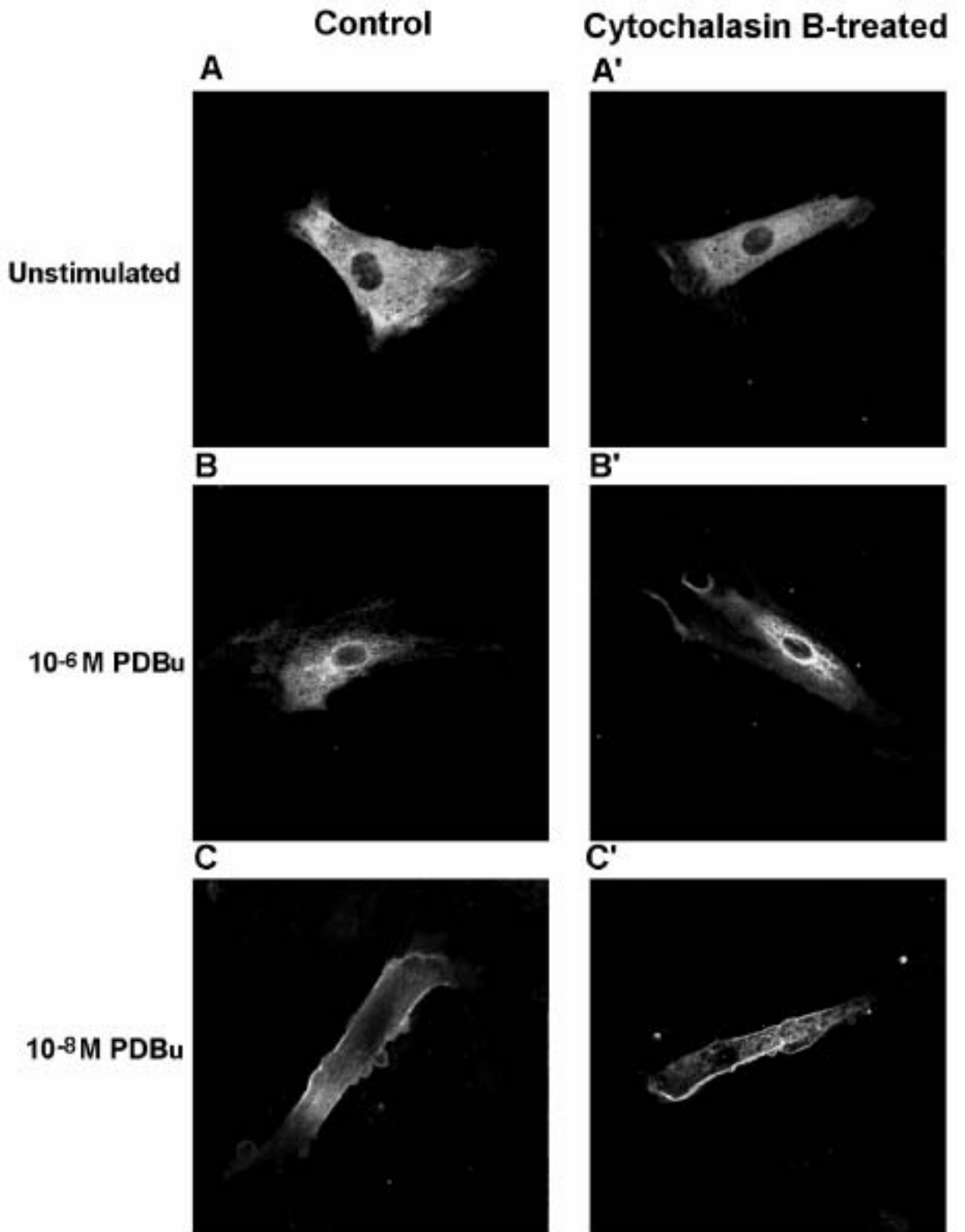
Figure 15.

Dual immunostaining of PKCα with nucleoporin p62 and PKCα with BiP/GRP78 in unstimulated A7r5 cells and cells treated with 10^{-6}M PDBu for 15 minutes. PKCα was visualized by standard immunostaining methods using unlabeled anti-PKCα primary antibody followed by Alexa 488-labeled anti-mouse IgG secondary antibody (green); p62 and BiP/GRP78 were visualized with Alexa 594-labeled secondary antibody (red). Images were collected in separate channels to prevent overlap of fluorophores. Yellow color indicates areas of colocalization of p62 or BiP/GRP78 and PKCα. Magnification was 400X. The micrographs reflect the results from 3 experiments in which a total of 78 cells were evaluated.

PKCα Translocation in Response to Different Contractile Agents

Translocation of PKCα-EGFP

Figures 16 through 20 compare the effects of PDBu, A23187, thapsigargin, Ang II and potassium on PKCα translocation in A7r5 cells expressing PKCα-EGFP. PDBu, A23187, and thapsigargin were effective contractile agonists, consistently causing approximately 85% of cells to visibly contract. Ang II and potassium, however, did not cause detectable constriction of A7r5 cells.

PKCα was diffusely distributed throughout the cell body in unstimulated cells (Figs. 16-20). The addition of PDBu to the medium resulted in a slow but robust relocation of PKCα to the plasma membrane leaving the cytosolic region of the cell devoid of fluorescence (Fig. 16). Translocation became clearly evident by 8 minutes and was usually complete within 10 to 20 minutes after addition of PDBu. Thereafter, PKCα remained localized along the cell periphery for at least 120 minutes.

The calcium ionophore A23187 (Fig. 17) and thapsigargin (Fig. 18) which elevates intracellular calcium through a blockade of endoplasmic reticulum calcium-ATPase activity, had similar effects on PKCα translocation. Each caused a robust but transient translocation of the PKCα to the cell membrane. Relocalization along the cell periphery was detectable within 1 minute and was completed within 4 minutes after addition of either agent to the medium. Subsequently, PKCα was observed to slowly redistribute back into the cytosolic region of the cell over an interval of 10 to 25 minutes.

By comparison with other agents studied, Ang II caused only a partial translocation of cellular PKCα which was extremely rapid in development, transient and highly site specific at the cell periphery. Ang II induced PKCα translocation to discrete areas of the cell periphery which began to be clearly visible as intensely fluorescing circular patches as early as 10 seconds after the addition of the drug to the medium (Fig. 19). This translocation response was further distinguished by the rapidly transient nature of PKCα localization at these sites. The depletion of PKCα from peripheral patches was often observed within 1 minute, with the distribution of the enzyme returning to that of the unstimulated cell by 5 minutes after Ang II addition.

Both the spatial and temporal patterns of the potassium-induced PKCα-EGFP translocation were different from the other agents studied. About 10 minutes after potassium stimulation, PKCα was observed to move slowly from the cytosol to the cell membrane, a process which continued to completion over an interval of approximately 20 minutes. At completion, most of the PKCα was localized at the cell membrane. However, detectable amounts were observed as granular structure scattered throughtout the cell body (Fig. 20).

Blockade of PKCα Translocation

A combination of calcium chelators has been previously demonstrated to block PKCγ translocation in response to A23187 but not to the phorbol ester 12-0-tetradecanoyl phorbol 13-acetate in COS-7 cells (Sakai et al., 1997). In order to determine if PKCα translocation exhibited similar calcium requirements in A7r5 smooth muscle cells, the

effects of a mixture of EGTA (2×10^{-3}M) and BAPTA-AM (10^{-5}M) were examined in
A23187- and PDBu-stimulated cells (Fig. 21). Addition of calcium chelators to the
medium completely blocked both PKCα translocation and the contraction of A23187-
treated cells. Similarly, calcium chelators blocked the translocation of PKCα in response
to PDBu and caused a partial inhibition of contraction (Fig. 21).

Staurosporine at high concentrations is an inhibitor of a broad spectrum of protein
kinases, but was expected to be selective for PKC activity at the concentration (10^{-8}M)
employed in the present experiments. Staurosporine had no effect on PKCα translocation
but blocked the contraction of PDBu-stimulated cells (Fig. 22). Staurosporine had no
effect on either PKCα translocation nor the contraction of cells treated with A23187.

Disruption of the microtubules by colchicine (40 μg/ml) had no effect on 10^{-8}M PDBu-
induced PKCα translocation to the cell membrane or cell contraction. By comparison,
disruption of actin filaments by treatment of cytochalasin B (1 μg/ml) showed no effect
on 10^{-8}M PDBu-induced PKCα translocation to cell membrane, however it partly blocked
the 10^{-8}M PDBu-induced cell contraction (Fig.23). Neither colchicine nor cytochalasin B
had a detectable effect on A23187-induced PKCα translocation to the cell membrane or
cell contraction (data not shown).

Incubation of cells in calcium-free medium blocked PDBu-induced PKCα translocation
to the cell membrane and attenuated cell contraction compared to PDBu-treated cells in

regular medium (Fig. 24). Both PKCα translocation and cell contraction in response to
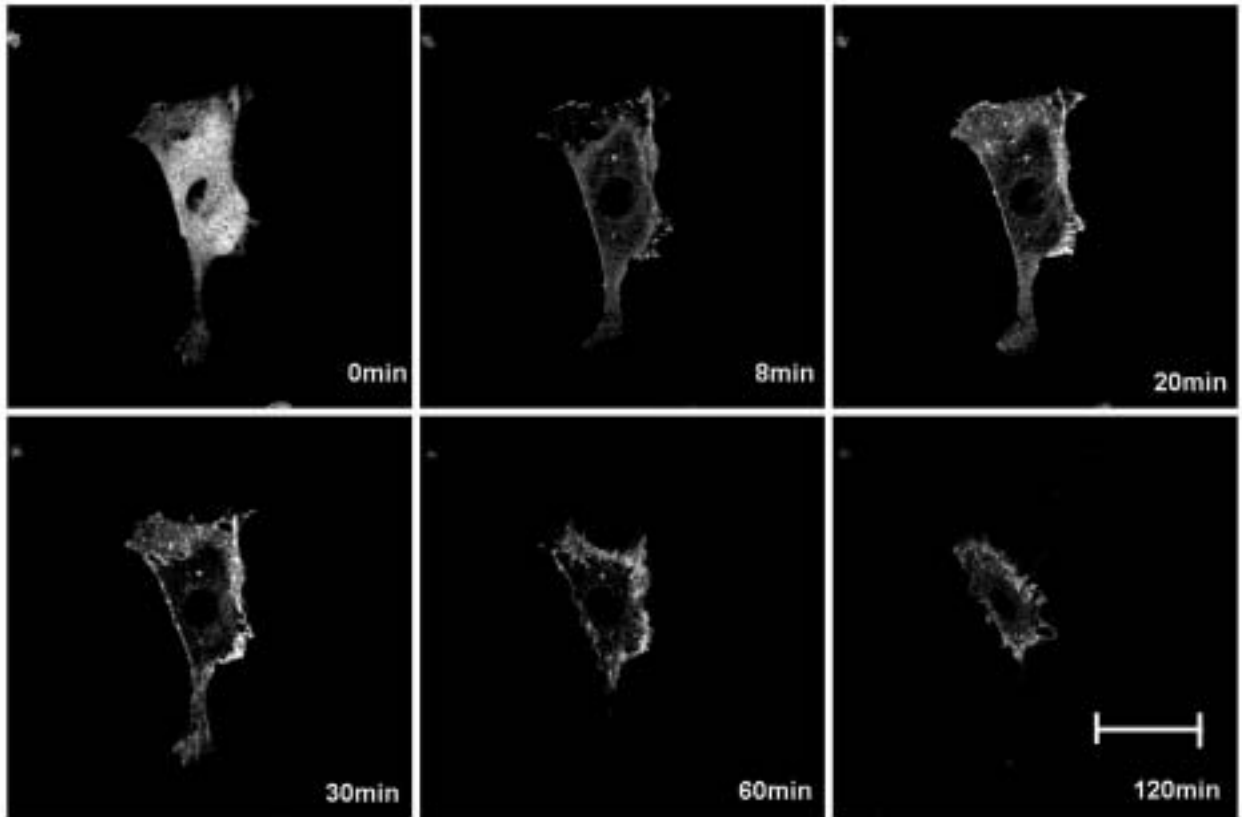
A23187 were blocked in calcium-free medium (Fig.24).

Figure 16.

Confocal micrographs showing the spatial and temporal translocation of PKCα-EGFP in a A7r5 cell stimulated with 10^{-8}M phorbol, 12, 13 dibutyrate (PDBu). Relocalization of the fusion protein from its diffuse distribution in the cytosol was complete within 10 to 20 minutes and was irreversible in the presence of PDBu. Results are representative of those obtained in 5 individual experiments in which total of 70 cells were evaluated. The original magnification was 400X. The bar indicates 50 microns.

Figure 17.

Confocal micrographs showing the spatial and temporal translocation of PKCα-EGFP in a A7r5 cell stimulated by 2 x 10^{-5}M A23187. Relocalization of the fusion protein from its diffuse distribution in the cytosol to the plasma membrane was completed within 1 to 4 minutes. Subsequently, the protein was seen to redistribute slowly into the cytosol over a 20 to 25 minute interval. Results are representative of those obtained in 5 individual experiments in which a total of 58 cells were evaluated. The original magnification was 400X. The bar indicates 50 microns.
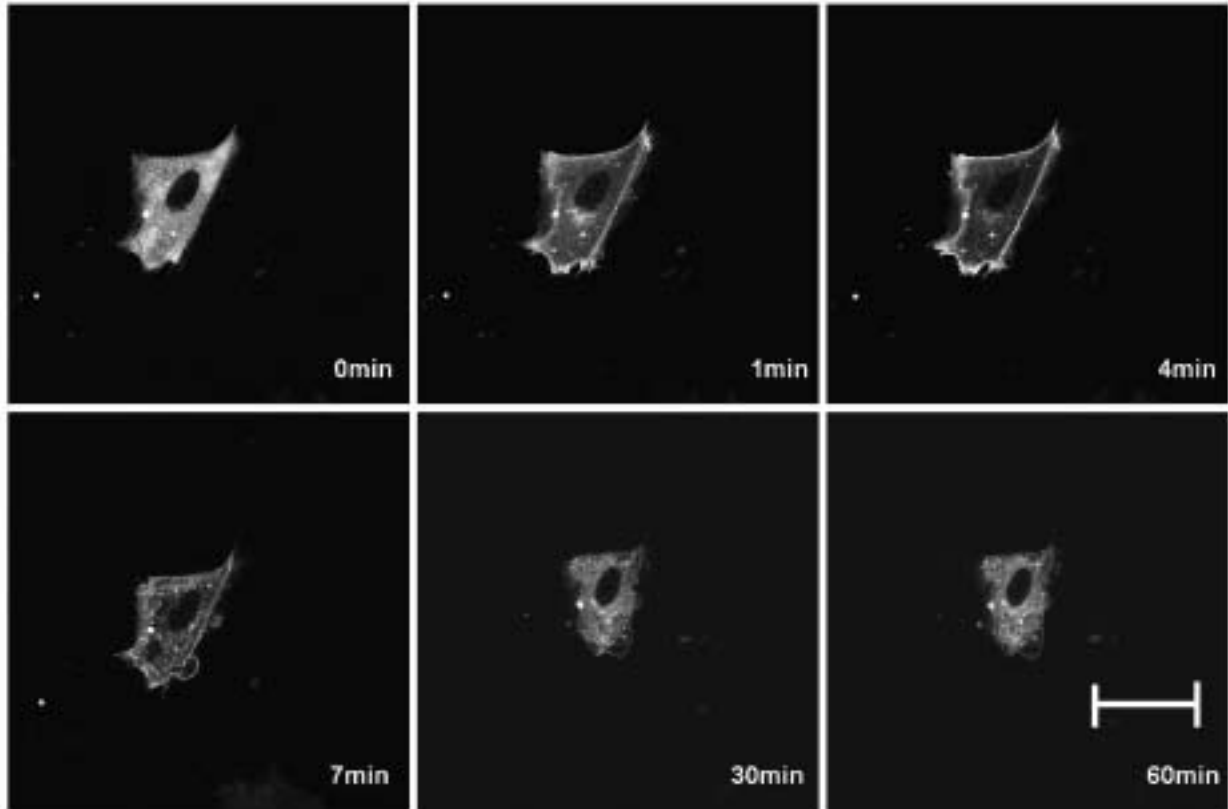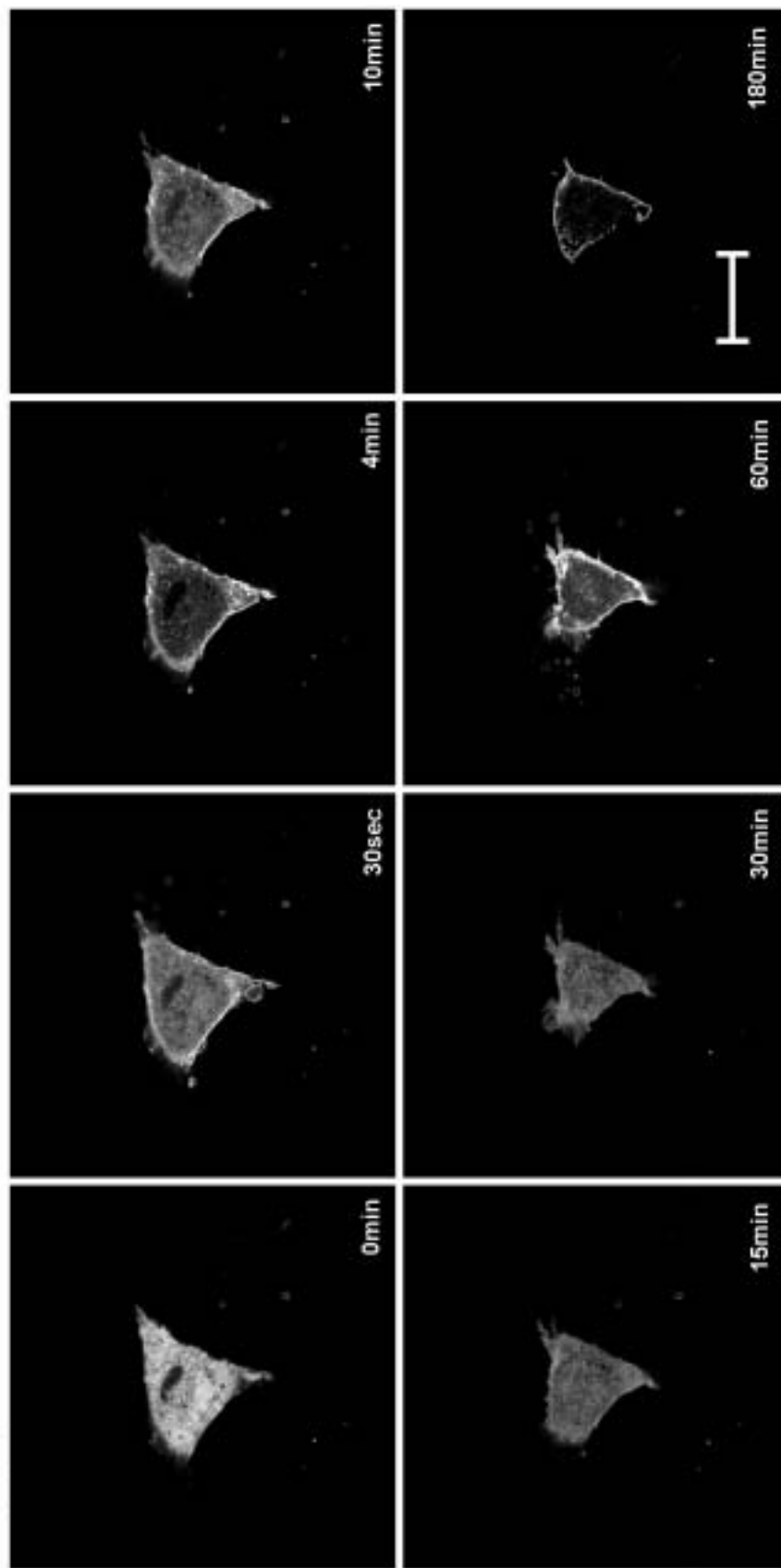
Figure 18.

Confocal images showing the spatial and temporal translocation of PKCα-EGFP in a A7r5 cell stimulated with 10^{-5}M thapsigargin. Thapsigargin stimulated PKCα-EGFP translocation from the cytosol to the plasma membrane within 0.5 to 1.0 minutes. Translocation was completed within 4 minutes. Subsequently, the protein was observed to slowly redistribute from the membrane to the cytosol over an interval of 5 to 10 minutes. At 60 min, the readministration of thapsigargin induced a second rapid, but not reversible, PKCα-EGFP translocation to the plasma membrane without further cell size change. Results are representative of those obtained in 3 individual experiments in which a total of 56 cells were evaluated. The original magnification was 400X. The bar indicates 50 microns.
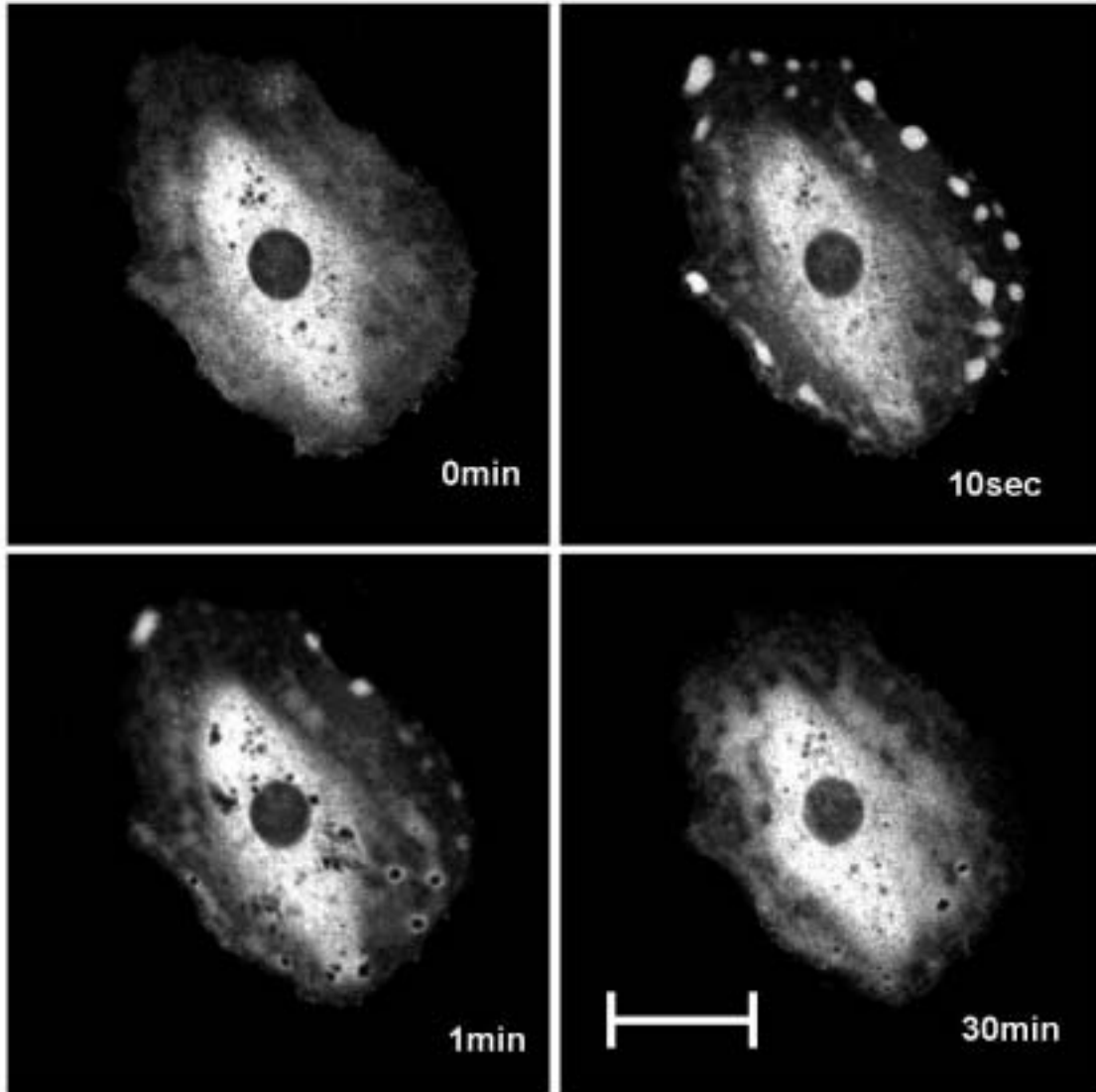
Tharpsigargin Treatment

0min 30sec 4min 10min

15min 30min 60min 180min

Figure 19.

Confocal micrographs showing the spatial and temporal translocation of PKCα-EGFP in A7r5 cells after addition of 10^{-6}M angiotensin II to the media. Translocation of the fusion protein was observed as early as 10 seconds after addition of the drug and was highly localized at brightly fluorescing patches at the cell periphery. Subsequently, the protein was observed to redistribute from the membrane to the cytosol over an interval of approximate 2 minutes. Note that no evidence of cell contraction was obtained in studies of angiotensin II. Results are representative of those obtained in 3 individual experiments in which a total of 30 cells was evaluated. The original magnification was 400X. The bar indicates 50 microns.

Potassium Treatment
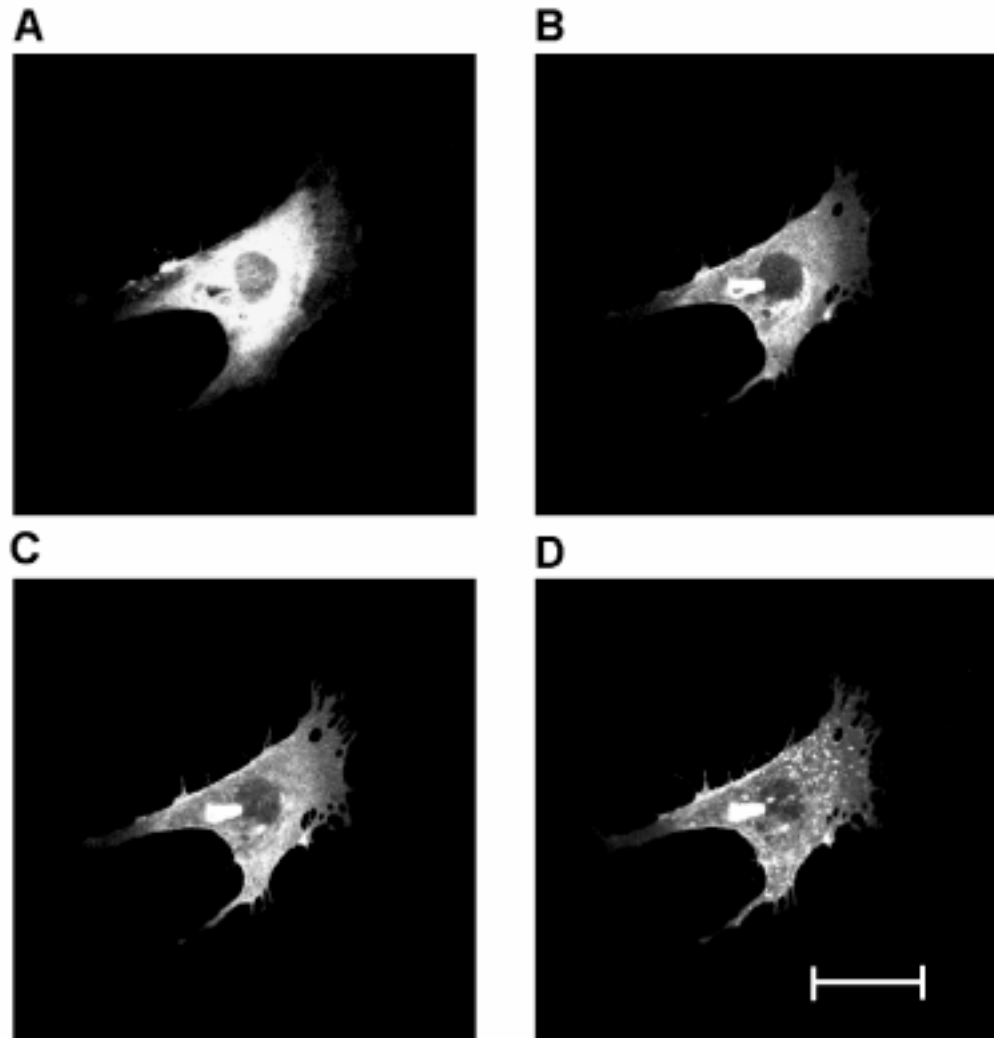
Figure 20.

Confocal images showing the spatial and temporal translocation of PKCα-EGFP in A7r5 cell stimulated with 10^{-2} M potassium. (A) Control, (B) relocalization of the PKCα was started within 10 minutes, (C) 20 minutes after potassium stimulation and (D) completed within 30 minutes. Translocation of PKCα was irreversible in the presence of potassium and most of PKCα-EGFP flourescence accumulated at the cell membrane. However, detectable amounts were observed as granular structures scattered throughtout the cell body. Results are representative of those obtained in 4 individual experiments in which a total of 50 cells were evaluated. The original magnification was 400X. The bar indicates 50 microns.

Figure 21.

Effect of the combination of 2 x 10^{-3}M EDTA and 10^{-5}M BAPTA-AM calcium chelators on the translocation of PKCα-EGFP in A7r5 cells stimulated with (A) A23187 or (B) PDBu. Calcium chelators blocked the translocation of the fusion protein in response to both agents. Micrographs are representative of results obtained in 3 individual experiments in which 30 cells were evaluated. The original magnification was 400X.

Effect of Calcium Chelator

A A23187 Treatment

0min 1min 4min 40min

B PDB Treatment

0min 10min 20min 40min
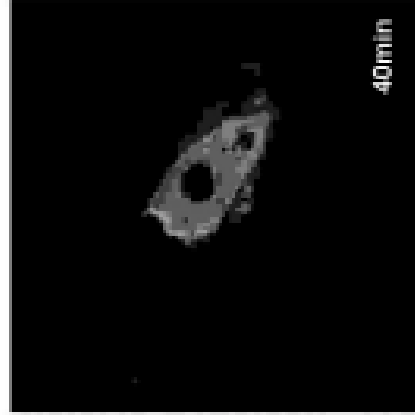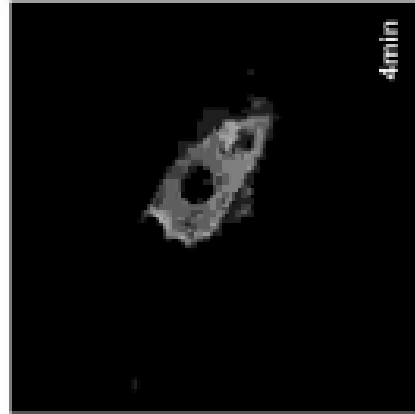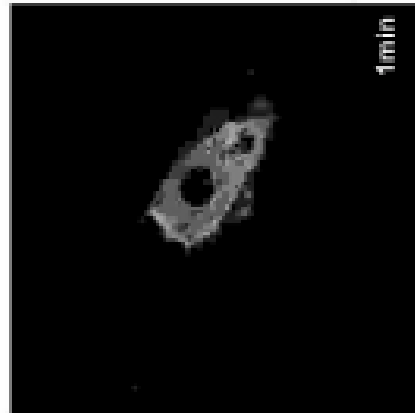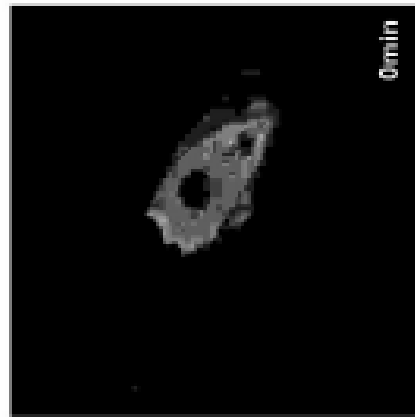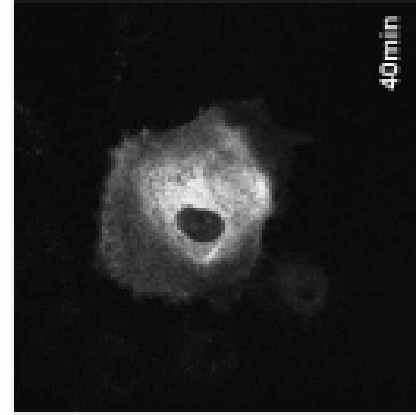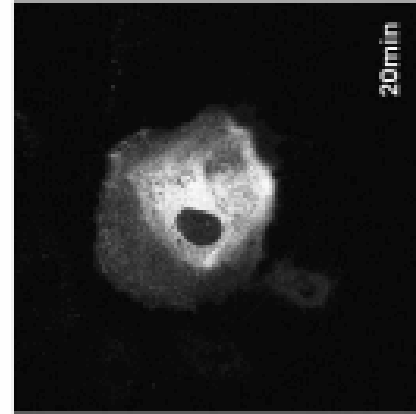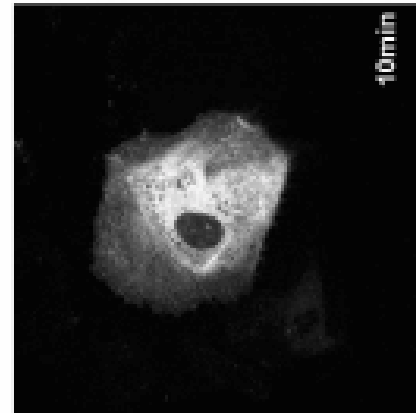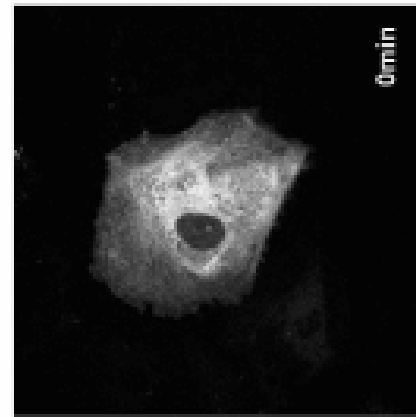
Figure 22.

Effect of the serine/threonine PKC activity inhibitor, staurosporine, on the translocation of PKCα-EGFP in A7r5 cells stimulated by additions of   A) 10^{-5}M PDBu and   B) 2 x 10^{-5}M A23187. Staurosporine had no effect on the translocation of the fusion protein in either treatment but blocked the contractile response to PDBu. Micrographs are representative of results obtained in 3 individual experiments in which a total of 35 cells were evaluated. The original magnification was 400X.

Effect of Staurosporine on PDB Treatment
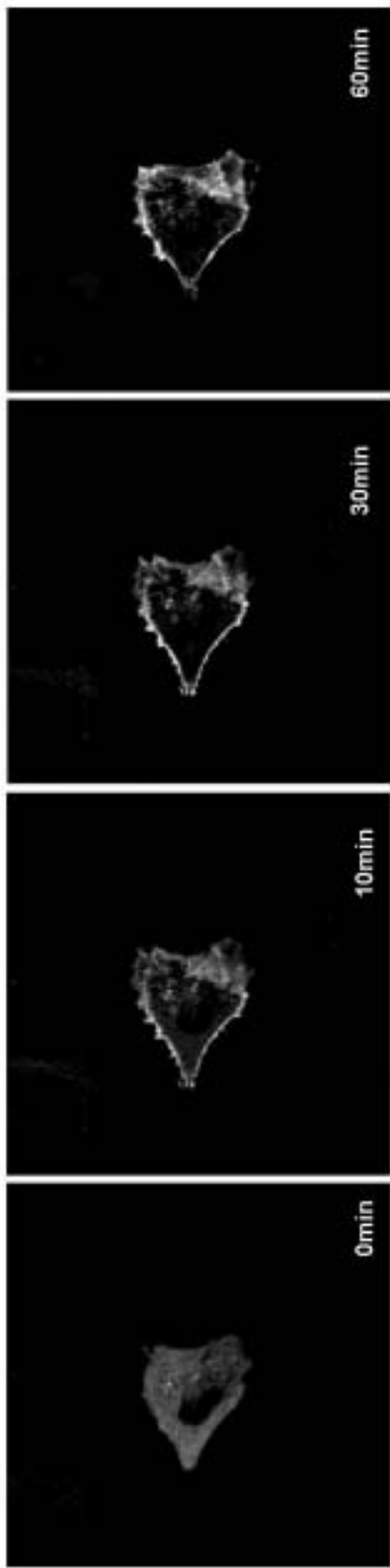
Effect of Staurosporine on A23187 Treatment

74
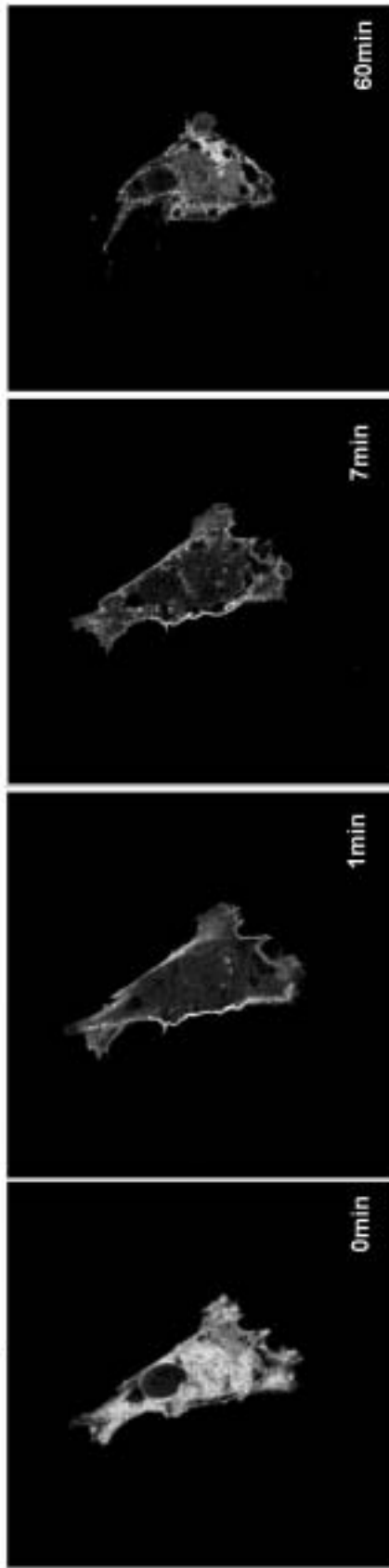
Figure 23.

Effect of cytochalasin B and colchicine on PKCα-EGFP translocation. Disruption of actin filaments with cytochalasin B did not affect A23187 or PDB-induced PKCα-EGFP translocation. It was also shown that disruption of microtubules with colchicine had no effect on PKCα-EGFP translocation from the cytosol to the plasma membrane. Micrographs are representative of results obtained in 3 experiments in which a total of 40 cells were evaluated. The original magnification was 400X. The bar indicates 50 microns.

Effect of colchicine on PDB Treatment
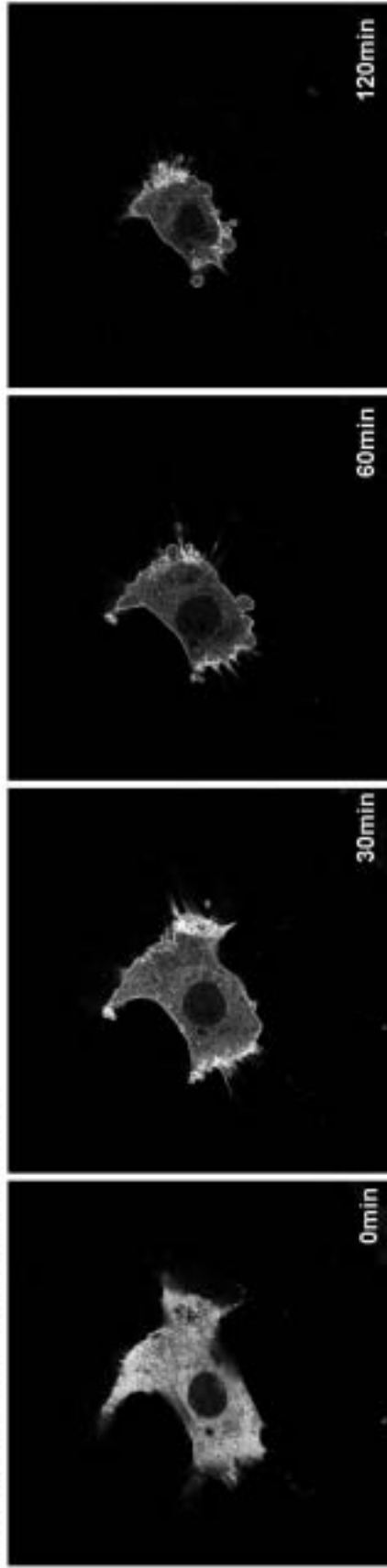
Effect of Cytochalasin B on PDB Treatment

76
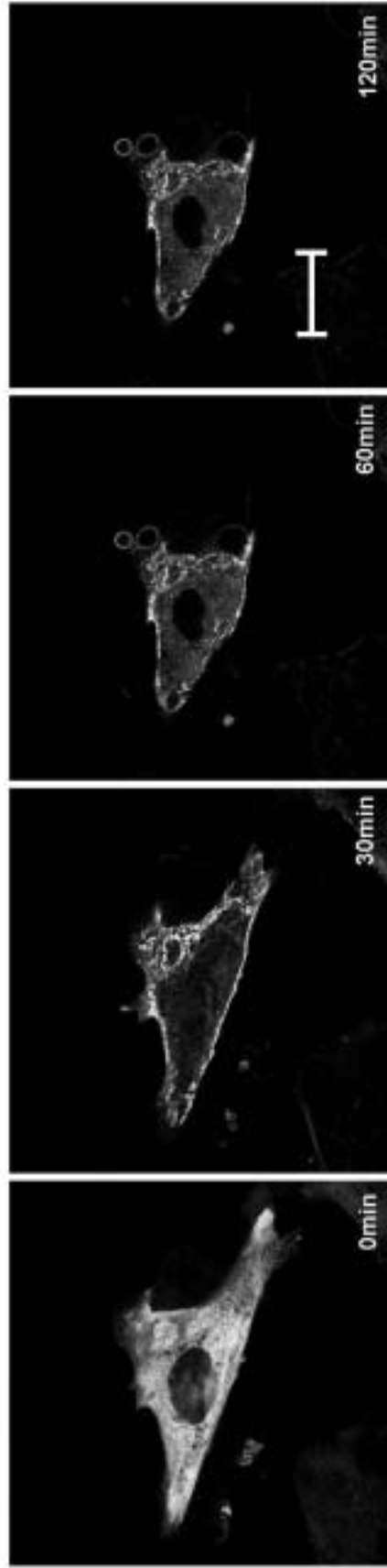
PDBu Treatment in Calcium-Free Medium

0 min 20 min 60 min
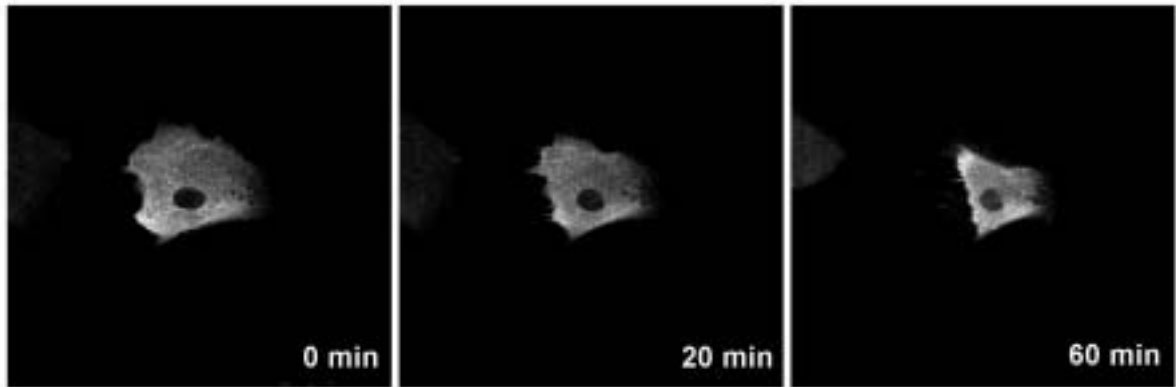
A23187 Treatment in Calcium-Free Medium

0 min 20 min 60 min
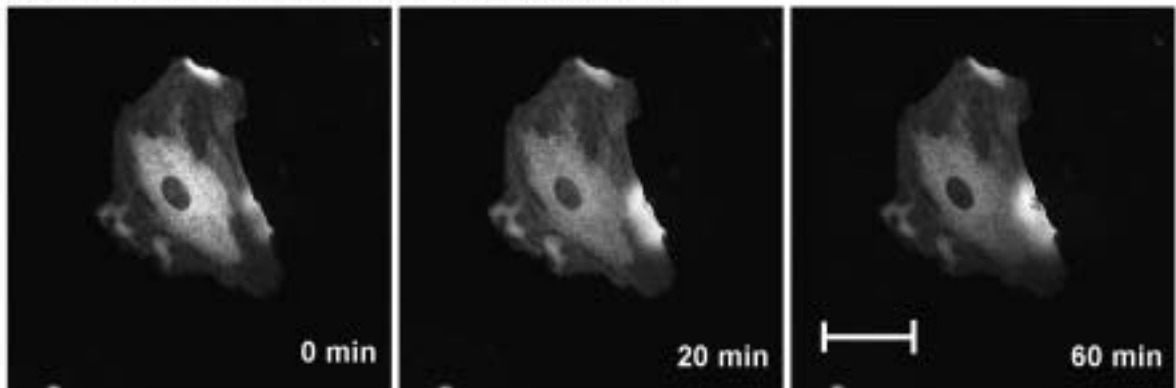
Figure 24.

Effect of PDBu and A23187 on PKCα-EGFP distribution and cells size change in a calcium-free medium. In the calcium-free medium, PDBu and A23187 failed to stimulate a significant translocation of PKCα-EGFP. PDBu stimulation induced a reduction of cell size while A23187 stimulation did not. Results are representative of those obtained in 3 individual experiments in which a total of 60 cells were evaluated. The original magnification was 400X. The bar indicates 50 microns.

Calcium-Dependent Actin Remodeling in Contracting A7r5 Cells

A7r5 Cell Contraction.

The effects of A23187 and thapsigargin were effectively identical on the contraction and dynamics of the actin cytoskeleton, suggesting that the mechanism of increased $[Ca^{2+}]i$ had little or no effect on A7r5 smooth muscle contraction. Both agents caused a sustained increase in $[Ca^{2+}]i$ which plateaued or continued to increase throughout the interval of observation. Figure 25 shows the results from a typical experiment examining the effect of A23187 and thapsigargin on $[Ca^{2+}]i$. The change in $[Ca^{2+}]i$ of 11 individual cells in response to thapsigargin is summarized in Table 2. Basal $[Ca^{2+}]i$ ranged between 60nM and 120nM ($\overline{X} = 81.4 \pm 6.4$ nM). The addition of thapsigargin (5×10^{-6}M) caused a biphasic response, with an initial slow phase of increase lasting about 10 minutes followed by a secondary increase in $[Ca^{2+}]i$. The maximum increase in $[Ca^{2+}]i$ ranged from 220 to 611 nM ($\overline{X} = 507.2 \pm 40.7$ nM), which typically occurred at about 17 minutes after the addition of thapsigargin. After an early phase of $[Ca^{2+}]i$ increase, periodic oscillations of varying frequency and amplitude were clearly observed. Such oscillations are a common feature of the increase in $[Ca^{2+}]i$ in stimulated cells of various types (Thaler et al., 1992). Administration of 2×10^{-5}M 4-Bromo-A23187 induced an immediate increase of $[Ca^{2+}]i$ which reached a plateau at 852 ± 21 nM. The calcium concentration then fell to baseline level over the next 4 to 6 minutes. After declining to the baseline level, the intracellular calcium did not respond to the addition of ionomyocin (Fig. 25), suggesting a possible leakage or inactivation of the Fura-2 dye. A further study of the uptake of Ca^{45} in ionophore-treated cells indicated that the intracellular calcium

levels were elevated by 2 to 6 times for at least 30 minutes after addition of 2×10^{-5}M

A23187 (Table 3).

Stimulation through the elevation of $[Ca^{2+}]i$ (A23187/thapsigargin) or the use of phorbol

ester (PDBu) resulted in different patterns of A7r5 cell contraction. The contractile

response to A23187 and thapsigargin was more rapid in onset, shorter in duration, and

less robust than that obtained with PDBu (Fig. 26). Cell constriction in response to

PDBu could be first observed at about 10 to 14 minutes and continued over an interval of

60 to 120 minutes. In the great majority of cells, contraction to PDBu was extremely

strong, such that the resolution of individual actin fibers was lost within 40 to 45 minutes.

By comparison, the responses to A23187 and thapsigargin elevations in $[Ca^{2+}]i$ were

observed as early as 2 to 6 minutes and were completed by 20 to 30 minutes. However,

the response was well maintained with little or no evidence of change in cell dimensions

after completion of constriction. Cell contraction by these agonists exhibited thread-like

extrusions and detached cell remnants on the glass substrate, indicating the forcible

detachment from peripheral adhesion sites. Disruption of actin filaments by treatment

with cytochalasin B (1 µg/ml) caused the precontracted cells to lose the ability to contract

further and there was a visible elongation in the cell x-axis (Fig. 27).

Actin Remodeling

Figure 28 shows the changes in β-actin stress cables during cell shortening in an A7r5

cell expressing β-actin-GFP. The β-actin cables shortened without evidence of

compression throughout the interval of contraction. Because individual fibers could be

identified throughout the interval of contraction, the results further indicate that

shortening was achieved without β-actin cable disassembly and reassembly of new structures. Staining of A23187-and thapsigargin-treated cells with phalloidin confirmed the presence of an extensive system of actin stress cables in contracted cells (Fig. 29); however, these experiments showed a degree of diffuse staining suggesting some loss in F-actin. Because diffuse staining was not noted in unstimulated cells (Fig. 29) nor was diffuse fluorescence observed in stimulated cells expressing β-actin-GFP (Fig. 28), the results suggest that the increase in $[Ca^{2+}]i$ was associated with loss in α-actin structure. Immunostaining of control A7r5 cells showed that α-actin was incorporated into thick stress cables similar in appearance to β-actin cables. Addition of A23187 or thapsigargin to elevate $[Ca^{2+}]i$ resulted in partial to complete dissolution of α-actin cables (Figs. 30). The dissolution of α-actin fibers started approximately 2 minutes after stimulation and was completed by approximately 15 minutes. Figure 31 shows enlarged images of both A23187- and thapsigargin-stimulated cells, indicating the partial to complete loss in α-actin fiber structure following elevation of $[Ca^{2+}]i$.

Previous work has demonstrated that the crosslinking protein, α-actinin, is colocalized with α-actin in the A7r5 cell, both in the resting cell and during PDBu-induced α-actin remodeling (Fultz et al., 2000). Similar to these findings, α-actinin was observed to form filamentous strands in unstimulated cells (Fig. 32 A, D). The addition of A23187 or thapsigargin to elevate $[Ca^{2+}]i$ resulted in the dispersal of the protein which was completed after 15 minutes of stimulation (Fig. 32 C, F), further indicating a general dissolution of α-actin. By comparison, the treatment did not significantly alter the

cellular distribution of talin (Fig. 33), suggesting that the effect was confined to the destabilization of α-actin cable structure.

Effect of Increased [Ca^{2+}]i on PDBu-Induced α-Actin Remodeling

PDBu caused remodeling of α-actin into brightly fluorescing peripheral bodies with a reduction in the numbers of α-actin fibers (Fig. 34B). The addition of A23187 (Fig. 34D) or thapsigargin (Fig. 34F) 30 minutes prior to the addition of PDBu resulted in the depolymerization of α-actin cables and blocked PDBu-induced remodeling. In corollary experiments, it was further shown that the addition of A23187 or thapsigargin to cells pretreated with PDBu also caused dissolution of remodeled α-actin peripheral bodies' structure (Fig. 35).

Effect of Ca^{2+}-Free Medium on Actin Remodeling

A7r5 cells incubated in calcium-free DMEM media for 1 hour did not contract in response to PDBu, A23187, or thapsigargin. Incubation in the calcium-free medium had no detectable effect on the integrity of β-actin cables in unstimulated cells or in the presence of the three agonists (Fig. 36 B, D, E, H and G). After changing back to regular media, PDBu, A23187, or thapsigargin did not show a detectable effect on β-actin cable structure (Fig. 36 C, F, I). By comparison, the calcium-free medium blocked α-actin disassembly by A23187 and thapsigargin and prevented PDBu-induced remodeling (Fig. 37 B, D, E, H, G). Similar to β-actin, no effect on the integrity of α-actin cables was noted in unstimulated cells incubated in calcium-free medium.   Cells returned to the calcium containing medium and examined immediately failed to show formation of

peripheral dense structure in response to PDBu or dissolution of α-actin cables in response to A23187 or thapsigargin (Fig. 37 C, F, I). Incubation in regular medium for 2 hours after the calcium-free medium, however, restored the effect of PDBu on formation of peripheral dense structure formation and the effects of A23187 or thapsigargin on dissolution of α-actin (data not shown).

Effect of Kinase Inhibitors on Depolymerization of α-Actin Structure

The effects of six different kinase inhibitors on calcium-induced α-actin cable dissolution were evaluated (Table 4). Staurosporine (ser/thre inhibitor), bisindolymaleimide (PKC inhibitor), H-89 (PKA inhibitor), KN-93 (CAMK II inhibitor), and genistein (tyrosine kinase inhibitor) had no detectable effect on A23187-or thapsigargin-induced α-actin cable disassembly. Only ML-7, a selective inhibitor of myosin light chain kinase (MLCK), caused a partial inhibition of this phenomenon (Fig. 38E, F).
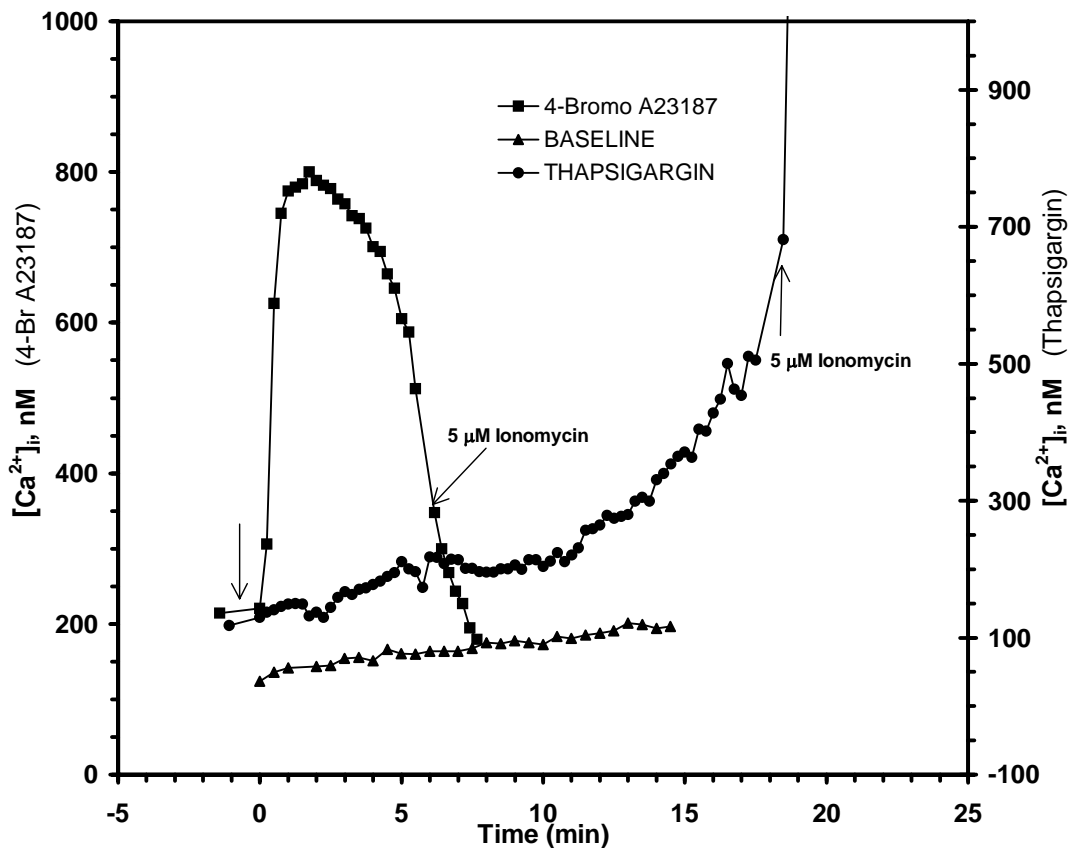
Figure 25.

The time course of increase in $[Ca^{2+}]i$ in A7r5 smooth muscle cells after the addition of 5 x 10^{-6}M thapsigargin or 2 x 10^{-5}M 4-Bromo-A_{23187}.   Cells were loaded with Fura-2AM approximately fifty minutes prior to imaging with a Nikon Diaphot TMD inverted fluorescence microscope. Tracings show the averaged results from eleven different control (baseline) and treated cells. Ionomycin was added at the termination of the experiment for calibration purposes and to demonstrate continued cell responsiveness. Cells were successively excited at 340nm and 380nm light and the fluorescence emitted at 510nm was captured on a DAGE-MTI video camera. $[Ca^{2+}]i$ was then calculated by the equation of Grynkiewicz et al. (1985).

Table 2. Thapsigargin increased $[Ca^{++}]_i$

The basal $[Ca^{++}]_i$ in individual A7r5 cells was determined in HBSS by using a ratio fluorescence microscopy procedure with Fura-2 as a fluorescent probe (see Materials and Methods). The magnitude of a 5 μM thapsigargin-induced increase in the $[Ca^{++}]_i$ in individual cells was calculated 17 minutes after the addition of thapsigargin.

Cell Number	$[Ca^{++}]_{i,}$ nM		Increase in $[Ca^{++}]_{i,}$ nM
	In HBSS	In 5 μM thapsigargin	
1	68	380	312
2	94	578	484
3	71	434	363
4	58	498	440
5	68	659	591
6	109	588	479
7	91	702	611
8	93	604	511
9	51	271	220
10	118	511	393
11	75	354	279

Table 3. ^{45}Ca-uptake by A7r5 cells at selected time intervals after addition of the ionophore A23187. Results reflect the averages from five or six individual cell cultures.

	5 min	10 min	30 min
Control	237 ± 15	193 ± 90	393 ± 120
A23187	653 ± 120*	1324 ± 102^{*+}	846 ± 109*

Data are presented as dpm/cell culture well. An (*) or (+) indicates significant difference from control and 5 minute value, respectively, $p < 0.05$.

Figure 26.

The contractile response of A7r5 smooth muscle cells to 10^{-8}M phorbol 12, 13 dibutyrate (PDBu); the calcium ionophore, A23187 (2×10^{-5} M); and 2×10^{-6}M thapsigargin. Cells were transfected with β-actin-GFP expression plasmid to enable visualization of single cell shortening. Cells are shown prior to stimulation (control) and at 30 and 60 minutes after the addition of agonists. Micrographs represent the results from 16 separate experiments in which a total of 76, 62, and 56 cells were examined in response to PDBu, A23187, and thapsigargin, respectively. The original magnification was 400X. The scale bar indicates 50 microns.
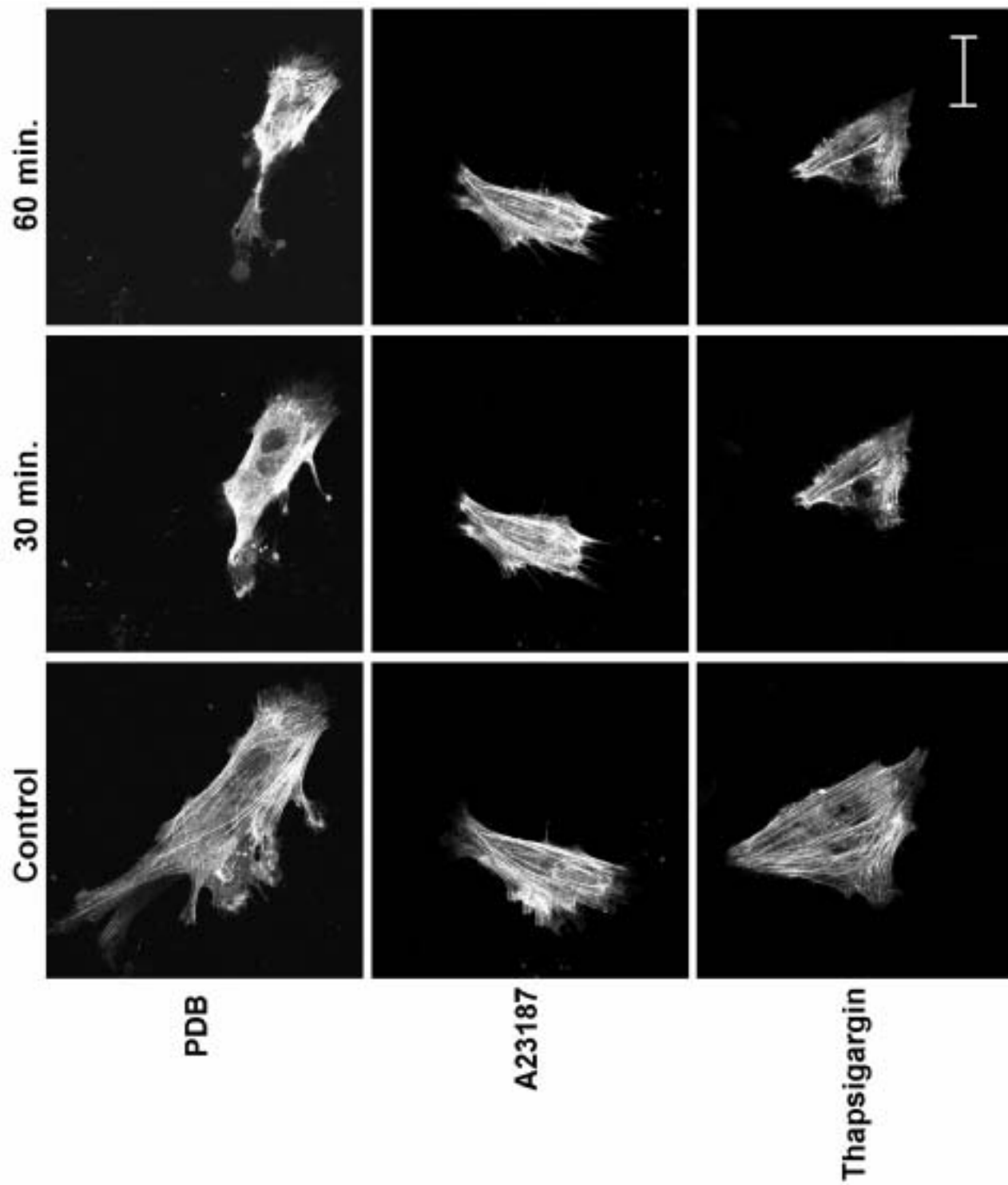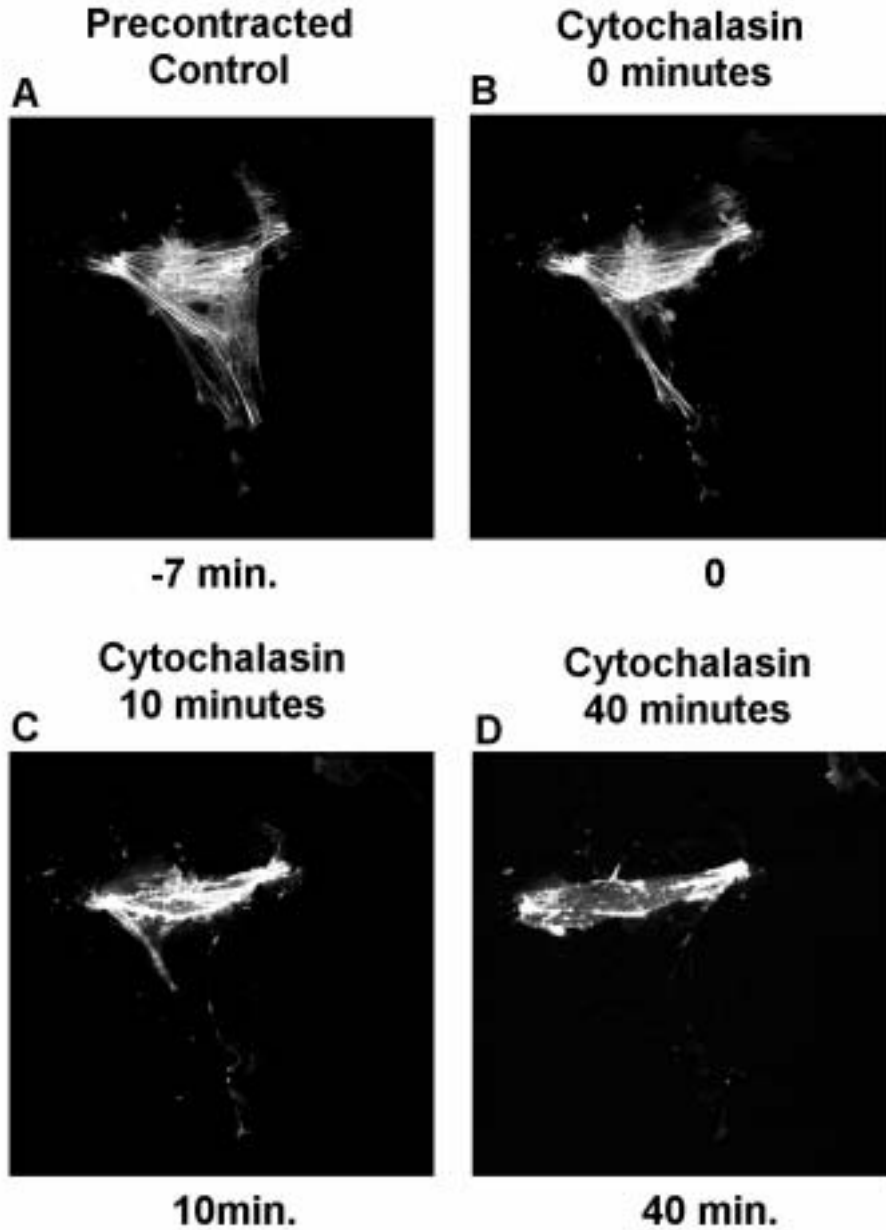
Figure 27.

The effect of cytochalasin-induced dissolution of the actin on cell length in the precontracted A7r5 cell. Cells were contracted by 10^{-8} M PDBu 30 minutes prior to the addition of 0.1 µg/ml cytochalasin B to the media for up to 40 minutes. A7r5 cell was transfected with an β-actin-GFP expression plasmid. The results show that within 10 minutes the cell began to elongate in the x-axis (arrow) parallel to the visible β-actin stress cables. Micrographs are representative of images collected in 3 separate experiments in which 8 cells were evaluated. The original magnification was 600X.
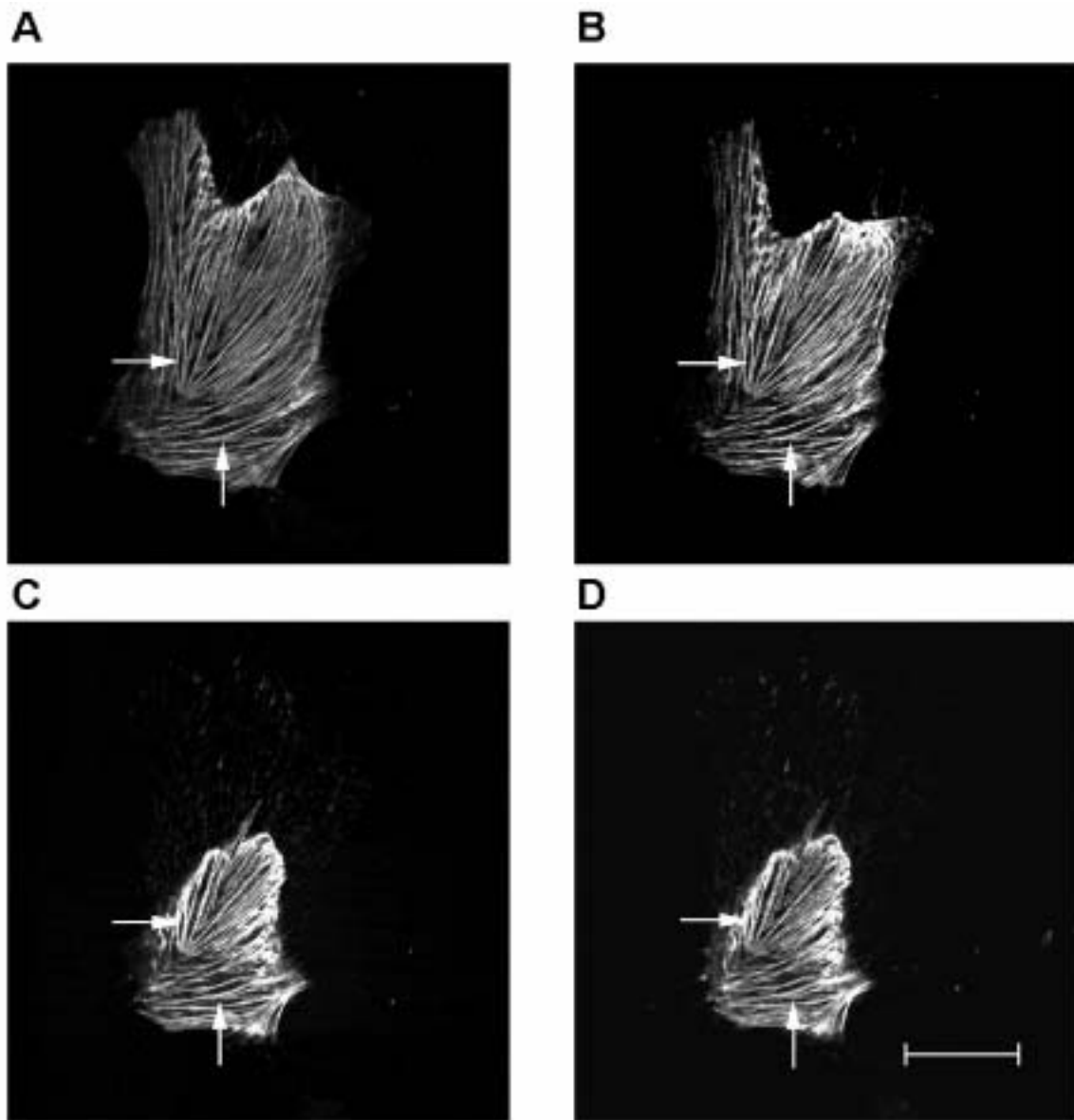
Figure 28.

The shortening of individual β-actin stress fibers during an A23187-induced contraction. A7r5 cells were transfected with β-actin-GFP expression plasmid 3 days prior to experimentation. Micrographs show the cell A) prior to stimulation and B) 10 minutes, C) 30 minutes, and D) 60 minutes after the addition of A23187. Arrows indicate two individual fibers that can be identified throughout the interval of contraction. The original magnification was 400X. The scale bar indicates 50 microns.
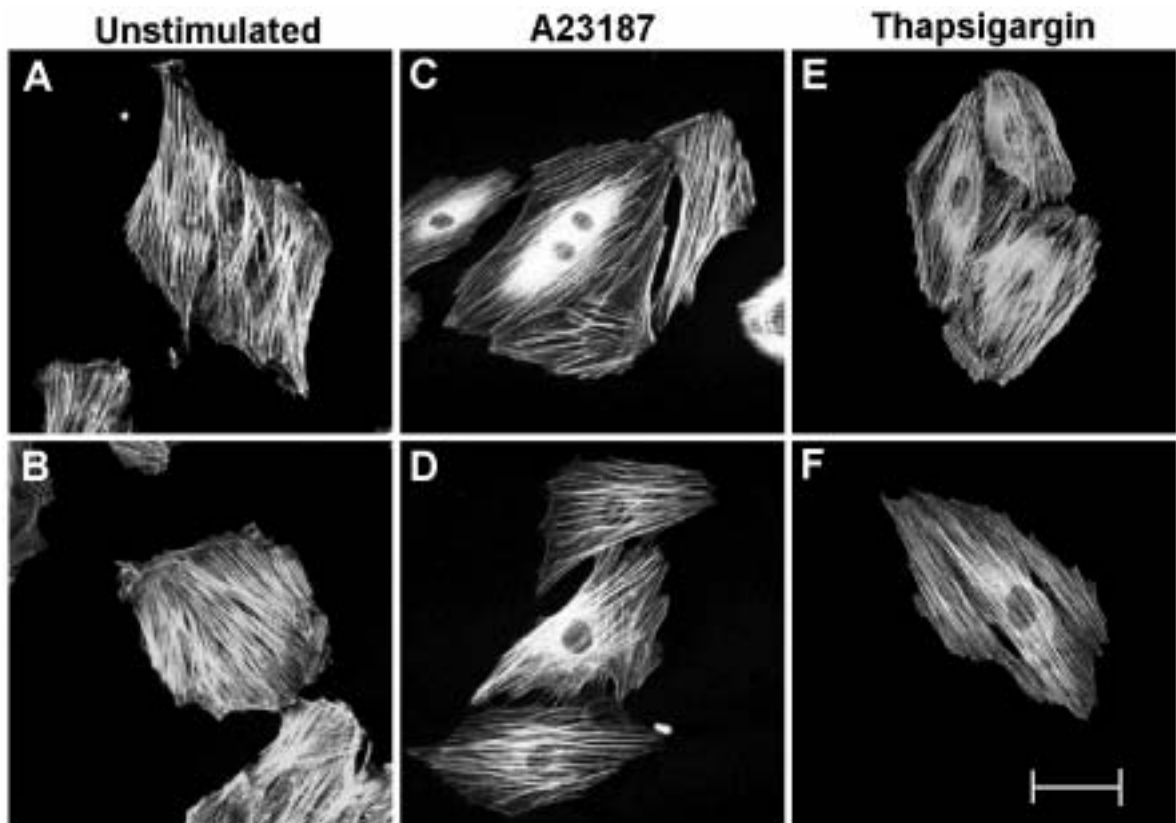
Figure 29.

Confocal micrographs showing the effects of A23187 and thapsigargin on cellular F-actin. A7r5 cells were stained with TRITC-labeled phalloidin prior to stimulation (A, B), 20 minutes after A23187(C, D), and 20 minutes after thapsigargin (E, F). Micrographs represent the results from 3 separate experiments in which a total of 106 unstimulated, 95 A23187-treated, and 96 thapsigargin-treated cells were evaluated. The original magnification was 400X. The scale bar indicates 50 microns.
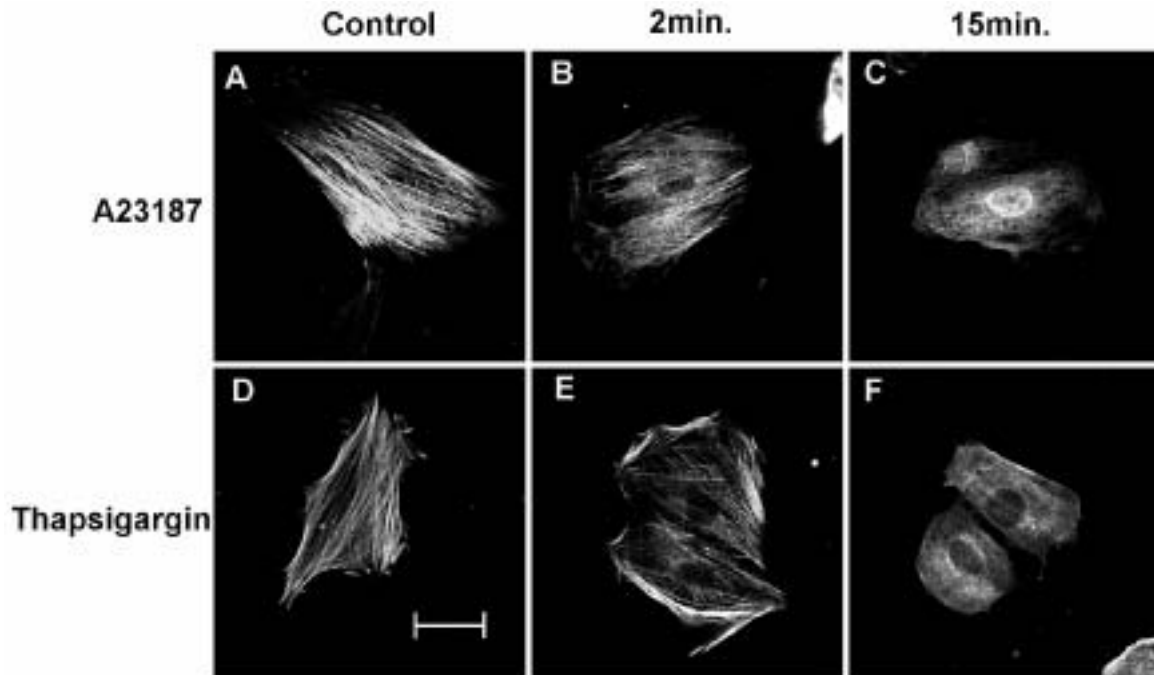
Figure 30.

Confocal micrographs of α-actin structure in unstimulated A7r5 cells (Control; A, D); cells treated with A23187 for 2 minutes (B) and 15 minutes (C); and cells treated with thapsigargin for 2 minutes (E) and 15 minutes (F). Cells were stained with monoclonal anti-α-smooth muscle actin clone 1A4FITC-labeled antibody. Micrographs represent the results of 4 separate experiments in which a total of 126 control, 198 A23187-treated, and 182 thapsigargin-treated cells were evaluated. An average of 76 ±3% of treated cells showed significant loss of α-actin fibers. The original magnification was 400X. The scale bar indicates 50 microns.
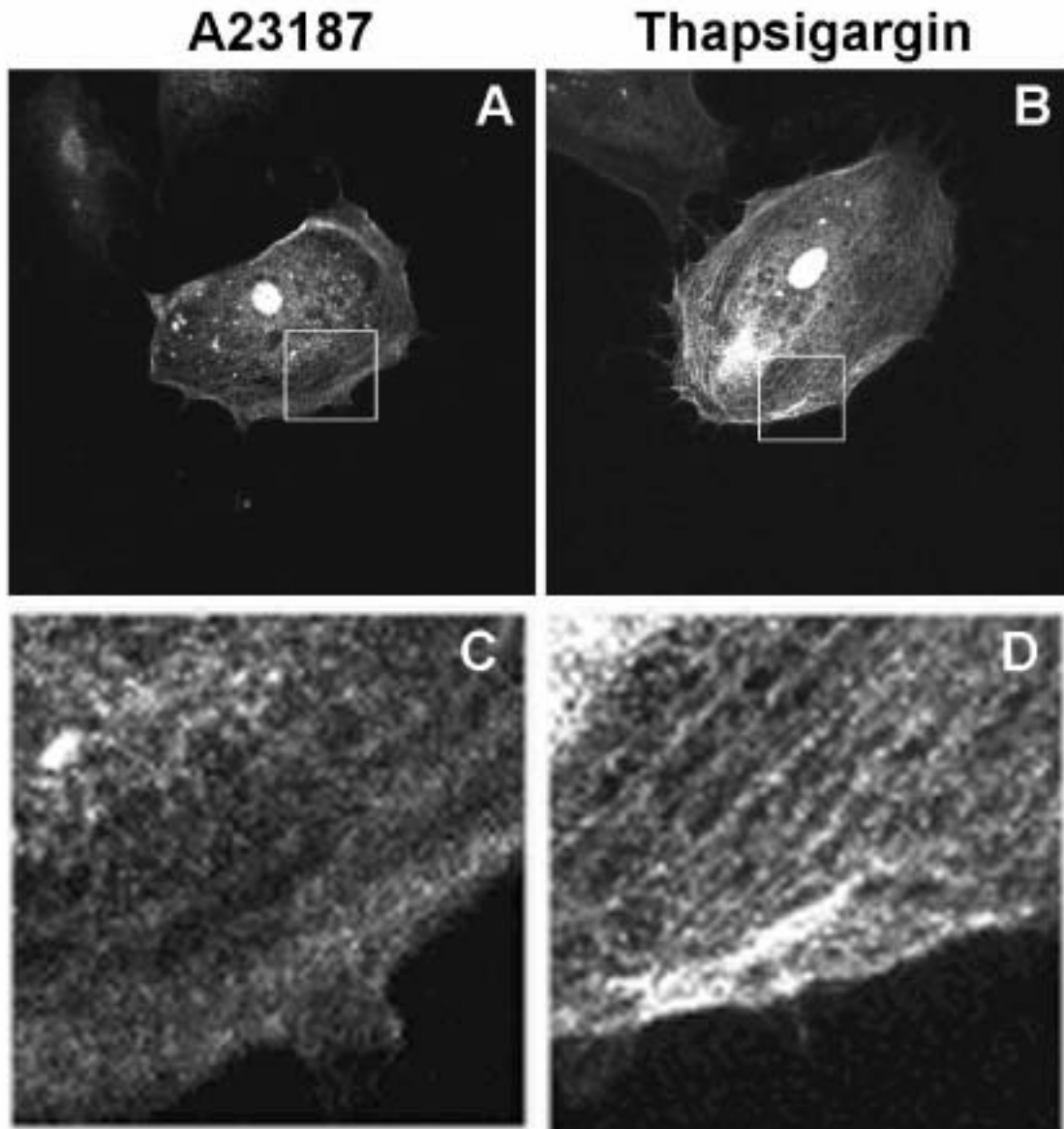
Figure 31.

High magnification imaging (2500X) of α-actin structure at 15 minutes after treatment with A23187 (C) and thapsigargin (D). Boxes indicate the portion of cell selected for visualization (A, B). Cells were stained with monoclonal anti-α-smooth muscle actin clone 1A4 FITC-labeled antibody. Images are representative of those obtained in 3 separate experiments indicating that treatment with either compound to elevate $[Ca^{2+}]i$ resulted in partial to complete depolymerization of the α-actin cytoskeletal structure.
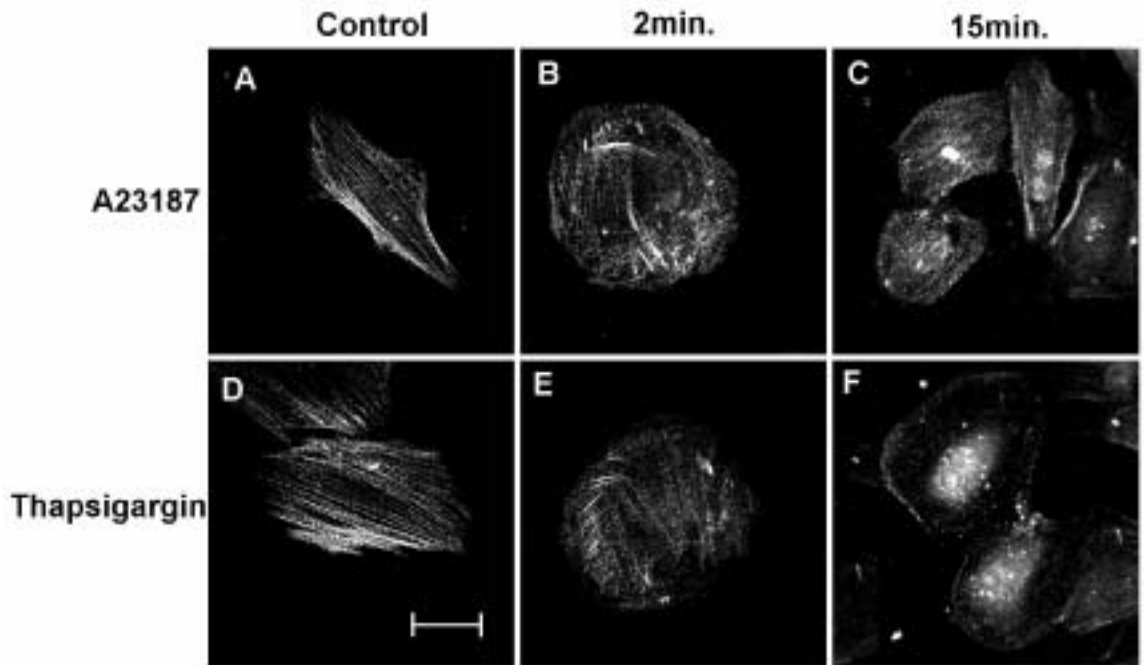
Figure 32.

Confocal micrographs showing the distribution of α-actinin in unstimulated control cells (A, D), cells stimulated with A23187 for 2 minutes (B) and 15 minutes (C), and cells stimulated with thapsigargin for 2 minutes (E) and 15 minutes (F). A7r5 cells were stained with anti-α-actinin primary antibody followed by Alexa 488-labeled secondary antibody. Micrographs represent the results from 3 separate experiments in which a total of 102 control, 110 A23187-treated, and 106 thapsigargin-treated cells were evaluated. An average of 80 ± 3% of treated cells showed dispersal of α-actinin. The original magnification was 400X. The scale bar indicates 50 microns.
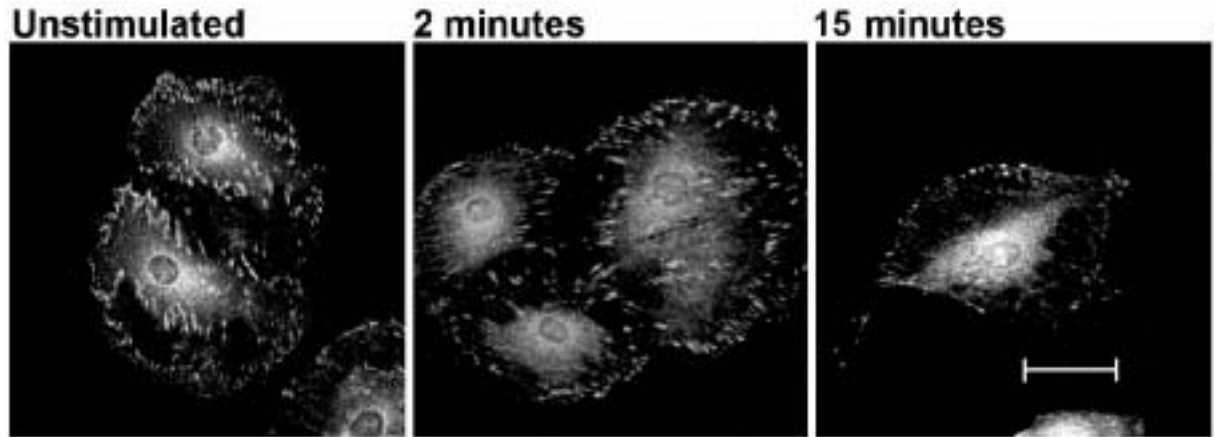
Figure 33.

Confocal images showing the distribution of talin in unstimulated control cells and in cells treated with A23187 for 2 minutes and 15 minutes. A7r5 cells were stained with anti-talin primary antibody followed by an Alexa 488-labeled secondary antibody. Micrographs represent the results of 3 separate experiments in which a total of 120 control and 130 A23187-treated cells were evaluated. An average of 95 ± 3% of treated cells were judged to be indistinguishable from control cells. The original magnification was 400X. The scale bar indicates 50 microns.

Figure 34.

A comparison of the effects of A23187 and thapsigargin on α-actin cytoskeletal structure in previously unstimulated cells (-PDBu) and cells in which PDBu was added to induce α-actin remodeling 20 minutes after the addition of A23187 and thapsigargin (+PDBu). Control panels show α-actin structure in unstimulated cells (A) and after PDBu alone (B). Other cells were incubated for 20 minutes with A23187 (C) or thapsigargin (E) or were successively these drugs for twenty minutes followed by an additional 30 minutes exposure to PDBu (D, F). Cells were stained with monoclonal anti-α-smooth muscle actin clone 1A4 FITC-labeled antibody. Images represent the results from 3 separate experiments in which a total of 205 A23187 + PDBu and 215 thapsigargin + PDBu cells were evaluated. The original magnification was 400X. The scale bar indicates 50 microns.

(+)PDB

(-)PDB

B

A

Control

D

A23187

F

E
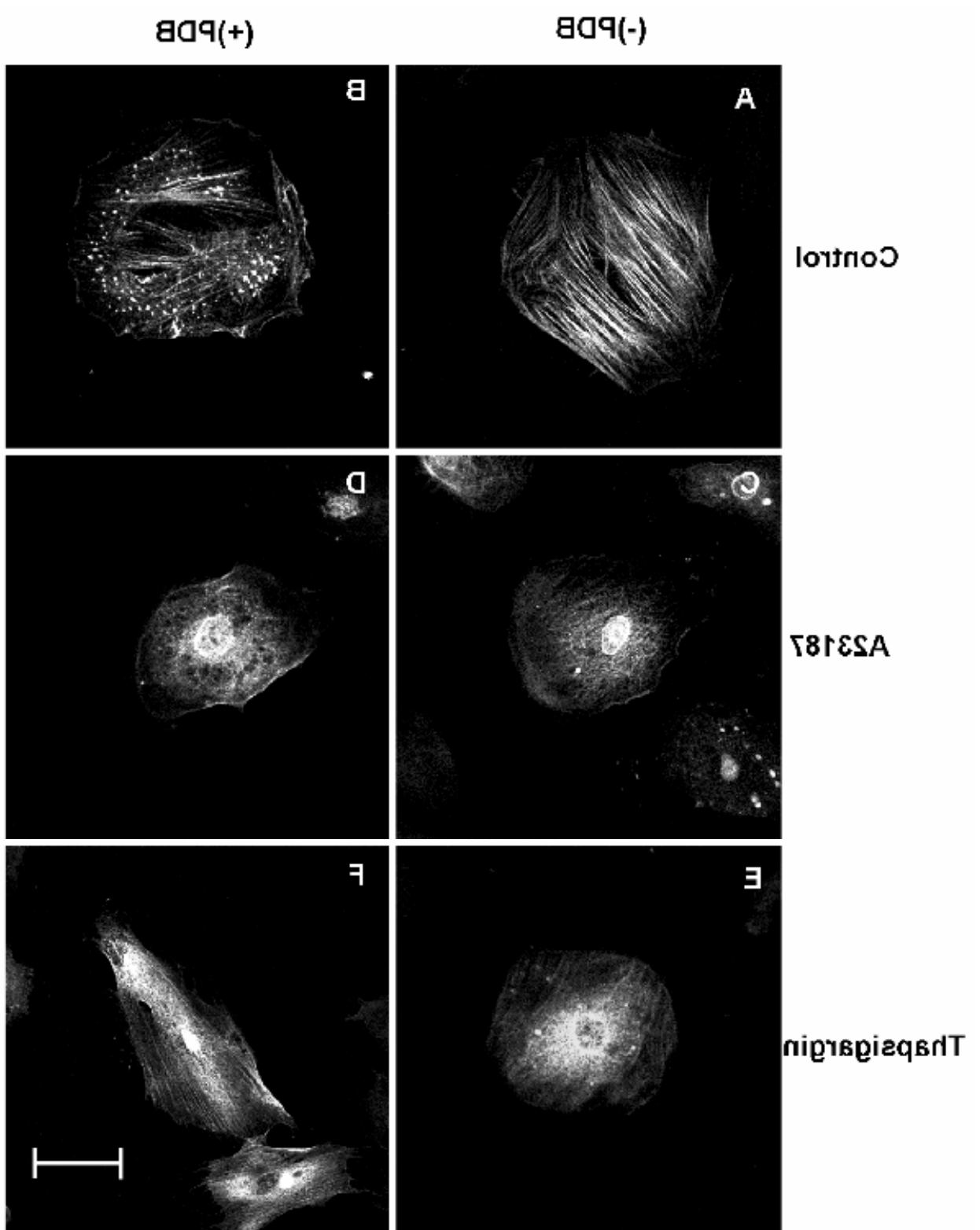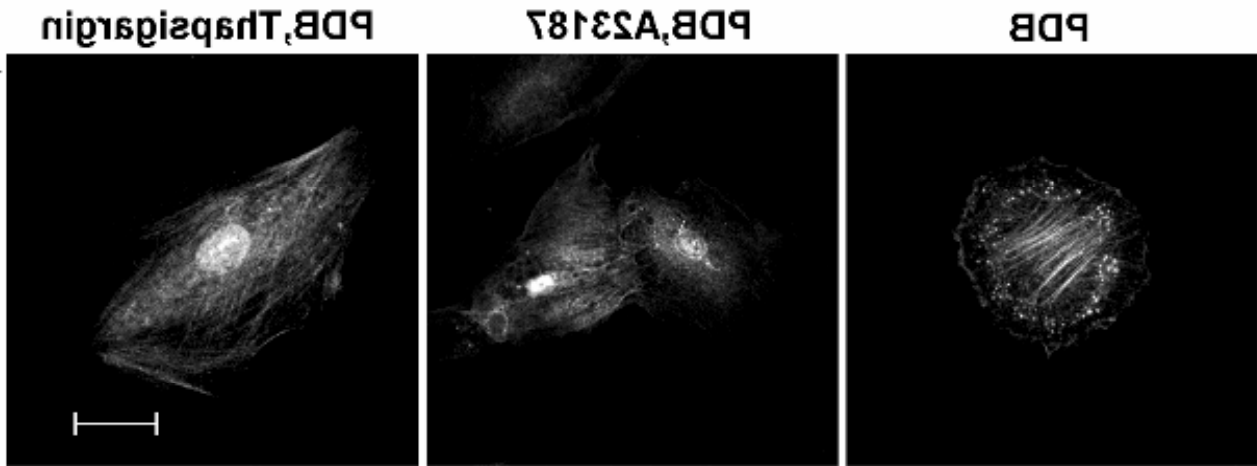
Thapsigargin

Figure 35.

The effect of A23187 and thapsigargin on α-actin cytoskeletal structure in A7r5 cells precontracted with 10^{-8}M PDBu. Cells were exposed to PDBu for 15 minutes to initiate remodeling and the A23187 or thapsigargin was added for an additional 15 minutes. α-Actin was visualized using a monoclonal anti-α-smooth muscle actin clone 1A4 FITC-labeled antibody. Micrographs represent results from 3 separate experiments in which an average 90 ± 3% of treated cells showed dissolution of α-actin structure. The original magnification was 400X. The scale bar indicates 50 microns.

Figure 36.

A study of the effect of PDBu, A23187 and thapsigargin on the distribution of B-actin stress fibers in calcium-free media. A7r5 cells were transfected with a β-actin-EGFP expression plasmid. PDBu treated cells (B), A23187 treated cells (D) and thapsigargin treated cells (G) show no loss of β-actin fibers. PDBu treated cells, PDBu + A23187 treated cells (E) and PDBu + thapsigargin treated cells (H) show no loss of β-actin fibers. The addition of calcium back to media did not cause any change of PDBu treated cells (C), PDBu + A23187 treated cells (F) or PDBu +thapsigargin treated cells (I). Micrographs represent the results from 3 separate experiments in which a total of 388 cells were evaluated. The original magnification was 400X. The scale bar indicates 50 microns.
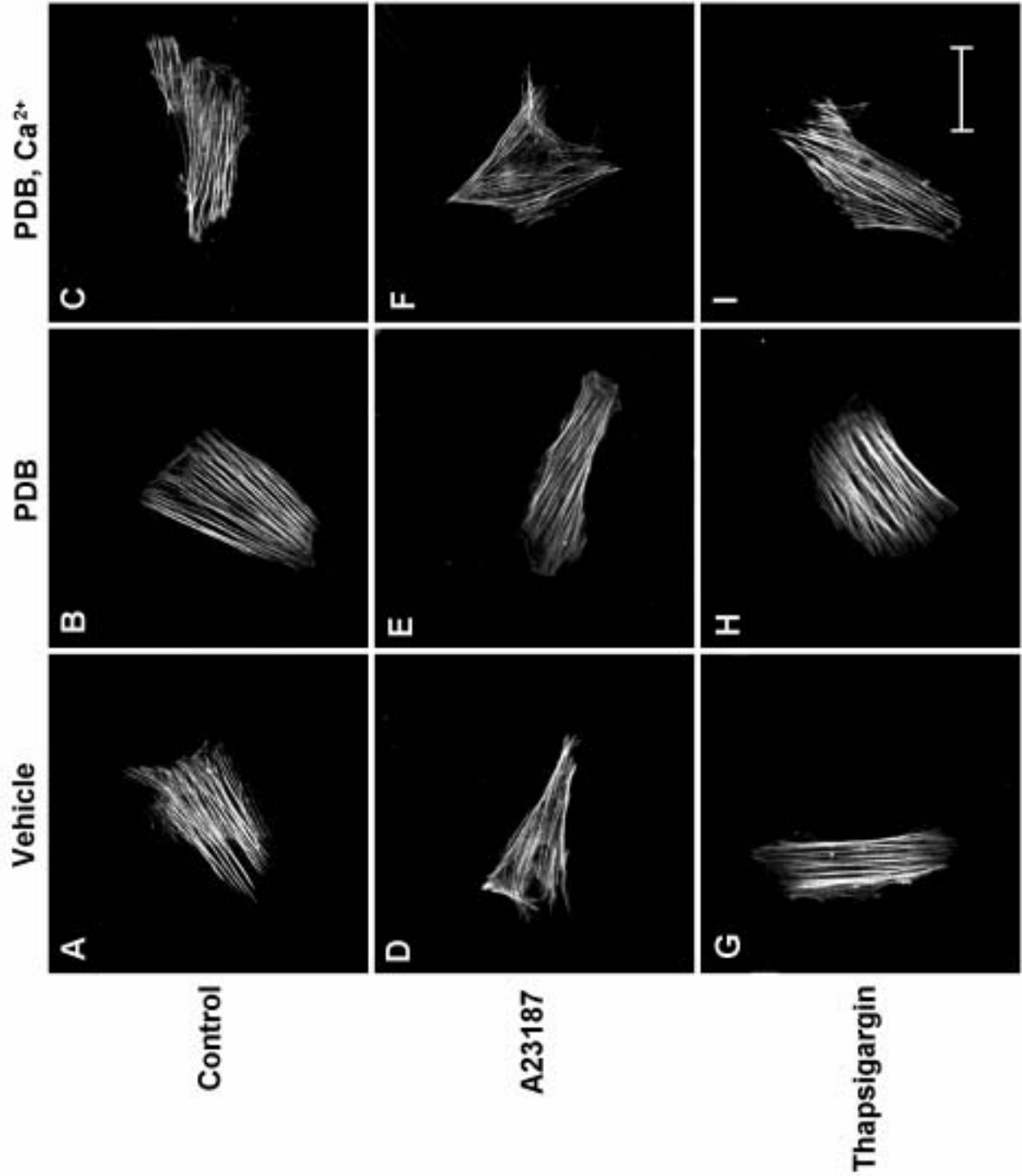
Figure 37.

A study of the effect of PDB, A23187 and thapsigargin on the distribution of α-actin stress fibers in calcium-free media. A7r5 cells were stained with a monoclonal anti-α-smooth muscle actin clone 1A4 FITC-labeled antibody. Control cells (A), A23187 treated cells (D) and thapsigargin treated cells (G) show no loss of α-actin fibers in calcium-free media. PDBu treated cells(B), PDBu + A23187 treated cells (E) and PDBu + thapsigargin treated cells (H) also have intact actin fiber structures. The addition of calcium back to media did not cause any change in PDB treated cells (C), PDBu + A23187 treated cells (F) or PDBu + thapsigargin treated cells (I). Micrographs represent the results from 5 separate experiments in which a total of 448 cells were evaluated. The original magnification was 400X. The scale bar indicates 50 microns.
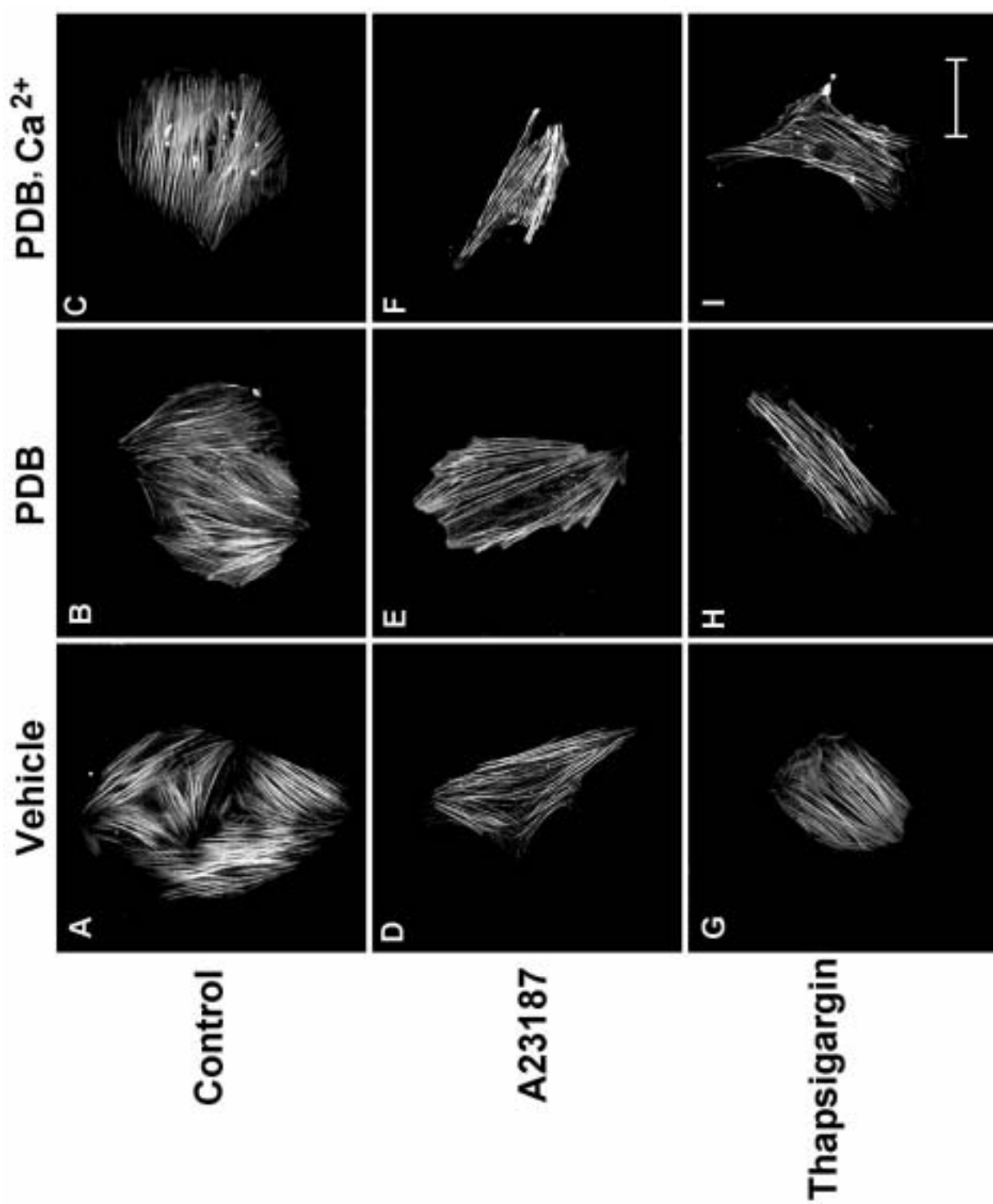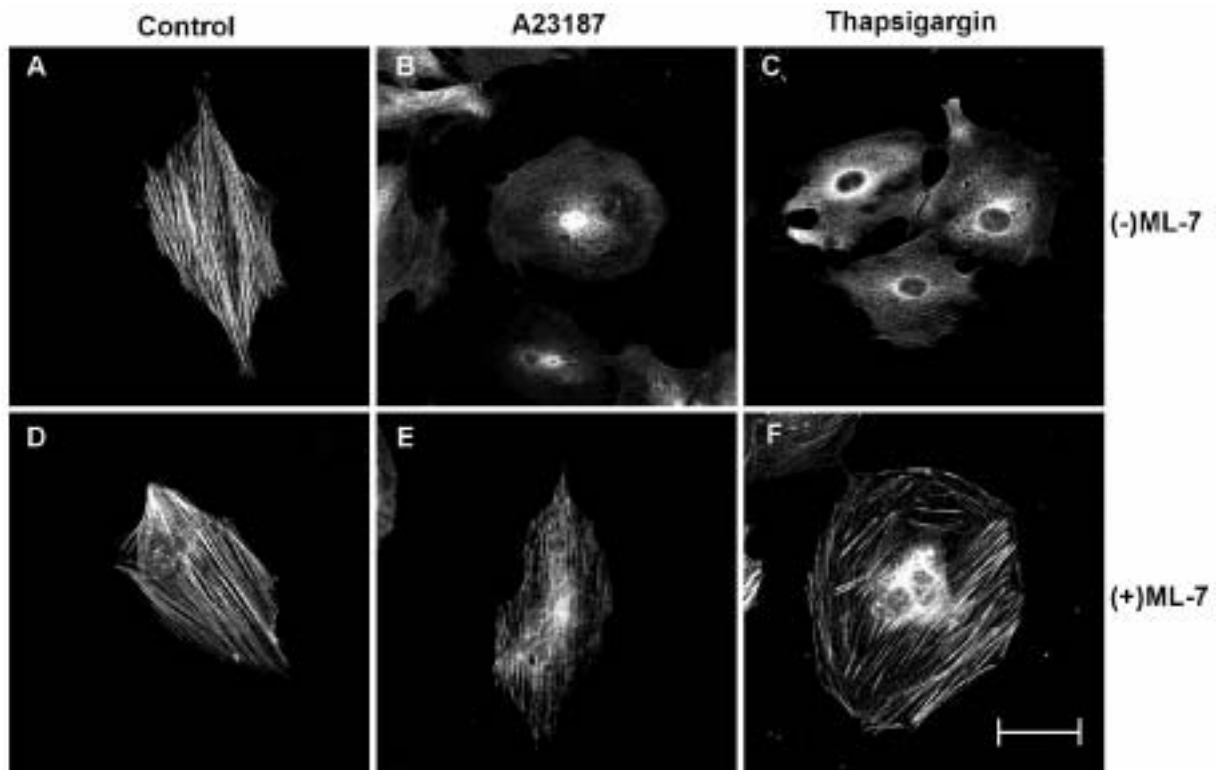
Figure 38.

The effect of myosin light chain kinase inhibitor, ML-7 on A23187 and thapsigargin-mediated dissolution of α-actin structure. Cells were visualized by staining with monoclonal anti-α-smooth muscle actin clone 1A4 FITC-labeled antibody. The dissolution of α-actin cables (B, C) was partially blocked by ML-7. Micrographs represent results from 3 separate experiments in which a total of 204 ML-7-treated cells were evaluated. The original magnification was 400X. The scale bar indicates 50 microns.

Table 4.   The effect of different kinase inhibitors on A23187-induced dissolution of α-actin structure.

Inhibitor	Target Kinase	Concentration	α-actin dissolution
Staurosporine	Ser/Thr	$7 \times 10^{-10}M$	- -
Bisindolymaleimide I	PKC	$1 \times 10^{-8}M$	- -
H-89	PKA	$3.7 \times 10^{-6}M$	- -
ML-7	MLCK	$5 \times 10^{-7}M$	+ -
KN-93	CAMK II	$3 \times 10^{-7}M$	- -
Genistein	Tyrosine Kinase	$2.5 \times 10^{-6}M$	- -

A negative (-) or positive (+) indicates no effect or an inhibitory effect, respectively, of the inhibitor against A23187-induced α-actin depolymerization.

Target kinase: general serine/threonine kinase inhibitor (ser/thr); protein kinase C(PKC); protein kinase A(PKA); myosin light chain kinase (MLCK); calmodulin kinase II (CAMK II).

IV Discussion

PKCα translocation

It is now thought that the various PKC isozymes differ in substrate specificity and sensitivity to activators. This conclusion is consistent with the observation of multiple isozymes within different cell types which indicate isozyme-specific functions despite apparently minor differences in amino acid composition (Chalfant et al., 1996). It is further thought that the high degree of PKC isoform specificity achieved in the cell is due to the localization of each isoform at specific subcellular sites. The translocation and compartmentalization of PKC isoforms in stimulated cells is thought to be of importance in enzyme activation and access to target substrates. Our experiments indicate that PKCα-EGFP fusion protein retained the enzymatic characteristics of PKCα and was a suitable probe for the study of translocation in A7r5 cells. Western blot analysis indicated that the fusion protein was effectively expressed and showed little or no evidence of degradation (Fig. 5). PKCα-EGFP retained kinase activity (Fig. 6) and showed a pattern of distribution identical to endogenous PKCα in unstimulated and PDBu-activated cells (Fig. 7). Translocation of PKCα-EGFP fusion protein was calcium dependent (Fig. 24). Moreover, the inactive phorbol ester 4α-PDD did not cause translocation, further suggesting that the cellular relocation of the fusion protein was due to the activation of PKC. These results are consistent with the findings of Sakai et al. (1997) who studied the translocation of PKCγ-GFP fusion protein in three different cell lines. They observed that the addition of GFP had no effect on distribution within the cell and concluded that the fusion protein provided a useful tool for the investigation of

the molecular mechanisms of PKCγ translocation. Others have successfully used the

expression of different GFP fusion proteins to study cytoskeletal dynamics in several

mammalian cell lines (Atten et al., 1998), further indicating the general utility of this type

of probe.

In recent work, Wang et al. (1999) have demonstrated a phorbol 12-myristate 13-acetate

(PMA) concentration-dependent translocation of PKCδ-GFP fusion protein in Chinese

hamster ovary cells. The present findings extend their observation, indicating a similar

phorbol ester concentration-dependent translocation of PKCα to the plasmalemma or

nucleus of A7r5 smooth muscle cells. The results suggest that the mechanism for

translocation of a specific PKC isoform to different primary target sites in response to

variation in stimulus strength may occur in widely differing cell types. The potentially

obligatory role of microtubules in phorbol ester-induced perinuclear translocation of

PKCα raises the possibility of unexpected complexity of PKC isoform regulatory activity

in different cells.

PKC activation is tightly linked to translocation. Therefore, translocation movements of

individual PKC isoforms have been investigated in different cell types under a variety of

stimulus conditions. The available evidence indicates that the target site of an individual

PKC isoform can vary among even closely related cell types. For example, PKCα has

been shown to translocate to the perinucleus of cultured cells derived from canine

pulmonary artery (Damron et al., 1998) and rat aorta (Haller et al., 1998) but is

translocated to the plasmalemma in freshly isolated ferret portal vein smooth muscle

(Khalil et al., 1996). It has been reported that PKCα is translocated to cytoskeletal structures in angiotensin II-stimulated cells derived from the adult rat aorta (Haller et al., 1998) and to both the cell nucleus and cell membrane focal adhesions when these cells are grown on fibronectin (Haller et al., 1998). Overall, research suggests that the translocation target site of an individual PKC isoform may be different among cell types and altered by different stimuli.

PKCs, which serve an important signal transduction function, interact with different components of the cytoskeleton and may play a central role in the regulation of cytoskeletal dynamics, while contributing to a variety of cytoskeletal-mediated cell functions. PKC isoforms have been shown to be extensively associated with cytoskeletal components and are thought to phosphorylate a large number of cytoskeletal-associated proteins (Atten et al., 1998; Meininger et al., 1999; Nakhost et al., 1998). It was demonstrated that PKCα associates with cytoskeletal filaments in angiotensin II-stimulated, but not PDGF-stimulated, vascular smooth muscle cells (Haller et al., 1998), suggesting that the association of this PKC isoform is specific to the stimulus utilized. Other research showed that PKC plays a key role in cell proliferation and differentiation (Montesano et al., 1985; Wang et al., 1997a; 1997b) as well as the contractile function of smooth muscle (Rasmussen et al., 1987; Wang et al., 1997B). Inhibition of PKC prevents cell spreading in nonmuscle (Vuori and Ruoslahti, 1993) and smooth muscle cells (Haller et al., 1998), suggesting a role in the formation (Clark and Brugge, 1995; Lewis et al., 1996; Walters et al., 1996) or disruption (Jaken et al., 1989) of cell focal adhesions. The role of PKC in smooth muscle contraction is not clearly understood. It

has been proposed that it is involved in several steps in the force generating mechanism ranging from increasing calcium influx through activation of voltage gated calcium channels to the phosphorylation of myosin light chain, myosin light chain kinase, myosin light chain phosphatase and several other proteins thought to regulate the interaction between myosin and actin filaments (Akiyama et al., 1986; Horowitz et al., 1996; Kebe and Hartshorne, 1985; Masuo et al., 1994; Sobue and Sellers, 1991). In light of the extensive literature linking PKC to cytoskeletal function and the activities of cytoskeletal-associated proteins, the inhibition of PKC translocation by disruption of the microtubules may reflect a cytoskeletal protein/PKCα interaction enabling movement to or docking at perinuclear sites. Alternatively, the results could be indicating an event mediated downstream of PKC activation that involves cytoskeletal components required, either directly or indirectly, for PKCα docking at the perinucleus. Because there was no clear evidence of colocalization of PKCα with microtubules during the interval of translocation (Fig. 13), suggesting that the mechanism does not require direct association of PKCα with microtubules, we consider an event downstream or parallel to PKCα activation a more likely explanation of the present results in A7r5 cells. The lack of an effect of cytochalasin B disruption of actin stress fibers on PKCα localization at either the cell membrane or perinucleus of PDBu-stimulated cells (Fig. 14) further indicates that the association between the cytoskeleton and PKCα translocation is highly specific to the microtubules.

It is interesting to note that perinuclear localization was observed at PDBu concentrations well above those necessary to fully activate PKC. One possibility is that high levels of

the phorbol ester resulted in the activation of other proteins affecting PKCα translocation. In addition to activation of the conventional and novel isoforms of PKC, substantial evidence now exists for phorbol ester-induced biological effects mediated via PKC-independent pathways (Rapuano and Bockman, 1997). At least 3 families of proteins have been identified as phorbol ester receptors (Kazanietz, 2000). The ras guanyl-releasing protein (ras-GRP) has been proposed to play a role in cell growth and malignant transformation through PKC-independent regulation of ras activity. The chimaerins are a family of proteins for which the α1 isoform has been demonstrated to exhibit GTPase-activating protein (GAP)-like activity for the GTP binding protein Rac, a central regulatory molecule in many cytoskeletal-related cell functions. Furthermore, the α2- and β2- chimaerins possess an N-terminal SH2 domain that may enable binding to phosphotyrosine proteins, suggesting that the chimaerins could be involved in more than one signaling pathway. Other potential phorbol ester receptors (Unc-13, Ca1DAG-GEF1) have been shown to bind phorbol esters with high affinity but are less well studied with regard to their biological properties. Hence, a number of phorbol ester-responsive proteins have been described which act through GTP-binding proteins to influence a variety of cell functions. To our knowledge, however, these or similar proteins have not been described in smooth muscle.

Within the cytosol, interactions of PKC with actin filaments, microtubules and intermediate filaments have been reported (Jaken and Jones, 1992). There are several other reports indicating a role of the cytoskeleton in the translocation response of PKCα. Schmaltz et al. (1996) showed that the transport of PKCα from the cytosol into the

nucleus of NIH 3T3 cells was blocked by disruption of either the microtubules or actin cytoskeleton without affecting the nuclear import of a karyophilic reporter protein containing a canonical nuclear localization sequence (NLS). Battistella-Patterson et al. (2000), however, found that colchicine disruption of microtubules but not cytochalasin disruption of actin microfilaments, blocked PDBu-induced perinuclear localization of PKCα in passaged smooth muscle cells. Their observations coupled with present findings suggest that the effects of colchicine are highly selective for perinuclear translocation and do not represent the nonspecific effect of a generalized loss in cytoskeletal integrity. It is observed that disruption of one kind of filament affects the integrity of others. Disruption of microtubules leads to a collapse of intermediate filaments into a ring around the nucleus (Murti et al., 1992). It is possible that PKCα perinucleus translocation is, in part, related to other cytoskeleton components.

Studies from several laboratories have established that the specific isoform PKCα is translocated from the cytosol in stimulated vascular smooth muscle cells. However, there has been considerable disagreement over the target site, suggesting that the spatial pattern of PKCα cellular movements may differ under the influence of a variety of factors. Plasticity in the signaling movements of an individual isoform could greatly expand its range of target substrates and could explain the multiple functional properties attributed to individual PKC isoforms by different laboratories. To investigate the potential for variable localization of PKCα at subcellular sites, we directly observed translocation in live cells expressing PKCα-EGFP. Studies were conducted in a single cell type under consistent cell culture conditions.

Our results confirm earlier reports that A7r5 cells retain responsiveness to vasoactive compounds (Byron et al., 1996) and may contract by both calcium-dependent and calcium-independent mechanisms (Nakajima et al., 1993). The absence of contractile response to Ang II (Fig. 19) further suggests that, while these cells exhibit clear responsiveness to the elevation of intracellular calcium concentration (thapsigargin, A23187) and activation of PKC (PDBu), they lacked the capability for receptor-mediated contraction to this compound.

The results indicate that the spatial and temporal relocalization of an individual PKC isoform (α) markedly differed depending on the stimulating agent. The direct activation of PKC with 10^{-8}M PDBu caused an irreversible relocalization of PKCα to the plasmalemma which required 10 to 20 minutes for completion (Fig. 16). Agents employed to elevate intracellular calcium concentration (A23187, Fig. 17; thapsigargin, Fig. 18) caused a rapidly transient translocation to the plasmalemma. In this case the relocalization of PKCα at the cell membrane was completed within 4 minutes with a slower redistribution back into the cytosol in the subsequent 25 minutes. By comparison, angiotensin II caused an extremely rapid transient location of PKCα to intensely fluorescing membrane patches (Fig. 19). In this case the translocation of PKCα to membrane sites was completed within seconds and return of the fusion protein to the cytosol within 1 or 2 minutes. Potassium stimulation induced a slow translocation of most of PKCα to the cell membrane, while small amounts were also observed as granular structures scattered throughout cytosol (Fig. 20). Because these experiments were

conducted under identical conditions, the results indicate a remarkable range in the temporal and spatial translocation movements of an individual PKC isozyme within a single cell type.

Our finding of concentration-dependent and agonist-dependent variations in PKCα translocation raises questions regarding the mechanisms which regulate PKC movements and/or docking at specific subcellular sites. We consider two possibilities likely: (1) an ATP-requiring transport process that involves active PKC protein translocation via a mechanism involving a microtubular component of the cytoskeleton; (2) simple diffusion may provide the driving force, while the targeting mechanisms center on the regulation of the availability of high-affinity binding sites at different subcellular location. To our knowledge, the possibility of active PKC translocation has not been investigated.

There are a number of potential mechanisms affecting PKC localization at specific subcellular sites. (1) Binding of calcium or diacylglycerol to PKC in the presence of phosphatidylserine causes a conformational change in the molecule that results in the exposure of the pseudosubstrate domain (Orr et al., 1992; Bosca and Moran, 1993) and increases hydrophobicity of the molecule, which, in turn, facilitates binding of the PKC to membrane lipids. (2) Phosphorylation of PKC would significantly affect the affinity of the protein for the lipid environment. Phosphorylation of PKC has been reported to be required for it to act as an effector-dependent kinase (Cazaubon and Parker, 1993). The phosphorylation sites of PKC have been identified as located in the catalytic domain in both α-PKC (Cazaubon and Parker, 1994) and β-PKC (Zhang et al., 1994). (3) It has

111

been suggested that PKC contains activator independent binding sites for arginine-rich

polypeptides distal to the catalytic site (Leventhal and Bertics, 1993). These binding sites

may allosterically activate PKC, but they may also allow targeting of PKC to specific

subcellular locations. (4) Specific receptors for PKC, such as RACKS, allow the

targeting of PKC to different subcellular sites.

Taken together, the evidence clearly suggests that the signaling movements of PKCα may

be significantly different depending on cell type or differentiation state (Batistalla-

Patterson et al., 2000, Li et al., 2001), cell environment (Haller et al., 1998), stimulus

intensity (Li et al., 2001), and stimulating agonist (present results). The localization of an

individual isoform at different subcellular sites may most likely be explained by concepts

of specific protein binding of PKC. However, mechanisms that acutely regulate the

availability of protein binding at substrate target sites have not been proposed or are

poorly defined. The magnitude of difference in the time requirement for visible

translocation and completion of relocalization at specific sites in response to different

agonists further suggests that the rate of PKC isoform activation or activation of binding

sites may play a role in PKCα translocation. The concept of simple diffusion of PKC

isoforms to available binding sites may not adequately explain the complex directional

signaling movements observed.

Summary

The results of present studies indicate that the A7r5 cell type has the capability to acutely

alter the translocation of an individual PKC isoform (PKCα) to a different subcellular

target site, depending upon the concentration of stimulating agent (PDBu) or the agonist employed. The translocation of PKCα to the perinucleus but not the plasma membrane is dependent on an intact microtubular cytoskeleton. Because PKCα perinuclear translocation does not involve direct association of PKCα with microtubules, it is unlikely that the cytoskeleton is directly involved in the directed movement of the PKCα isoform. This further suggests the role of the cytoskeleton may center on events downstream or parallel to PKC activation that enable PKCα movement to and/or docking at a specific location. The spatial and temporal characteristics of PKCα translocation were markedly different in A7r5 cells stimulated with different contractile agents. The results may explain how individual isoforms can exert multiple functional effects through the selective phosphorylation of different substrates via translocation to different locations in a single cell type. Mechanisms which regulate the selective PKC binding to different subcellular sites are not known.

Actin remodeling in the Contracting A7r5 Cell

It is well accepted that the temporal and spatial regulation of intracellular calcium concentration is crucial in the regulation of contractility in smooth muscle (Somlyo, 1985). However, repeated observations of dissociation between $[Ca^{2+}]i$ and force development have led to the concept of modulated calcium sensitivity of the smooth muscle contractile protein. Fay et al. (1979) provided the first simultaneous measurements of $[Ca^{2+}]i$ and tension in single smooth muscle cells, demonstrating a transient increase in light emission in aequorin-injected cells from toad stomach muscle which decreased to near pre-stimulus levels before the onset of mechanical events.

Morgan and Morgan (1982 and 1984) subsequently showed that receptor-mediated contraction of vascular smooth muscle evoked a transient elevation of $[Ca^{2+}]i$ with peak concentration reached at activation followed by a decline to near basal levels at the completion of force development and the subsequent plateau and maintenance of tension. This pattern of calcium transient and dissociation of $[Ca^{2+}]i$ and force has been confirmed by numerous laboratories using different techniques in a variety of smooth muscle cell types (Ishii et al., 1989; Ozaki et al., 1989; Rembold and Murphy, 1986; Himpens and Casteels, 1987; Himpens et al., 1988; Cross et al., 2000). Remarkably, one class of contractile agonist, phorbol esters, has been reported to cause contraction of smooth muscle without an elevation of $[Ca^{2+}]i$ (Sybertz et al., 1986; Itoh and Lederis, 1987; Jiang and Morgan, 1987). Others, however, have noted increased $[Ca^{2+}]i$ in phorbol ester-induced contractions (Rembold and Murphy, 1988; Nakajima et al., 1993; Kaneda et al., 1995; Murthy et al., 2000), suggesting these agonists do have at least a low level calcium requirement which could differ among cell types. In the present studies with A7r5 cells, A23187 and thapsigargin caused a sustained or increasing elevation of $[Ca^{2+}]i$ during the interval of observed cell contraction. This suggests to us that the conditions of increased $[Ca^{2+}]i$ were not physiological but may more closely reflect events initiated at high Ca^{2+} concentration normally occurring during the early phase of force development following cell activation.

The present work extends previous findings of different modes of α-and β-actin remodeling to contractions elicited by increased $[Ca^{2+}]i$. Both A23187 and thapsigargin caused visible constriction of cells in which β-actin cables were observed to shorten

without evidence of disassembly (Fig. 28). By comparison, the elevation of $[Ca^{2+}]i$ resulted in the destabilization and loss of α-actin structure in the majority of cells by the completion of cell contraction (Figs. 30, 31). Dissolution of actin filaments in the presence of high calcium concentration has been previously observed (Miyauchi et al., 1994) and may be explained by the activation of known microfilament severing proteins such as gelsolin (Ebisawa et al., 1985; Kwiatkowski, 1999). However, the concomitant dispersal of the α-actin-associated crosslinking protein, α-actinin (Fig. 32), the absence of change in the cellular distribution of talin (Fig. 33), and the lack of an effect on the integrity of the system of β-actin stress cables (Fig. 28) suggest that the destabilizing effect of increased $[Ca^{2+}]i$ was highly specific to α-actin cable structure.

The present results support the contention of Fultz et al. (2000) that the separation into distinct domains (Small et al., 1986) as well as the different modes of α- and β-actin remodeling, reflect different functions of the two isoforms during contraction. The shortened duration of the contractile response with concomitant, selective loss of α-actin cytoskeletal structure in A23187-and thapsigargin-treated cells is consistent with a direct involvement of α-actin in force development. Similarly, the maintenance of the cell in the contracted configuration at the cessation of cell shortening and after the depolymerization of α-actin, concomitant with normal β-actin cable shortening and stability, is consistent with a role of β-actin cable in tension maintenance.

We consider it probable that the degree of α-actin depolymerization seen in present studies represents an exaggerated response due to the sustained high levels of $[Ca^{2+}]i$

115

induced by the agonists employed. This conclusion is supported by the further observation that PDBu-mediated α-actin remodeling was also blocked by high $[Ca^{2+}]i$. Finally, incubation of cells in a calcium-free medium indicated that the loss of α-actin structure was indeed due to the elevation in $[Ca^{2+}]i$. Interestingly, these latter experiments also indicated that the calcium-free medium inhibited PDBu-induced α-actin remodeling, suggesting that this activity has a requirement for at least low $[Ca^{2+}]i$ levels. Taken together, these results suggest that the pattern of transient increase in $[Ca^{2+}]i$ induced by physiological agonists could be important in the sequential activation of different Ca^{2+} concentration-dependent contractile activities. In addition to activating myosin ATPase activity and rapid force development, the initial high levels of $[Ca^{2+}]i$ of the calcium transient could also serve to initiate α-actin destabilization preparatory to remodeling and a slower mode of force development. Alternatively, the peak in $[Ca^{2+}]i$ could serve to inhibit α-actin remodeling during the initial phase of force development. The inhibition of high $[Ca^{2+}]i$-induced α-actin depolymerization by ML-7 suggests that myosin light chain kinase (MLCK) could act as part of a pathway regulating the stability of α-actin cytoskeletal structure. However, we emphasize the need for caution in the interpretation of results from these experiments. Although studied at 10X, its IC_{50} concentration, ML-7 was, at most, only partially effective in preventing the loss in α-actin cable structure (Fig. 38). Moreover, the general serine/threonine kinase inhibitor, staurosporine, which was expected to inhibit MLCK at the concentration used, had no effect on α-actin dissolution by increased $[Ca^{2+}]i$. In light of these observations, the protective effect of ML-7 on α-actin structure was likely not due to a direct effect of the inhibition of MLCK on α-actin dynamics. Studies of calcium-dependent stress relaxation

of smooth muscle have suggested that the relaxant response to stretch involves remodeling of the actin cytoskeleton triggered by the strain placed on the tension bearing elements of the system (Wright and Battistella-Patterson, 1998). By way of speculation, initial force development due to spiking of $[Ca^{2+}]i$ in the activated cell could provide an obligatory perturbation in the distribution of strain on actin cables for triggering remodeling activity. Hence, an action of ML-7 to reduce or inhibit initial force development could indirectly influence actin remodeling.

Summary

The present results confirm earlier observations of different modes of remodeling of α-actin and β-actin isoforms in the contracting A7r5 cell and extend these findings to include contractions induced through the elevation of $[Ca^{2+}]i$. Our findings are consistent with separate primary functional roles, namely, the direct involvement of α-actin in force development and the remodeling of β-actin to maintain tension. Based on present findings, we speculate that the calcium transient reported in receptor-mediated activation of smooth muscle cells is of physiological importance in regulating the appropriate sequence of primary contractile events. In addition to activating maximal myosin ATPase activity and early force development, the peak in $[Ca^{2+}]i$ may trigger destabilization of α-actin cable structure, enabling active remodeling as $[Ca^{2+}]i$ declines.

Based on the present results and other recent findings (Fultz et al., 2000), we propose a modification of an earlier proposed mechanism of smooth muscle contraction by Battistella-Patterson et al. (1997). Figure 39A depicts a theoretical system indicating that

α-actin and β-actin are segregated into separate cytoskeletal domains. Immediately following agonist stimulation and elevation in $[Ca^{2+}]i$, the cell complement of α-actin/myosin contractile protein contracts, resulting in relatively rapid early force development and perturbation in the distribution of mechanical strain in the system (Fig. 39B). This, in turn, initiates a cycle of β-actin stress cable shortening to preserve gains in tension (Fig. 39C) and α-actin remodeling to modulate mechanical advantage of the contractile protein (Figs. 39 D, E, F). In preloaded tissues or cells, the attainment of equilibrium between force generating capacity and opposing load would result in the plateau of active tension and restoration of balance in mechanical strain within the system (Fig. 39G). The plateau in tension would be characterized by very low level remodeling and contractile protein activity with the establishment of a stable tension bearing system (Wright and Hurn, 1994). The model predicts (1) an unexpectedly high level of force generating capacity due to modulation of mechanical advantage at the contractile protein; (2) slow force development during combined remodeling and contractile protein activity; (3) virtually unfettered shortening in length of unloaded cells and; 4) low energy tension maintenance cost.
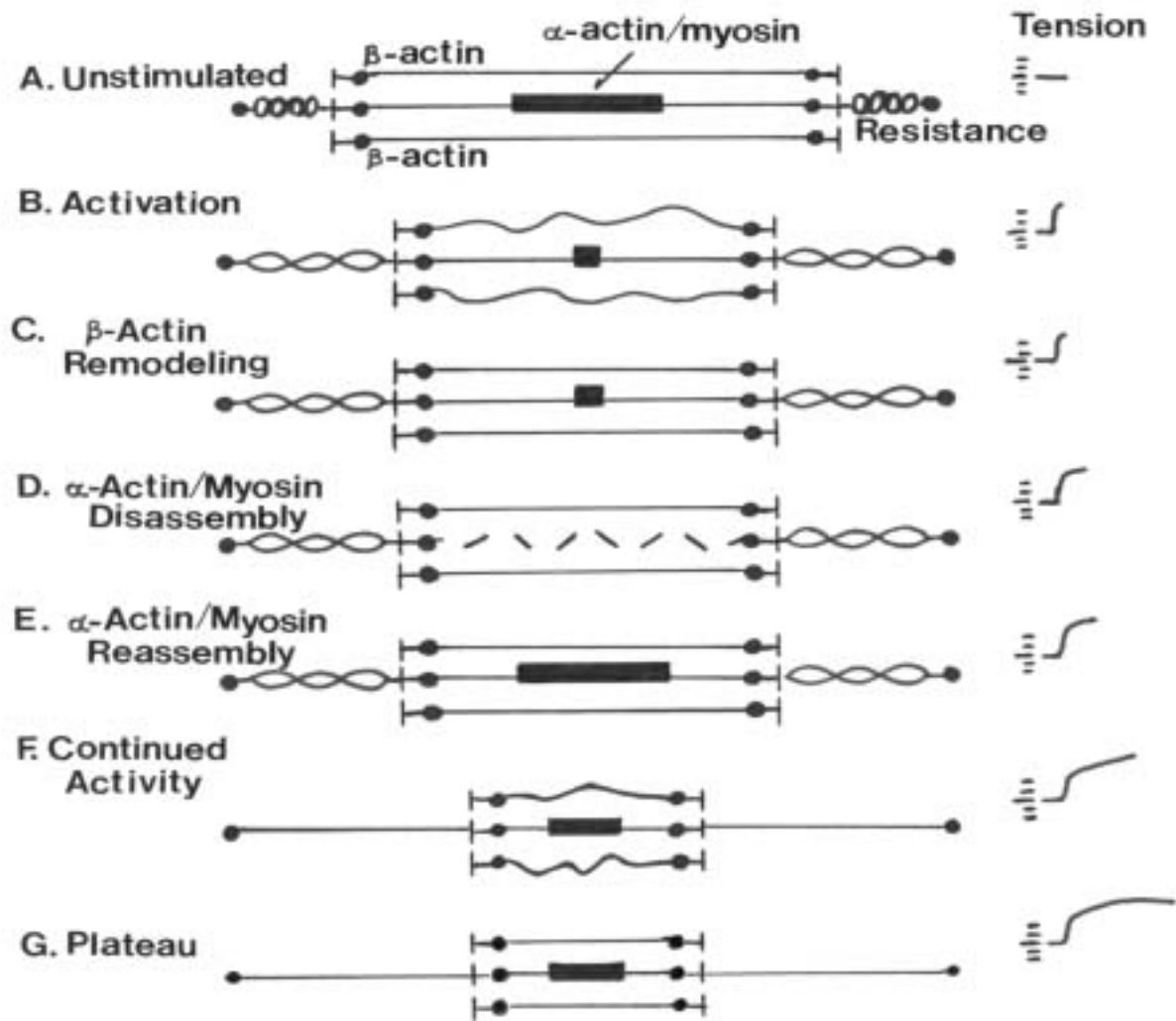
Figure 39.
Proposed model explaining force development and maintenance of active tension in smooth muscle. Resting mode with inactive contractile protein and associated β-actin stress bearing cables (A). Agonist stimulation of increased $[Ca^{2+}]i$, activation of early force development, and alteration in the distribution of strain (B). Activation of β-actin remodeling (C) serving to preserve gains in tension during α-actin disassembly (D). α-Actin reassembly (E) serving to optimize actin/myosin overlap for additional contractile activity at shortened length (F). Plateau in active force development with cessation of remodeling and establishment of a stable system of tension bearing elements (G).

V Literature Cited

Adam, L.P., Franklin, M. T., Raff, G.J. & Hathaway, D. R. Activation of mitogen-activated protein kinase in porcine carotid arteries. Circ Res 76: 183-190, 1995.

Akiyama T, Nishida E, Ishida J, Saji N, Ogawara H, Hoshi M, Miyata Y, Sakai H. Purified protein kinase C phosphorylates microtubule-associated protein-2. J Biol Chem 261(3): 15648-15651, 1986.

Allen LH, Aderem A. A role for MARKS, the alpha isozyme of protein kinase C and myosin I in zymosan phagocytosis by macrophages. J Exp Med 182(3):829-840, 1995.

Andrea JE, Walsh MP. Protein kinase C of smooth muscle. Hypertension 20: 585-595, 1992.

Atten MJ, Attar BM, Holian O. Cytoskeletal PKC and ERK/MAPK activation in response to N-nitrosamines and phorbol 12-myristate 13-acetate in gastric adenocarcinoma cells. Anticancer Res 18(6A): 4377-4382, 1998.

Avila J. Microtubule functions. Life Sci. 50:327-334, 1991.

Barkalow K. and Hartwig J.H. The role of actin filament barbed-end exposure in cytoskeletal dynamics and cell motility. Biochem. Soc. Trans. 23: 451-456, 1995.

Batistella-Patterson AS, Fultz ME, Li C, Geng W, Norton M, Wright GL. PKCα translocation is microtubule-dependent in passaged smooth muscle cells. Acta Physiol Scand 170: 87-97, 2000.

Battistella-Patterson AS, Wang S and Wright GL. Effect of disruption of the cytoskeleton on smooth muscle contraction. *Can J Physiol Pharmacol* 75: 1287-1299, 1997.

Benndorf R, Hayess K, Ryazantsev S, Wieske M, Behlke J, and Lutsch G. Phosphorylation and supramolecular organization of murine small heat shock protein HSP25 abolish its actin polymerization-inhibiting activity. J Biol Chem 269: 20780-20784, 1994.

Bershadsky A.D. and Vasiliev. J.M. Mechanisms of regulation of pseudopodal activity by the microtubule system. Symp. Soc. Exp. Biol. 47:353-373, 1993.

Blobe G. C., Stribling D. S., Fabbro D., Stabel S., and Hannun Y. A. Protein kinase C beta II specifically binds to and is activated by F-actin. [Erratum published in J. Biol. Chem. Vol. 271, p. 30297.] J. Biol. Chem. 271, 15823-15830, 1996.

Bond M, Somlyo AV. Dense bodies and actin polarity in vertebrate smooth muscle. J Cell Biol. 95(2 Pt 1): 403-13, 1982.

Bosca L., Morgan F. Circular dichroism analysis of ligand-induced conformational change in protein kinase C. Mechanism of translocation of the enzyme from the cytosol to the membrane and its implications. Biochem J. 290: 827-32, 1993.

Brinkley B. Microtubule organizing centers. Ann. Rev. Cell. Biol. 1:145-172, 1985.

Butt E, Immler D, Meyer HE, Kotlyarov A, Laass K, and Gaestel M. Heat shock protein 27 is a substrate of cGMP-dependent protein kinase in intact human platelets. Phosphorylation-induced actin polymerization caused by Hsp27 mutants. J Biol Chem 276: 7108-7113, 2001.

Byron, K.L. Vasopressin stimulates Ca^{2+}-spiking activity in A7r5 vascular smooth muscle cells via activation of phospholipase A_2. Circ. Res. 78: 813-820, 1996.

Carter S.B. Effects of cytochalasins on mammalian cells. Nature. 213:261-264, 1967.

Cazaubon S., Bornancin F., Parker P.J. Threonine-497 is a critical site for permissive activation of protein kinase C alpha. Biochem J. 301: 443-8, 1994.

Cazaubon S., Parker P.J. Identification of the phosphorylated region responsible for the permissive activation of protein kinase C. J. Biol. Chem. 268: 17559-63, 1993.

Chalfant CE., Ohno S., Konno Y., Fisher AA., Bisnauch LD., Watson JE., Cooper DR. A carboxy-terminal deletion mutant of protein kinase C beta II inhibits insulin-stimulated 2-deoxyglucose uptake in L6 rat skeletal muscle cells. Mol Endocrinol. 10: 1273-81, 1996.

Chapline C., Mousseau B., Ramsay K., Duddy S., Li Y., Kiley S. C., and Jaken S. Identification of a major protein kinase C-binding protein and substrate in rat embryo fibroblasts. Decreased expression in transformed cells. J. Biol. Chem. 271, 6417-6422,1996.

Chou YH, Bischoff JR, Beach D, Goldman RD. Intermediate filament reorganization during mitosis is mediated by p34cdc2 phosphorylation of vimentin. Cell 62(6): 1063-1067, 1990.

Clark EA, Brugge JS. Integrins and signal transduction pathways: the road taken. Science 268(5208): 233-239, 1995.

Cooper J.A. Effects of cytochalasin and phalloidin on actin. J. Cell Biol. 105:1473-1478,1987.

Cooper JA, Buhle EL Jr, Walker SB, Tsong TY, Pollard TD. Kinetic evidence for a monomer activation step in actin polymerization. Biochemistry, 26; 22(9):2193-202, 1983.

Coussens L, Parker PJ, Rhee L, Yang-Feng TL, Chen E, Waterfield MD,Francke U, Ullrich A. Multiple, distinct forms of bovine and human protein kinase C suggest diversity in cellular signaling pathways. Science 233: 859-66, 1986.

Cross KML, Dahm LM and Bowers CW. Simultaneous measures of contraction and intracellular calcium in single, cultured smooth muscle cells. *In Vitro Cell Dev Biol Animal* 36: 50-57, 2000.

Csukai, M., Chen, C. H., De Matteis, M.A., and Mochly-Rosen, D. The coatomer protein beta-COP, a selective binding protein (RACK) for protein kinase C epsilon. J. Biol. Chem. 272: 29200-29206, 1997.

Damron DS, Nadim HS, Hong SJ, Darvish A, Murray PA. Intracellular translocation of PKC isoforms in canine pulmonary artery smooth muscle cells by ANG II. Am J Physiol 274: L278-L288, 1998.

Daria MR, and Gordon AS. Anchoring protein for protein kinase C: a means for isozymes selectively. FASEB J. 12: 35-42, 1998.

Dekker LV, Parker P. Protein kinase C--a question of specificity. TIBS 19:73-77, 1994.

Devin CE, Somlyo AV and Somlyo AP. Sarcoplasmic reticulum and excitation-contraction coupling in mammalian smooth muscle. J Cell Biol. 52: 690-718, 1972.

Dresel P.E. and Knickle L. Cytochalasin B and phloretin depress contraction and relaxation of aortic smooth muscle. Eur. J. Pharm. 144:153-157, 1987.

Dresel P.E. and Ogbaghebriel A. Bolckade of the inotropic effect of BayK 8644 by cytochalasin B and phloretin. Br. J. Pharmacol. 94:552-556, 1988.

Ebisawa K, Maruyama K and Nonomura Y. Ca^{2+} regulation of vertebrate smooth muscle thin filaments mediated by an 84K Mv actin-binding protein: purification and characterization of the protein. *Biomed Res* 6: 161-173, 1985.

Fay F.S., Fujiwara K., Rees D.D. and Fogerty K.E. Distribution of α-actinin in single isolated smooth muscle cells. J. Cell Biol. 96:783-795, 1983.

Fay FS., Shlevin HH., Grannger WC Jr., Taylor SR. Aequorin luminescence during Activation of single isolated smooth muscle cells. Nature. 280: 506-8, 1979.

Firulli AB, Han D, Kelly-Roloff L, Kateliansky VE, Schwartz SM, Olson EN, Miano JM A comparative molecular analysis of four smooth muscle cell lines. In Vitro Cell Dev Biol 34: 217-26,1998.

Fowler L. J., Everitt J., Stevens J. L., and Jaken S. Redistribution and enhanced protein kinase C-mediated phosphorylation of alpha- and gamma-adducin during renal tumor progression. Cell Growth Differ. 9, 405-413, 1998.

Frieden C. Polymerization of actin: mechanism of the Mg2+-induced process at pH 8 and 20 degrees C. Proc Natl Acad Sci 80(21): 6513-7, 1983.

Fultz ME, Li C, Geng W, and Wright GL Remodeling in the contracting A7r5 smooth muscle cell. *J Mus Res Cell Motil* 21: 775-787, 2000.

Gallagher, P.J., Herring, B.P., Griffin, S.A. & Stull, J.T. Molecular characterization of a mammalian smooth muscle myosin light chain kinase. J Biol Chem 266, 23936-23944, 1991.

Gallagher, P.J., Herring, B.P.&Stull, J.T. Myosin light chain kinases (review). J Muscle Res Cell Motil 18, 1-16. 34:217-226, 1997.

Garcia-Rocha M., Avila J., and Lozano J. The zeta isozyme of protein kinase C binds to tubulin through the pseudosubstrate domain. Exp. Cell Res. 230, 1-8, 1997.

Geiger B., Volk T. and Volberg T. Molecular heterogeneity of adherens junctions. J. Cell Biol. 101:1523-1531, 1985.

Godman G.C. The effect of colchicines on striated muscle in tissue culture. Exp. Cell Res. 8:488-499, 1955.

Grynkiewicz G, Poenie M, Tsien RY. A new generation of Ca^{2+} indicators with greatly improved fluorescence properties. J. Biol Chem. 260 (6): 3440-50, 1985.

Gunst SJ, Wu MF, and Smith DD Contraction history modulates isotonic shortening velocity in smooth muscle. *Am J Physiol* 265(Cell Physiol. 34): C467-C476, 1993.

Gusev NB, Pritchard K, Hodgkinson JL, and Marston SB. Filamin and gelsolin influence calcium-sensitivity of smooth muscle thin filaments. J Muscle Res Cell Motil 15: 672-681, 1994.

Haller H, Smallwood JI, Rasmussen H. Protein kinase C translocation in intact vascular smooth muscle strips. Biochem J 270: 375-381, 1990.

Haller H, Ziegler W, Lindschau C, Luft FC. Endothelial cell tyrosine kinase receptor and G-protein coupled receptor activation involves distinct protein kinase C isoforms. Arterioscler Thromb Vasc Biol 16: 678-686, 1996.

Haller H, Lindschau C, Maasch C, Olthoff H, Kurscheid D, Luft FC. Integrin-induced protein kinase C translocation to focal adhesions mediates vascular smooth muscle cell spreading. Circ Res 82:157-165, 1998.

Haller H, Maasch C, Lindschau C, Brackmann M, Buchner K, Luft FC. Intracellular targeting and protein kinase C in vascular smooth muscle cells: specific effects of different membrane-bound receptors. Acta Physiol Scand 164:599-609, 1998.

Hanson PI, Kapiloff MS, Lou LL, Rosenfeld MG, Schulman H. Expression of a multifunctional Calcium/calmodulin-dependent protein kinase and mutational analysis of its autoregulation. Neuron 3(1): 59-70, 1989.

Hanson PI, Schulman H. Neuronal Calcium/calmodulin-dependent protein kinases. Annu Rev Biochem 61: 559-601, 1992.

Harris DE and Warshaw DM. Length vs active force relationship in single isolated smooth muscle cells. *Am J Physiol* 260(29): C1104-C1112, 1991.

Harris DE and Warshaw DM Slowing of velocity during isotonic shortening in isolated smooth muscle cells. *J Gen Physiol* 96: 581-601, 1990.

Hartshorne, D.J. Biochemistry of the contractile process in smooth muscle. In: L.R.Johnson (ed) Physiology of the Gastrointestinal Tract, pp. 423-482. Raven Press, New York. 1987.

Hayakawa, K., Okagaki, T., Higashi-Fujime, S.& Kohama, K. Bundling of actin filaments by myosin light chain kinase from smooth muscle. Biochem Biophys Res Commun 199, 786-791, 1994.

Hedges JC, Dechert MA, Yamboliev LA, Martin JL, Hickey E, Weber LA, and Gerthoffer WT. A role for p38 (MAPK)/HSP27 pathway in smooth muscle cell migration. J Biol Chem 274: 24211-24219, 1999.

Herman I.M. Actin isoforms. Curr. Opin. Cell Biol. 5:48-55, 1993.

Himpens B., and Casteels R. Measurement of Quin-2 of change of the intracellular calcium concentration in strips of the rabbit ear artery and of the guinea-pig ileum. Pflugers Arch 408: 32-7, 1987.

Himpens B, Matthÿs G, Somlyo AV, Butler TM and Somlyo AP. Cytoplasmic Free calcium, myosin light chain phosphorylation, and force in phasic and tonic smooth muscle. *J Gen Physiol* 92: 713-729, 1988.

Holden, H.M., Ito, M., Hartshorne, D.J.& Rayment, I. X-ray structure determination of telokin, the C-terminal domain of myosin light chain kinase, at 2,8 A resolution. J Mol Biol 227, 840-851, 1992.

Horowitz A, Menice CB, LaPorte R, Morgan KG. Mechanisms of smooth muscle contraction. Physiol Rev 7614: 967-1003, 1996.

Horowitz A., and Simons M. Regulation of syndecan-4 phosphorylation in vivo. J. Biol. Chem. 273,10914-10918, 1998.

Horowitz A., and Simons M. Phosphorylation of the cytoplasmic tail of syndecan-4 regulates activation of protein kinase Calpha. J. Biol. Chem. 273, 25548-25551, 1998.

Hoshi M, Nishida E, Miyata Y, Sakai H, Miyoshi T, Ogawara H, Akiyama T.Protein kinase C phosphorylates tau and induces its functional alterations. FEBS Lett 217 (2): 237-141, 1987.

House C., and Kemp B.E. Protein kinase C contains pseudosubstrate prototope in its regulatory domain. Science 238: 1726-1728, 1987.

Hundle B., McMahon T., Dadgar J., Chen C.H., Mochly-Rosen D., and Messing R.O., An inhibitory fragment derived from protein kinase C epsilon prevents enhancement of nerve growth factor responses by ethanol and phorbol ester. J. Bioo. Chem. 272: 15028-35, 1997.

Hyatt S., Liao L., Chapline C., and Jaken S. Identification and characterization of α-protein kinase C binding proteins in normal and transformed REF52 cells. Biochemistry 33. 1223-1228, 1994.

Ibitayo AI, Sladick J, Tuteja S, Louis-Jacques O, Yamada H, Groblewski G, Welsh M, and Bitar KN. HSP27 in signal transduction and association with contractile proteins in smooth muscle cells. Am J Physiol Gastrointest Liver Physiol 277: G445-G454, 1999.

Inagaki M, Gonad Y, Matsuyama M, Nishizawa K, Nishi Y, Sato C. Intermediate filament reconstitution in vitro. The role of phosphorylation in the assembly-disassembly of desmin. J Biol Chem 263 (12): 5970-5978, 1988.

Ishii N, Simpson AW, and Ashley CC . Free calcium at rest during "catch" in Single smooth muscle cells. *Science* 243 (4896): 1367-1368, 1989.

Itoh H and Lederis K. Contraction of rat thoracic aorta strips induced by phorbol 12 myristate 13-acetate. *Am J Physiol* 252: C244-C247, 1987.

Jaken S., and Jones W.A. PKV interaction with intracellular components. In Protein Kinase C , Current Concepts and Future Perspectives PP 237-273, Ellis Horwood, Ltd., W. Sussex, UK. 1992.

Jaken S, Leach K, Klauck T. Association of type 3 protein kinase C with focal contracts in rat embryo fibroblasts. J Cell Biol 109(2): 697-704, 1989.

Jensen PE, Gong MC, Somlyo AV, Somlyo AP. Separate upstream and convergent downstream pathways of G-protein-and phorbol ester-mediated Ca^{2+} sensitization of myosin light chain phosphorylation in smooth muscle. Biochem J 318: 469-475, 1996.

Jiang MJ and Morgan KG. Intracellular calcium levels in phorbol ester-induced contractions of vascular smooth muscle. *Am J Physiol* 253: H1365-H1371, 1987.

Johnson, J., Grey, M., and Mochly-Rosen, D. A protein kinase C translocation inhibitor as an isozyme selective antagonist of cardiac function. J. Biol. Chem. 271: 24962-66, 1996.

Kamm, K.E. & Stull, J.T. Myosin phosphorylation, force, and maximal shortening velocity in neutrally stimulated tracheal smooth muscle. Am J Physiol 249, C238-C247, 1985.

Kargacin GJ, Cooke PH, Abramson SB, Fay FS. Periodic organization of the contractile apparatus in smooth muscle revealed by the motion of dense bodies in single cells. J Cell Biol. 108(4):1465-75, 1989.

Kaneda T, Shimizu K, Nakaiyo S and Urakawa N. Effect of phorbol ester, 12 deoxyphorbol 13-isobutylate (DPB), on muscle tension and cytosolic Ca^{2+} in rat anococcygeus muscle. *Jpn J Pharmacol* 69: 195-204, 1995.

Kazanietz MG. Eyes wide shut: Protein kinase C isozymes are not the only receptors for the phorbol ester tumor promoters. Mol Carcinog 28:5-11, 2000.

Kebe M, Hartshorne DJ. Phosphorylation of smooth muscle myosin at two distinct sites by myosin light chain kinase. J Biol Chem 260 (18):10027-10031, 1985.

Keenan C, Kelleher D. Protein kinase C and the cytoskeleton. Cell Signal 10 (4):225-232, 1998.

Kemp, B.E. & Pearson, R.B. Intrasteric regulation of protein kinases and phosphatases, Biochim Biophys Acta 1094: 67-76, 1991.

Keranen LM, and Newton AC. Ca^{2+} differentially regulates conventional protein kinase Cs' membrane interaction and activation. J. Biol. Chem. 272: 25959-67, 1997.

Khalil RA, Lajore C, Morgan KG. In situ determination of $[Ca^{2+}]$; threshold for translocation of the alpha protein kinase C isoform. Am J Physiol 266: C1544-C1551, 1994.

Khalil RA, Morgan KG. Enzyme translocations during smooth muscle activation. In Biochemistry of Smooth Muscle Contraction. San Diego, CA, Academic. Vol. 24, pp 307-318, 1996.

Kimes BW, Brandt BL. Characterization of two putative smooth muscle cell lines from rat thoracic aorta. Exp Cell Res 98: 349-366,1976.

Klauck T. M., Faux M. C., Labudda K., Langeberg L. K., Jaken S., and Scott J. D. Coordination of three signaling enzymes by AKAP79, a mammalian scaffold protein. Science 271: 1589-1592, 1996.

Knighton D.R., Pearson R.B., Sowadski J.M., Means AR, Ten Eyck LF, Taylor SS, Kemp BE. Structural basis of the intrasteric regulation of myosin light chain kinases. Science 258:130-135, 1992.

Korn E.D. Actin polymerization and its regulation by proteins from non-muscle cells. Physiol. Rev. 62:672-737, 1982.

Kwiatkowski DJ. Functions of gelsolin: motility, signaling, apoptosis, cancer. *Curr Opin Cell Biol* 11: 103-108, 1999.

Lambert H, Charette SJ, Bernier AF, Guimond A, and Landry J. HSP27 multimerization mediated by phosphorylation-sensitive intermolecular interactions at the amino terminus. J Biol Chem 274: 9378-9385, 1999.

Lavoie JN, Gingras-Breton G, Tanguay RM, and Landry J. Induction of Chinese hamster HSP27 gene expression in mouse cells confers resistance to heat shock. HSP27 stabilization of the microfilament organization. J Biol Chem 268: 3420-3429, 1993a.

Lavoie JN, Hickey E, Weber LA, and Landry J. Modulation of actin microfilament dynamics and fluid phase pinocytosis by phosphorylation of heat shock protein 27. J Biol Chem 268: 24210-24214, 1993b.

Lehrich RW, Forrest JN. Protein kinase C zeta is associated with the mitotic apparatus in primary cell cultures of the shark rectal gland. J Biol Chem 269(51):32446-32450, 1994.

Leventhal PS., Bertics PJ. Activation of protein kinase C by selective binding of arginin-rich polypeptides. J Biol. Chem. 268: 13906-13, 1993.

Lewis JM, Cheresh DA, Schwartz MA. Protein kinase C regulates alpha v beta 5-dependent cytoskeletal associations and focal adhesion kinase phosphorylation. J Cell Biol 134: 1323-1332, 1996.

Li C., M.E. Fultz, W. Geng, S. Ohno, M. Norton and G.L. Wright. Concentration-dependent phorbol-stimulation of PKCα localization at the nucleus or subplasmalemma in A7r5 cells. Pflügers Archive 443(1):38-47, 2001.

Masuo M, Reardon S, Ikebe M, Kitazawa T. A novel mechanism for the Ca^{2+}-sensitizing effect of protein kinase C on vascular smooth muscle: inhibition of myosin light chain phosphatase. J Gen Physiol 104:265-286, 1994.

Mehta D and Gunst SJ. Actin polymerization stimulated by contractile activation regulates force development in canine tracheal smooth muscle. *J Physiol (Lond)* 519(3): 829-840, 1999.

Meininger GA, Moore EDW, Schmidt DJ, Lifshitz LM, Fay FS. Distribution of active protein kinase C in smooth muscle. Biophysical J 77: 973-984, 1999.

Meller N., Liu Y. C., Collins T. L., Bonnefoy-berard N., Baier G., Isakov N., and Altman A. Direct interaction between protein kinase C theta (PKC theta) and 14-3-3 tau in T cells: 14-3-3 overexpression results in inhibition of PKC theta translocation and function. Mol. Cell. Biol. 16, 5782-5791, 1996.

Meyer T, Hanson PI, Stryer L, Schulman H. Calmodulin trapping by calcium-calmodulin-dependent protein kinase. Science 256(5060): 1199-202, 1992.

Mineo C., Ying Y. S., Chapline C., Jaken S., and Anderson R.G. Targeting of protein kinase Xalpha to caveolae. J. Cell Biol. 141, 601-610, 1998.

Miron T, Vancompernolle K, Vanderkerckhove J, Wilchek M, and Geiger B. A 25-kD inhibitor of actin polymerization is a low molecular mass heat shock protein. J Cell Biol 114: 255-261, 1991.

Miron T, Wilchek M, and Geiger B. Characterization of an inhibitor of actin polymerization in vinculin-rich fraction of turkey gizzard smooth muscle. Eur J Biochem 178: 543-553, 1988

Miyauchi Y, Oishi K and Uchida MK. Actin severing and Ca^{2+}-induced reversal of smooth muscle contraction that is independent of Ca^{2+}. *Gen Pharmac* 25 (4): 691-695, 1994.

Mochly-Rosen, D. Localization of protein kinases by anchoring proteins: A theme in signal transduction. Science 268: 247-251, 1995.

Mochly-Rosen D, Khaner H, Lopez J. Identification of intracellular receptor proteins for activated protein kinase C.   Proc Natl Acad Sci USA 88:3997-4000, 1991.

Mochly-Rosen D., Miller K. G., Scheller, R. H., Khaner, H., Lopez, J., and Smith, B. L. p65 fragments, homologous to the C2 region of protein kinase C, bind to the intracellular receptors for protein kinase C. Biochemistry 31: 8120-8124, 1992.

Montesano R, Orci L. Tumor promoting phorbol esters induce angiogenesis *in vitro*. Cell 42: 469-477, 1985.

Morgan JP and Morgan KG. Stimulus-specific patterns of intracellular calcium levels in smooth muscle of the ferret portal vein. *J Physiol (Lond)* 351: 155-167, 1984.

Morgan JP and Morgan KG. Vascular smooth muscle: The first recorded Ca^{2+} transients. *Pflugers Arch* 395 (1): 75-77, 1982.

Murphy A, Breen KC, Long A, Feighery C, Casey EB, Kelleher D. Neurofilament expression in human T lymphocytes. Immunology 79 (1): 167-170, 1993.

Murthy KS, Yee YS, Grider JR and Makhlouf GM. Phorbol-stimulated Ca^{2+} Mobilization and contraction in dispersed intestinal smooth muscle cells. *J Pharmacol Exptl Therapeutics* 294(3): 991-996, 2000.

Murti KG, Kaur K, Goorha RM. Protein kinase C associates with intermediate filaments and stress fibers. Exp Cell Res 202 (1): 36-44, 1992.

Nakajima S, Fujimoto M and Veda M. Spatial changes of $[Ca^{2+}]i$ and contraction By phorbol esters in vascular smooth muscle cells. *Am J Physiol* 265: C1138-C1145, 1993.

Nakhost A, Forscher P, Sossin WS. Binding of protein kinase C isoforms to actin in Aplysai. J Neurochem 71 (3): 1221-1231,1998.

Newton AC, Johnson JE. Protein Kinase C: Paradigm for regulation of protein function by two membrane-targeting modules. Biochem Biophys Acta 1376(2): 155-172, 1998.

Newton, D., Klee, C., Woodgett, J. & Cohen, P. Selective effects of CAPP calmodulin on its target proteins. Biochim Biophys Acta 845: 533-539, 1985.

North A.J., Gimona M. Cross R.A. and Small J.V. Calponin is localized in both the contractile apparatus and the cytoskeleton of smooth muscle cells. J. Cell Sci. 107: 437-444, 1994a.

North A.J., Gimona M. Lando Z. and Small J.V. Actin isoform compartments in chicken gizzard smooth muscle cells. J. Cell Sci. 107: 445-455, 1994b.

Oakley C.E. and Oakley B.R. Identification of gamma-tubulin, a new member of the tubulin superfamily encoded by a mipA gene of Aspergillus nidulans. Nature. 338: 662-664, 1989.

Obara K. and Yabu H. Effect of cytochalasin B on intestinal smooth muscle cells. Eur. J Pharm. 255: 139-147, 1994.

Oh E. S., Woods A., and Couchman J. R. Multimerization of the cytoplasmic domain of syndecan-4 is required for its ability to activate protein kinase C. J. Biol. Chem. 272, 11805-11811, 1997.

Oh E. S., Woods A., and Couchman J. R. Syndecan-4 proteoglycan regulates the distribution and activity of protein kinase C. J. Biol. Chem. 272, 8133-8136, 1997.

Ohno S, Kawasaki H, Imajoh S, Suzuki K, Inagaki M, Yokokura H, Sakoh T, Hidaka H Tissue-specific expression of three distinct types of rabbit protein kinase C. Nature 325: 161-166, 1987.

Oka N., Yamamoto M., Schwencke C., Kawabe J., Ebina T., Ohno S., Couet J., Lisanti M. P., and Ishikawa Y. Caveolin interaction with protein kinase C. Isoenzyme dependent regulation of kinase activity by the caveolin scaffolding domain peptide. J. Biol. Chem. 272:33416-33421, 1997.

Olson, D.B. & Eckstein, F. High-efficiency oligonucleotide-directed plasmid mutagenesis. Proc Natl Acad Sci USA 87, 1451-1455, 1990.

Omary MB, Baxter GT, Chou CF, Riopel CL, Lin WY, Strulovici B. PKC epsilon-related kinase associates with and phosphorylates cytokeratin 8 and 18. J Cell Biol 117(3): 583-593, 1992.

Ono Y, Fujii T, Lagrashi K, Kuno T, Tanaka C, Kikkawa, and Nishizuka Y. Phorbol ester binding to protein kinase C requires a cysteine-rich-finger-like sequence. Proc. Natl. Acad. Sci. USA. 86: 4868-71, 1989.

Orr JW., Keranen LM., Newton AC. Reversible exposure of the pseudosubstrate domain of protein kinase C by phosphatidylserine and diacylglycerol. J Biol. Chem. 267: 15263-6, 1992.

Owen PJ, Johnson GD, Lord JM. Protein kinase C delta associates with vimentin intermediate filaments in differentiated HL60 cells. Exp Cell Res 225 (2):366-37, 1996.

Ozaki H, Sato K, Sakata K and Karaki H. Endothelin dissociates muscle tension From cytosolic Ca^{2+} in vascular smooth muscle of rat carotid artery. *Jpn J Pharmacol* 50: 521-524, 1989.

Pease DC, and Molinari S. Electron microscopy of muscular arteries: pial vessels of the cat and monkey. J. Ultrastruct. Res. 3: 447-468, 1960.

Persechini, A., Gansz, K.J. & Paresi, R.J. Activation of myosin light chain kinase and nitric oxide synthase activities by engineered calmodulins with duplicated or exchanged EF hand pairs. Biochemistry 35: 224-228, 1996.

Persechini, A., McMillan, K. & Leakey, P. Activation of myosin light chain kinase and nitric oxide synthase activities by calmodulin fragments. J Biol Chem 269: 16148-16154, 1994.

Pollard T.D. and Cooper J.A. Actin and actin-binding proteins. A critical evaluation of mechanisms and functions. Ann. Rev. Biochem. 55: 987-1035, 1986.

Potier, M. C., Chelot, E., Pekarsky, Y., Gardiner, K., Rossier, J. & Turnell, W.G. The human myosin light chain kinase (MLCK) from hippocampus: Cloning, sequencing, expression, and localization to 3qcen-q21. Genomics 29: 562-570, 1995.

Prekeris R., Hernandez R. M., Mayhew M. W., White M. K., and Terrian D. M. Molecular analysis of the interactions between protein kinase C-epsilon and filamentous actin. J. Biol. Chem. 273, 26790-26798, 1998.

Prekeris R., Mayhew M. W., Cooper J. B., and Terrian D. M. Identification and localization of an actin-binding motif that is unique to the epsilon isoform of protein kinase C and participates in the regulation of synaptic function. J. Cell Biol. 132, 77-90, 1996.

Puls A., Schmidt S., Grawe F., and Stabel S. Interaction of protein kinase C zeta with ZIP, a novel protein kinase C-binding protein. Proc. Natl. Acad. Sci. USA 94, 6191-6196, 1997.

Rapuano BE, Bockman RS. Protein kinase C-independent activation of a novel nonspecific phospholipase C pathway by phorbol myristate acetate releases arachidonic acid for prostaglandin synthesis in MC3T3-EY osteoblasts. Prostaglandins 53: 163-187, 1997.

Rasmussen H, Takuwa Y and Park S. Protein kinase C in the regulation of smooth Muscle contraction. *FASEB J* 1: 177-185, 1987.

Reddy S., Ozgur K. Lu M. Chang W. Mohan S.R. Kumar C.C. and Ruley H.E. Structure of the human smooth muscle alpha-actin gene. Analysis of a cDNA and 5' upstream region. J. Biol. Chem. 265: 1683-1687, 1990.

Rembold CM and Murphy RA. [Ca^{2+}]i-dependent myosin phosphorylation in Phorbol diester-stimulated smooth muscle contraction. *Am J Physiol* 255: C719-C723, 1988.

Rembold CM. and Murphy RA . Myoplasmic calcium, myosin phosphorylation andregulation of the crossbridge cycle in swine arterial smooth muscle. *Circ Res* 58: 803-815, 1986.

Ron D., Chen C. H., Caldwell J., Jamieson L., Orr, E., and Mochly-Rosen D. Cloning of an intracellular receptor for protein kinase C: a homolog of the beta subunit of G proteins.

Proc. Natl. Acad. Sci USA 91: 839-843, 1994.

Ron D., Jiand Z., Yao L., Vagts A. J., Diamond I., and Gordon A.S. Coordinated Movement of RACKI with activated Beta II PKC. J.Biol.Chem. 274: 27039-46, 1999.

Ron D., Lou J., and Mochly-Rosen, D. C2 region-derived peptides inhibit translocation and function of beta protein kinase C in vivo. J. Biol.Chem. 270: 24180-7, 1995.

Rousseau S, Houle F, Landry J, and Huot J. p38 MAP kinase activation by vascular endothelial growth factor mediates actin reorganization and cell migration in human endothelial cells. Oncogene 15: 2169-2177, 1997.

Sakai, N., K. Sasaki, N. Ikegaki, Y. Shirai, Y. Ono and N. Saito. Direct visualization of the translocation of the γ-subspecies of protein kinase C in living cells using fusion proteins with green fluorescent protein. J. Cell Biol. 139: 1465-1476, 1997.

Sanger F, Nicklen S, Coulson AR. DNA sequencing with chain-terminating inhibitors. Proc Natl Acad Sci U S A. Dec;74(12):5463-7, 1977.

Sato, M., Ye, L.-H. & Kohama, K. Myosin light chain kinase from vascular smooth muscle inhibits the ATP-dependent interaction between actin and myosin by binding to actin. J Biol Chem 118: 1-3, 1995.

Schlaepfer DD, Broome MA, and Hunter T. Fibronectinstimulated signaling from a focal adhesion kinase-c-Src complex: involvement of the Grb2, p130cas, and Nck adaptor proteins. Mol Cell Biol 17: 1702-1713, 1997.

Schlaepfer DD, Hanks SK, Hunter T, and Van Der Geer P. Integrin-mediated signal transduction linked to Ras pathway by GRB2 binding to focal adhesion kinase. Nature 372: 786-791,1994.

Schmalz D, Kalkbrenner F, Hucho F, Buchner K. Transport of protein kinase C alpha to the nucleus requires intact cytoskeleton while the transport of a protein containing a canonical nuclear localization signal does not. J Cell Sci 109 (9): 2401-2406, 1996.

Schneider GB, Hamano H, and Cooper LF. In vivo evaluation of hsp27 as an inhibitor of actin polymerization: hsp27 limits actin stress fiber and focal adhesion formation after heat shock. J Cell Physiol 177: 575-584, 1998.

Schroeder T.E. The contractile ring. I. Fine structure of dividing mammalian (HeLa) cells and the effects of cytochalasin B.Z. Zellforsch. Mikrosk. Anat. 109:431-449, 1970.

Schworer CM, Rothblum LI, Thekumkara TJ, Singer. Identification of novel isoforms of the delta subunit of Calcium/calmodulin-dependent protein kinase II. Differential expression in rat brain and aorta. J. Biol.Chem. 268(19): 14443-9, 1993.

Sellers, J.R. & Pato, M.D. The binding of smooth muscle myosin light chain kinase and phosphatases to actin and myosin. J Biol Chem 259: 7740-7746, 1984.

Shen X, Wu MF, Tepper RS and Gunst SJ. Mechanisms for mechanical response Of airway smooth muscle to length oscillation. *J Appl Physiol* 83 (3): 731-738, 1997.

Singer HA and Baker KM. Calcium dependence of phorbol 12, 13 dibutyrate-Induced force and myosin light chain phosphorylation in arterial smooth muscle. *J Pharmacol Exptl Therapeutics* 243 (3): 814-821, 1987.

Small JV, Furst DO and DeMeys L. Localization of filamin in smooth muscle. *J Cell Biol*102: 210-220, 1986.

Sobue K, Sellers JR. Caldesmon, a novel regulatory protein in smooth muscle and nonmuscle actomyosin systems. J Biol Chem 266 (19): 12115-12118, 1991.

Somlyo AP. Excitation-contraction coupling and the ultrastructure of smooth muscle. *Circ Res* 57: 497-501, 1985.

Somlyo, A.P. & Somlyo, A.V. Signal transduction and regulation in smooth muscle. Nature 372: 231-236, 1994.

Spudich J.A. Effects of cytochalasin B on actin filaments. Cold spring Harbor Symposia on Quantitative Biology. 37: 585-593, 1972.

Spudich J.A. and Lin S. Cytochalasin B, Its interaction with actin and actomyosin from muscle. Proc. Nat. Acad. Sci. 69: 442-446, 1972.

Stull JT, Hsu LC, Tansey MG, Kamm KE. Myosin light chain kinase phosphorylation in tracheal smooth muscle. J Biol Chem 265(27): 16683-90, 1990.

Stull, J.T., Nunnally, M.H. & Michnoff, C.H. Calmodulin-dependent protein kinases. In: E.G. Krebs & P.D.Boyer (eds), The Enzymes, pp. 113-166. Academic Press, New York, 1986.

Sweeney, H.L., Bowman, B.F. & Stull, J.T. Myosin light chain phosphorylation in vertebrate striated muscle: regulation and function. Am J Physiol 264: C1085-C1095, 1993.

Sybertz EJ, Desiderio DM, Tetzloff G and Chiu PJS. Phorbol dibutyrate contraction in rabbit aorta: calcium dependence and sensitivity to nitrovasodilators and 8-BR-cyclic GMP. *J Pharmacol Exptl Ther.* 239: 78-83, 1986.

Tang DD and Gunst SJ. Depletion of focal adhesion kinase by antisense oligonucleotides depresses contractile activation of smooth muscle. Am J Physiol Cell Physiol 280: C874-C883, 2001.

Tang DD, Mehta D, and Gunst SJ. Mechanosensitive tyrosine phosphorylation of paxillin and focal adhesion kinase in tracheal smooth muscle. Am J Physiol Cell Physiol 276: C250-C258, 1999.

Tansey MG, Word RA, Hidaka H, Singer HA, Schworer CM, Kamm KE, Stull JT. Phosphorylation of myosin light chain kinase by the multifunctional calmodulin-dependent protein kinase II in smooth muscle cells. J Biol Chem 267(18): 12511-6, 1992.

Thaler CD and Haimo LT. Control of organelle transport in melanophores: regulation of Ca^{2+} and cAMP levels. *Cell Motil Cytoskel* 22(3): 175-184, 1992.

Tobacman LS, Brenner SL, Korn ED. Effect of Acanthamoeba profiling on the pre-steady state kinetics of actin polymerization and on the concentration of F-actin at steady state. J Biol Chem. 25; 258(14): 8806-12,1983.

Tseng S., Kim R. Kim T. Morgan K.G. and Hai C.M. F-actin disruption attenuates agonist induced [Ca++], myosin phosphorylation, and force in smooth muscle. Am.J. Phys 272:Cell Phys. 41: C1960-1967, 1997.

Vandekerckhove J. and Weber K. At least six different actins are expressed in a higher mammal: an analysis based on the amino acid sequence of the amino-terminal tryptic peptide. J.Mol.Biol. 126: 783-802, 1978.

Vandekerckhove J. and Weber K. Actin typing on total cellular extracts: A highly sensitive protein-chemical procedure able to distinguish different actins. Eur. J. Biochem. 113: 595-603, 1981.

Volberg T. Sabanay H. and Geiger B. Spatial and temporal relationships between vinculin and talin in the developing chicken gizzard smooth muscle. Differentiation. 32: 34-43, 1986.

Vuori K, Ruoslahti E. Activation of protein kinase C precedes alpha 5 beta 1 integrin-mediated cell spreading on fibronectin. J Biol Chem 268: 21459-21462, 1993.

Wang S, Desai D, Wright G, Niles R, Wright GL. Effects of protein kinase Cα overexpression of A7r5 smooth muscle cell proliferation and differentiation. Exp Cell Res 236: 117-126, 1997a.

Wang S, Wright G, Geng W, Wright GL. Retinol influences contractile function and exerts an anti-proliferative effect on vascular smooth muscle cells through an endothelium-dependent mechanism. Pflugers Arch - Eur J Physiol 434: 669-677, 1997b.

Wang QJ, Bhattacharyya D, Garfield S, Narco K, Marquez VE, Blumberg PM. Differential localization of protein kinase C delta by phorbol esters and related

compounds using a fusion protein with green fluorescent protein. J Biol Chem 274(52): 37233-37239, 1999.

Walters D, Garrone B, Gobert G, Williams S, Gardiner R, Lavin M. Bistratene A causes phosphorylation of talin and redistribution of actin microfilaments in fibroblasts:possible role for PKC-delta. Exp Cell Res 229 (2): 327-335, 1996.

Wessells N.K. Microfilaments in cellular and developmental processes. Science. 171: 135-143, 1971.

Wiche G., Krepler R. Artlieb U. Pytela R. and Denk H. Occurrence and immunolocalization of plectin in tissues. J.Cell Biol. 97: 887-901, 1983.

Wright GL and Battistella-Patterson AS. Involvement of the cytoskeleton in calcium-dependent stress relaxation of rat aortic smooth muscle. *J Mus Res and Cell Motil* 19: 405-414, 1998.

Wright G and Hurn E. Cytochalasin inhibition of slow tension increase in rat aortic rings. *Am J Physiol* 267 (Heart Circ. Physiol. 36): H1437-H1447, 1994.

Xiao B., Smerdon S. J., Jones D. H., Dodson G. G., Soneji Y., Aitken A., and Gamblin S. J. Structure of a 14-3-3 protein and implications for coordination of multiple signaling pathways. Nature (London) 376, 188-191, 1995.

Xu X. Z., Choudhury A., Li X., and Montell C. Coordination of an array of signaling proteins through homo and heteromeric interactions between PDZ domains and target proteins. J. Cell Biol. 142, 545-555, 1998.

Yao L., Suzuki H., Ozawa K., Deng J., Lehel C., Fukamachi H., Anderson W., Kawakami Y., and Kawakami T. Interactions between protein kinase C and pleckstrin homology domain: inhibition by phosphoatidylinositol 4,5-bisphosphate and phorbol 12-myristate 13-acetate. J. Biol. Chem. 272, 13033-13039, 1997.

Yedovitzky J.A., Mochly-Rosen D., Ron D., Gary M.O., Johnson J.A., Abramovitch E., Cerasi E. and Nesher R. Translocation inhibition define specificity of protein kinase C isozymes in pancreatic beta cells. J. Biol.Chem. 272: 1417-20, 1997.

Zhange J., Wang L., Schwartz J., Bond RW., Bishop WR. Phosphorylation of Thr 642 is an early event in the processing of newly synthesized protein kinase C betaI and is essential for its activation. J Biol. Chem. 269:19578-84, 1994.

Zheng Y., Jung M. and Oakley B.R. Gamma-gubulin is present in Drosophila melanogaster and Homo sapiens and is associated with the centrosome. Cell 65: 817-823, 1991.

Zhang Z.H., Johnson J.A., Chen l., EL-Sherif N., Mochly-Rosen D., and Boutjdir D. C2 region-drived peptides of beta-protein kinase c regulate Ca^{2+} channels. Circ. Res. 80: 720-9, 1997.